Mathematical Modeling and Simulation for Epidemic Models

Hyojung Lee

Department of Mathematical Sciences

Graduate School of UNIST

Mathematical Modeling and Simulation for Epidemic Models

A dissertation
submitted to the Graduate School of UNIST
in partial fulfillment of the
requirements for the degree of
Doctor of Philosophy

Hyojung Lee

12.14.2016
Approved by

Advisor
Chang Hyeong Lee

Mathematical Modeling and Simulation for Epidemic Models

Hyojung Lee

This certifies that the dissertation of Hyojung Lee is approved.

12.14.2016

Advisor: Chang Hyeong Lee

Pilwon Kim: Thesis Committee Member #1

Chang-Yeol Jung: Thesis Committee Member #2

Jin Hyuk Choi : Thesis Committee Member #3

Sunmi Lee: Thesis Committee Member #4

I dedicate this dissertation to my parents

Abstract

Mathematical modeling has been important to explore transmission dynamics and construct effective control strategies to prevent the spread of disease. Most simple mathematical model is deterministic model. However, we need to take account into the stochastic model when the system involves the intrinsic fluctuations or randomness. Moreover, stochastic models can capture exactly the dynamics of individuals in a small population. But generally, it is difficult to solve the stochastic system. Since bio-chemical reaction is described according to the law of mass action which is used to construct epidemic model. We derive the explicit formula of the solution in terms of block matrices. We formulate mathematical models for epidemic disease. Then, we apply the stochastic computational methods such as the stochastic simulation algorithm (SSA) and the moment closure method (MCM) to the model. First, we apply the stochastic methods to an disease transmission model with government′s control policies against the 2009 H1N1 influenza in Korea. We investigate the impact of various vaccination and antiviral treatment intervention scenarios to prevent the spread of disease. As the result, it is verified that the earlier vaccination is more effective. Second, we consider the two-strain dengue transmission model with seasonality for sequential infection. Despite of having no autochthonous dengue outbreaks in Korea, the potential risk of dengue transmission in Jeju Island increases. We investigate the possible impacts of the potential outbreak of dengue fever in Jeju Island considering climate change based on Representative Concentration Pathways (RCP) scenarios and the migration of infected international travel. Finally, if there are a small number of cases at the initial stage of the epidemic. Infection processes occur randomly. Transmission dynamics involve the probabilistic properties in the system. Therefore, stochastic model provides more accurate predictions. We compare the dynamics of epidemic outbreaks quantitatively under stochastic and deterministic models. We investigate that as the initial number of infectives increases, the difference between the deterministic and stochastic solutions decreases.

Contents

*This work was published as: H. Lee and CH Lee, ''An Analytic Approach to a Stochastic Enzyme Kinetic Model", MATCH-Communications in Mathematical and in Computer Chemistry, vol. 73, pp.691-704 (2015)

**This work was published as: H.Lee, S. Lee and CH Lee, ''Stochastic methods for epidemic models: An application to the 2009 H1N1 influenza outbreak in Korea", Applied Mathematics and Computation, vol. 286, pp.232-249 (2016)

List of Figures

List of Tables

1

Introduction

1.1 Overview

Some infectious diseases such as dengue fever or malaria have occurred recurrently for centuries, and new pathogens such as the Middle East Respiratory Syndrome (MERS) coronavirus emerged in 26 countries. Infectious disease were responsible for 60% of global deaths. The importance of mathematical modeling is constantly growing, since it allows us to estimate the transmission dynamics and prevent the spread of disease. The classical epidemic models are described by deterministic systems such as ordinary differential equations (ODEs) or partial differential equations (PDEs). If the individuals are assumed to be mixed uniformly, the models can be expressed as a system of ODEs. One of the most famous ODE models is the Susceptible-Infectious- Recovery (SIR) model presented by McKendrick and Kermack [2, 3], which is a three compartment model with each compartment describing the number of Susceptible, Infectious and Recovered individuals respectively at a time of interest. PDE-based modeling involves several independent variables and is suitable for systems in heterogeneous real-world environments. For example, the cholera disease dynamics have different infection rates depending on the age of humans. Alexanderian [4] constructed age-structured PDEs by adding an age variable into the ODEs. Lotfi [5] studied a reaction-diffusion SIR model considering the spatial effect due to the mobility of people.

However, the transmission dynamics of infectious diseases involve the probabilistic properties in the system, while the deterministic models can only describe the average behaviors of collective variables under the uniformly mixed population assumption. Therefore, the time evolution of individuals in a small population cannot be captured exactly by deterministic models. Moreover, intrinsic fluctuations or noises appear in the reaction events of the system. Some studies [6, 7] had introduced stochastic thresholds and investigate the relationships between the deterministic and stochastic models in terms of thresholds, especially for basic reproduction number. For a case of large populations, the ODE system shows outbreaks with only

a few initial infected individuals if the basic reproduction number $R_0 > 1$, but the epidemic may not occur in a stochastic system [8]. In those cases, stochastic models provide a more detailed understanding of an epidemic. Therefore, even if the deterministic model is commonly used, the importance of the stochastic model is raised. The stochastic epidemic model was first introduced by Kendall [9] and was studied profoundly by Bartlett [10]. In Allen [11], the discrete-time stochastic Susceptible-Infectious-Susceptible (SIS) and SIR models with constant population size are studied, and stochastic solutions are compared with the deterministic solutions. Stochastic models for the vector-host diseases are also developed Samat and Cao [12, 13]. For example, the dengue transmission with seasonality in a short time scale is studied using a stochastic model [14].

Most commonly used stochastic epidemic models are based on continuous-time Markov chain in terms of standard Poisson processes by a random time change representation. However, it is difficult or inapplicable to solve the system analytically, since the epidemic models are generally nonlinear and deal with the high dimensionality. Therefore, various numerical computation methods are developed for solving stochastic systems. One computational algorithms is the stochastic simulation algorithm (SSA) presented by Gillespie [15]. The SSA is widely used to simulate stochastic chemical reactions where the small size of molecules often invalidates the deterministic differential equations. The SSA is a simple procedure generating trajectories of a stochastic system. However, this method is slow when computing a system with frequent reactions. Therefore, there have been many modifications and adaptations to reduce the computational costs significantly [16, 17], and the moment closure method (MCM) is one of stochastic computational methods. There are several studies about the applications of the moment closure method for the stochastic epidemic models. Lloyd [18] showed that the behavior of stochastic Susceptible-Exposed-Infectious-Recovery (SEIR) model depends on the population size and the seasonal forcing by using the MCM. Furthermore, a second-order MCM is used for the SI and SIS models based on the beta binomial distribution approximation in [19]. The higher-order MCMs including the second-order MCM are developed rigorously in [20]. We apply this method to the stochastic epidemic models which has the higher order dimension and large population size.

1.2 Infectious disease

Infectious diseases are caused by pathogenic microorganisms, such as bacteria, viruses, parasites or fungi. These diseases can be spread directly from person to person or indirectly. Here, H1N1 influenza and dengue fever are typical examples of infectious diseases. H1N1 is a new influenza virus which can effectively cause infection through contact among people. On the other hand, dengue fever is a vector-borne viral disease which is transmitted by the bite of female *Aedes* mosquitoes.

H1N1 influenza

More than 20 kinds of influenza viruses have been detected since the 20th century. The worldwide influenza pandemics in history are the 1918 Spanish Flu, the 1957 Asian Flu and the 1968 Hong Kong Flu. The 1918 Spanish Flu (H1N1) was a severe pandemic with three major outbreaks resulting in approximately 50 million deaths. The Asian Flu (H2N2) was first identified in the Far East. Approximately 2 million global deaths were estimated during a pandemic of 1957-1958. In early 1968, a new virus (H3N2) broke out in Hong Kong and the first cases in the United States were detected in September. It still caused about 34,000 deaths until March 1969. Though, it was the mildest influenza pandemic in the 20th century among the three pandemics since the United States was not severely affected.

Recently, a novel H1N1 pandemic influenza broke out in 2009 all over the world, but the damage was mild compared to three major pandemics. In April 2009, an influenza A H1N1 virus was first identified in Mexico and the United States. Since the population had no immunity against the new virus, it spread quickly in almost every area throughout the country within 4 - 6 weeks. World Health Organization (WHO) has declared a flu pandemic on June 11, 2009, and it reported about 30,000 cases of infection in 74 countries. Over 300 thousand infected cases in 135 countries were reported as of September 20, 2009. The Centers for Disease Control and Prevention (CDC) reported that the 2009 H1N1 pandemic influenza is back and the 2013–2014 influenza season is ongoing worldwide.

In South Korea, the first infection was a woman returning from Mexico on May 2, 2009. As of July 24, more than one thousand cases were detected and no death was reported. As of March 31, 2010, 260 deaths were reported. The Korea Centers for Disease Control and Prevention (KCDC) issued the alert of the epidemic influenza on January, 2, 2014. Fortunately, the vaccine for 2013-2014 flu season included the 2009 H1N1 influenza vaccine since then. thus, it is not considered as a severe pandemic. However, the pandemic influenza has the unpredictable occurrence and severity while frequently appearing on average of every 10 to 40 years. It is necessary to prepare control strategies to prevent the spread of disease and socio-economic crisis.

Dengue Fever

Dengue fever is a mosquito-borne viral disease transmitted by the bite of female *Aedes* mosquitoes. Dengue is endemic in more than 100 countries of Africa, America, Asia and the Western Pacific with tropical climates. Dengue is a major international public health concern with more than 55% of the world population at risk in recent decades. Dengue has four serotypes denoted by DENV1-4. The dengue fever caused by one serotype has non-fatal symptoms such as high fevers, headache, muscle ache, and joint pain. The primary infection only provides the life-long immunity to that serotype but short-term partial immunity against other serotypes.

Moreover, the antibody dependent enhancement (ADE) occurs when the pre-existing antibodies generated by the previous dengue infection enhances the replication of the secondary serotype. Due to the ADE, secondary heterologous infections can develop into sever diseases such as dengue hemorrhagic fever (DHF) and dengue shock syndrome (DSS). Fig.1-1 given by CDC [21] shows the life cycle of mosquitoes which is composed of four stages including egg, larvae, pupae, and adult stage. Climate change has indirect impact on the mosquito population such as the infection rate and incubation period [22]. Currently, there are no antiviral drugs or effective vaccines against all serotypes of dengue virus.

The mathematical models with multi-strain have been developed to study the life-threatening transmission process of dengue virus in the absence of seasonality [23, 24, 25]. The SEIR model with all four strains has been studied considering the seasonal population dynamics of mosquitoes [26]. It is reported that dengue incidence in Thailand, Taiwan, Singapore, Brazil have been associated with seasonal patterns [26, 27, 28, 29]. The seasonal patterns, including temperature, relative humidity, and rainfall, play a significant role in the dengue transmission in terms of statistical approaches [30, 22]. The dengue transmission model incorporates the temperature dependent entomological parameters, including the effect of temperature on the population of *Aedes* mosquitoes [27, 31]. The temperature dependent parameters have been obtained from the laboratory data which remains in the range from $10°C$ to $37°C$ in [32, 33].

In South Korea, 367 cases of dengue fever were reported during 2006–2010, and all infected people were travelers returning from the endemic countries [34]. Several studies describe that the risk of autochthonous dengue outbreaks grows as the number of the international travels to endemic areas increases [35, 36]. The SEIR type model with migration and immigration has been introduced [37, 38]. Since *Aedes* mosquitoes have been found in Jeju Island. Due to the effects of increased international travel and climate change, the potential risk of autochthonous dengue outbreaks in Jeju Island is greater than other regions of Korea.

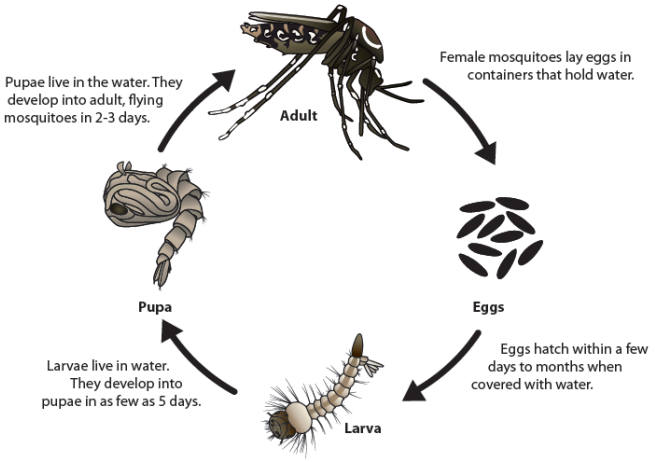

Figure 1-1: Life cycle of *Aedes* aegypti mosquitoes.

1.3 Summary of contents

In chapter 2, we introduce deterministic compartment models such as SEIR model and Suceptible-Latent-Symptomatic Infectious-Asymptomatic Infectious-Recovery (SLIAR) model. First, we consider the extension of SLIAR model by adding the treatment compartments. Second, we explain the calculation of the basic reproduction number and final size relation for the treatment model. Finally, we describe the stochastic modeling of the epidemic models and computational methods such as SSA and MCM.

In chapter 3, we consider the simple model of the enzyme-substrate reaction system to solve the stochastic system analytically. We describe an explicit representation of the solution of stochastic model in terms of the eigenvalues and eigenvectors of block matrices. This approach reduces the computational cost. We carry out numerical simulations to investigate the accuracy and efficiency of the method.

In chapter 4 and chapter 5, we apply stochastic methods for computation to disease transmission models. In chapter 4, we present stochastic models by applying government's countermeasures to prevent the 2009 H1N1 influenza transmission dynamics in Korea. We apply the MCM into the model to find the stochastic solutions for a large population. Moreover, the deterministic solution is compared with the mean of stochastic model. As a result, the discrepancy between the two solutions is observed, when the number of initial infectives is small. We investigate the effect of control scenarios such as vaccination and antiviral treatment on the dynamics of infectives. As a result, earlier vaccination was more effective than increasing antiviral treatment.

In chapter 5, we formulate the two-strain dengue fever transmission model with seasonality. We investigate the effect of international travel on the dengue outbreak in Jeju Island in Korea. We incorporate the inflow factor corresponding to imported dengue cases. We explore how the climate change and international travel influence on dengue transmission dynamics in Jeju Island of Korea in terms of seasonal reproduction number and the annual peak size. Moreover, we compare the dynamics of dengue incidence between the stochastic model and the deterministic model depending on the size of infected individuals initially.

2

Mathematical Modeling

2.1 Deterministic modeling

2.1.1 SEIR type model

In this section, we introduce an expended form of SIR model such as the SEIR model and SLIAR model described in [39]. The SEIR model is an extended form obtained by adding the compartment E to the SIR model. The compartment E refers to the exposed individuals at time t. The compartment D represents the individuals who died of the disease. Only susceptible individuals can get infected. After an infectious period, an infected individual proceed to either recover or die. Let $N(t) = S(t) + E(t) + I(t) + R(t)$ denote the total population size. This model neglects the natural birth and death. The dynamics of the SEIR model with death are written as

$$\begin{aligned} \frac{dS}{dt} &= -\beta(N)SI \\ \frac{dE}{dt} &= \beta(N)SI - \kappa E \\ \frac{dI}{dt} &= \kappa E - \alpha I \\ \frac{dR}{dt} &= f\alpha I, \\ \frac{dD}{dt} &= (1-f)\alpha I, \end{aligned} \tag{2.1.1}$$

$\beta(N)$ is the transmission rate for contacts with infected individuals. Susceptible individual makes $\beta(N)N$ contacts with anyone per unit time and the probability of the contact with an infective is I/N, then the rate of new infections per susceptible is $\beta(N)N(I/N) = \beta I$, where a rate of new infections $\beta(N)N(I/N)S = \beta SI$. We define $\beta_0 = \beta(N)N$ as the average number of population who make contacts. For simplicity, β is used instead of $\beta(N)$. i.e., $\beta_0 = \beta N$. $1/\kappa$ is the latent period and $1/\alpha$ is the infectious period. $(1-f)$ is the fatality

rate of infectives. The basic reproduction number, R_0 is defined by the number of secondary infections produced by a single infected individual. The initial conditions are $S(0) = S_0, I(0) = I_0, E(0) = R(0) = 0, N(0) = S_0 + I_0$. The system (2.1.1) has a disease−free equilibrium with (S, E, I, R)=$(S_0, 0, 0, 0)$. The basic reproduction number R_0 is derived by using next generation method [40].

$$R_0 = \frac{\beta S_0}{\alpha}$$

There were approximately 33% asymptomatic infectives among people with influenza. Infectious people are divided into symptomatic and asymptomatic infectious individuals to account for the significant people who are infectious but never show symptoms. The SLIAR model in Fig.2-1 consists of five compartments which are susceptible (S), latent (L), infectious and symptomatic (I), asymptomatic but infectious (A), and recovered (R). The dynamics of the SLIAR model with death is described by the following set of ODEs [41, 42].

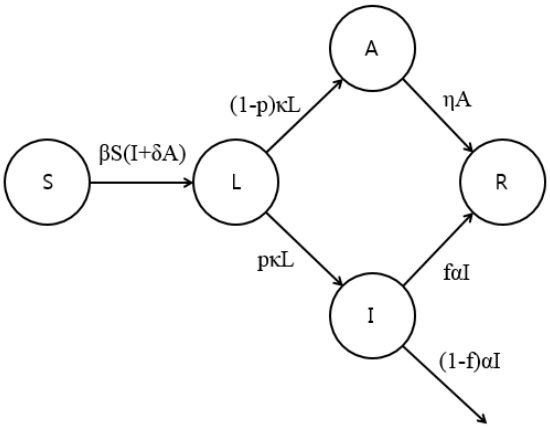

Figure 2-1: SLIAR model

$$\begin{aligned}
\frac{dS}{dt} &= -\beta S(I + \delta A) \\
\frac{dL}{dt} &= \beta S(I + \delta A) - (1-p)\kappa L - p\kappa L \\
\frac{dI}{dt} &= p\kappa L - f\alpha I - (1-f)\alpha I \\
\frac{dA}{dt} &= (1-p)\kappa L - \eta A \\
\frac{dR}{dt} &= f\alpha I + \eta A \\
\frac{dD}{dt} &= (1-f)\alpha I.
\end{aligned} \tag{2.1.2}$$

Here, a fraction δ represents the reduced transmissibility of the asymptomatic infectives. A fraction p of latent individuals who show a symptom moves to compartment I. The rest

$(1-p)$ proceeds to the compartment A. $1/\kappa$ is the latent period. The parameters $1/\alpha$ and $1/\eta$ indicate the infectious period of I and A, respectively. The fraction $(1-f)$ is fatality rate of symptomatic infectives, I. The initial conditions are $S(0) = S_0, I(0) = I_0, L(0) = A(0) = R(0) = 0, N(0) = S_0 + I_0$. The system (2.1.2) has a disease−free equilibrium with (S, L, I, A, R)=$(S_0, 0, 0, 0, 0)$. The basic reproduction number R_0 is given by

$$R_0 = \beta S_0 \left[\frac{p}{\alpha} + \frac{\delta(1-p)}{\eta} \right]$$

2.1.2 SLIAR with treatment model without vaccination during the epidemic

The SLIAR model is extended to the SLIAR with treatment model by adding the treatment compartments based on [42]. This model in Fig.2-2 includes the control parameters such as vaccination before the epidemic and antiviral treatment during the epidemic. ϕ_I and ϕ_A represent a fraction of the antiviral treatment that that have reduced infectivity for I and A, respectively. In this section, there are two modifications on the previous model for simplicity:

1) To focus on the dynamics of short-time scale, it does not occur the relapses from treatment compartments of I_T, A_T to disease compartments of I, A, respectively.

2) It seldom occurs for the people in latent class to receive the treatment, i.e, we do not consider ϕ_L by letting $\phi_L = 0$.

$S_T(t), L_T(t), I_T(t)$ and $A_T(t)$ are defined as the number of individuals in the treated susceptible (or vaccinated susceptible), treated latent, treated symptomatic infectious, and treated asymptomatic infectious compartments, respectively. The fraction m is the rate of pre-epidemic vaccination with $S(0) = (1-m)S_0 > 0, S_T(0) = mS_0$. Treatment compartments have the factors σ_I, σ_A that reduce the infectivity for I_T and A_T, respectively. The parameters $1/\kappa_T$,$1/\alpha_T$ and $1/\eta_T$ denote the latent period in L_T and the infectious periods of I_T and A_T, respectively A factor σ_S represents the effect on reducing the susceptibility through the vaccination. As the σ_S is closer to 1, the vaccination has less effect for susceptible individuals. The fraction $p\tau$ of L_T is developed into symptomatic infectious I_T. A fraction q reduces the contact rate for people who show a symptom. The fraction $(1-f)$ and $(1-f_T)$ are fatality rates of I and I_T, respectively.

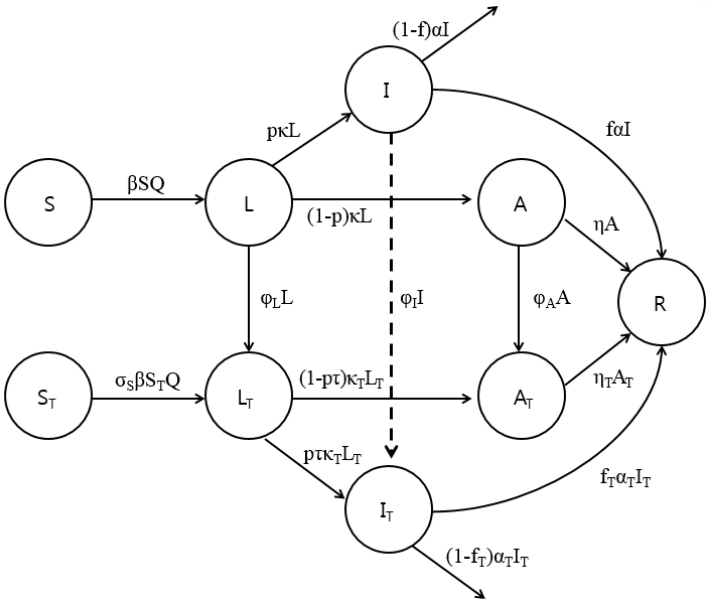

Figure 2-2: SLIAR with treatment model without vaccination during the epidemic.

The ODEs can be written as

$$
\begin{aligned}
\frac{dS}{dt} &= -\beta SQ && (2.1.3)\\
\frac{dS_T}{dt} &= -\sigma_s \beta S_T Q - \mu S_T && (2.1.4)\\
\frac{dL}{dt} &= \beta SQ - \kappa L \\
\frac{dL_T}{dt} &= \sigma_s \beta S_T Q - \kappa_T L_T \\
\frac{dI}{dt} &= p\kappa L - \alpha I - \phi_I I \\
\frac{dI_T}{dt} &= p\tau\kappa_T L_T - \alpha_T I_T + \phi_I I && (2.1.5)\\
\frac{dA}{dt} &= (1-p)\kappa L - \eta A - \phi_A A \\
\frac{dA_T}{dt} &= (1-p\tau)\kappa_T L_T - \eta_T A_T + \phi_A A \\
\frac{dR}{dt} &= f\alpha I + f_T\alpha_T I_T + \eta A + \eta_T A_T \\
\frac{dD}{dt} &= (1-f)\alpha I + (1-f_T)\alpha_T I_T \\
Q &= (1-q)I + (1-q)\sigma_I I_T + \delta A + \delta\sigma_A A_T,
\end{aligned}
$$

where $S(0) = (1-m)S_0 > 0, S_T(0) = mS_0, I(0) = I_0 > 0, L(0) = L_T(0) = A(0) = A_T(0) = I_T(0) = R(0) = D(0) = 0$.

2.1.3 Basic reproduction number

The next generation method is general approach to derive the reproduction number. We summarize the procedure to find the next generation matrix described in [40]. We sort individuals into either the disease compartment or non-disease compartment. Suppose that there are m non-disease compartment and n disease compartments including infected and not necessarily infectious individuals.

$$\begin{cases} x_i' = \mathcal{F}_i(x,y) - \mathcal{V}_i(x,y) & i = 1, ...n \\ y_j' = g_j(x,y) & j = 1, \ldots, m \end{cases} \tag{2.1.6}$$

x represents the subpopulations of infected compartments, y represents the subpopulations of susceptible compartments. $\mathcal{F}_i$ is the new infection rate in i^{th} disease compartment and cannot be negative. $\mathcal{V}_i$ is the transition rate from disease compartment i. Let $\mathcal{V}_i = \mathcal{V}_i^- - \mathcal{V}_i^+$ where $\mathcal{V}_i^+$ is the inflow rate into the i^{th} compartment and $\mathcal{V}_i^-$ is the outflow rate out of the i^{th} compartment [43, 44].

The n $\times$ n matrices F, V are defined by

$$F = \left[\frac{\partial \mathcal{F}_i}{\partial x_j}(0, y_0)\right], \quad V = \left[\frac{\partial \mathcal{V}_i}{\partial x_j}(0, y_0)\right]$$

where $(0, y_0)$ is the disease$-$free equilibrium. F(i, j) is the new infection rate in i^{th} compartment by infected one of j^{th} compartment. (i, j) entry of V^{-1} is the expected time of spending in compartment i after being introduced into j^{th} compartment. FV^{-1} matrix represents as the next generation matrix at the disease-free equilibrium. (i, j) entry of FV^{-1} is the average number of secondary infections in i^{th} compartment by individual which firstly transmitted in j^{th} compartment. The reproduction number is defined as spectral radius of next generation matrix.

$$R_0 = \rho(FV^{-1})$$

The disease-free equilibrium is locally asymptotically stable if $R_0 < 1$. It indicates that the number of infectives decreases monotonically to zero and disease disappears. Whereas, if $R_0 > 1$, the endemic equilibrium is locally asymptotically stable and this is an epidemic. In the system (2.1.5), the corresponding reproduction number yields to the control reproduction number. The control reproduction number R_c is defined as the reproduction number with the control measures. Here, we derive the control reproduction number R_c for the system (2.1.5). It has the disease-free equilibrium $x_0 = (S_0, S_{T0}, 0, 0, 0, 0, 0, 0)$. Let X$= (L, L_T, I, I_T, A, A_T, S, S_T)$,

the model (2.1.5) can be written as $X' = \mathcal{F}(X) - \mathcal{V}(X)$, where

$$\mathcal{F}(X) = \begin{pmatrix} \beta SQ \\ \sigma_s \beta S_T Q \\ 0 \\ 0 \\ 0 \\ 0 \end{pmatrix}, \mathcal{V}(X) = \begin{pmatrix} \kappa L \\ \kappa_T L_T \\ -p\kappa L + (\alpha + \phi_I) I \\ -p\tau\kappa_T L_T - \phi_I I + \alpha_T I_T \\ -(1-p)\kappa L + (\eta + \phi_A) A \\ -(1-p\tau)\kappa_T L_T - \phi_A A + \eta_T A_T \end{pmatrix}.$$

The Jacobian matrices of F and V are $6\times$ 6 matrices given by

$$\mathbf{F} = \begin{pmatrix} 0 & 0 & \beta(1-m)S_0(1-q) & \beta(1-m)S_0(1-q)\sigma_I & \beta(1-m)S_0\delta & \beta(1-m)S_0\delta\sigma_A \\ 0 & 0 & \sigma_s\beta m S_0(1-q) & \sigma_s\beta m S_0(1-q)\sigma_I & \sigma_s\beta m S_0\delta & \sigma_s\beta m S_0\delta\sigma_A \\ 0 & 0 & 0 & 0 & 0 & 0 \\ 0 & 0 & 0 & 0 & 0 & 0 \\ 0 & 0 & 0 & 0 & 0 & 0 \\ 0 & 0 & 0 & 0 & 0 & 0 \end{pmatrix},$$

$$\mathbf{V} = \begin{pmatrix} \kappa & 0 & 0 & 0 & 0 & 0 \\ 0 & \kappa_T & 0 & 0 & 0 & 0 \\ -p\kappa & 0 & \alpha + \phi_I & 0 & 0 & 0 \\ 0 & -p\tau\kappa_T & -\phi_I & \alpha_T & 0 & 0 \\ -(1-p)\kappa & 0 & 0 & 0 & \eta + \phi_A & 0 \\ 0 & -(1-p\tau)\kappa_T & 0 & 0 & -\phi_A & \eta_T \end{pmatrix}$$

The inverse of the matrix V is given by

$$\mathbf{V^{-1}} = \begin{pmatrix} \frac{1}{\kappa} & 0 & 0 & 0 & 0 & 0 \\ 0 & \frac{1}{\kappa_T} & 0 & 0 & 0 & 0 \\ \frac{p}{\alpha+\phi_I} & 0 & \frac{1}{\alpha+\phi_I} & 0 & 0 & 0 \\ \frac{p\phi_I}{\alpha_T(\alpha+\phi_I)} & \frac{p\tau}{\alpha_T} & \frac{\phi_I}{\alpha_T(\alpha+\phi_I)} & \frac{1}{\alpha_T} & 0 & 0 \\ \frac{(1-p)}{\eta+\phi_A} & 0 & 0 & 0 & \frac{1}{\eta+\phi_A} & 0 \\ \frac{(1-p)\phi_A}{\eta_T(\eta+\phi_A)} & \frac{1-p\tau}{\eta_T} & 0 & 0 & \frac{\phi_A}{\eta_T(\eta+\phi_A)} & \frac{1}{\eta_T} \end{pmatrix}$$

Especially, since the matrix F has rank 1, the spectral radius of FV^{-1} is equal to the trace of FV^{-1} [45]. Therefore, the control reproduction number R_c for the system (2-2) is presented in [1] as follows;

$$
\begin{aligned}
R_c &= \varrho(FV^{-1}) \\
&= \beta S_0 \left[\frac{(1-q)p}{(\alpha+\phi_I)} + \frac{(1-q)\sigma_I p\phi_I}{\alpha_T(\alpha+\phi_I)} + \frac{\delta(1-p)}{(\eta+\phi_A)} + \frac{\delta\sigma_A\phi_A(1-p)}{\eta_T(\eta+\phi_A)} \right] \\
&+ \sigma_s\beta S_{T0} \left[\frac{(1-q)\sigma_I p\tau}{\alpha_T} + \frac{\delta\sigma_A(1-p\tau)}{\eta_T} \right].
\end{aligned}
$$

The control reproduction number R_c is rewritten by

$$R_c = (1-m)R_u + mR_v$$

where m is the fraction of vaccinated susceptible before infection and R_u, R_v are defined by.

$$
\begin{aligned}
R_u &= \beta S_0 \left[\frac{(1-q)p}{(\alpha+\phi_I)} + \frac{(1-q)\sigma_I p\phi_I}{\alpha_T(\alpha+\phi_I)} + \frac{\delta(1-p)}{(\eta+\phi_A)} + \frac{\delta\sigma_A\phi_A(1-p)}{\eta_T(\eta+\phi_A)} \right] \\
R_v &= \sigma_s\beta S_0 \left[\frac{(1-q)\sigma_I p\tau}{\alpha_T} + \frac{\delta\sigma_A(1-p\tau)}{\eta_T} \right]
\end{aligned}
$$

In addition, the basic reproduction number R_0 is equal to the control reproduction number R_c with $\phi_A = \phi_I = m = 0$.

2.1.4 Final size relation

The final size is the number of individuals that remain in each non−disease compartment during the epidemic. We investigate a relation between the control reproduction number and the final size. We introduce the notations for non−negative continuous function $f(t)$.

$$f_\infty = \lim_{t\to\infty} f(t), \quad \hat{f} = \int_0^\infty f(t)dt$$

For given $n = 6$ of disease compartment and $m = 2$ of non-disease compartment, the system (2-2) is expressed as

$$
\begin{aligned}
x &= [L\ L_T\ I\ I_T\ A\ A_T]^T := [x_L\ x_I\ x_A]^T \\
y &= [S\ \ S_T]^T \\
x(0) &= [0\ 0\ \ I_0\ 0\ 0\ 0]^T \\
y(0) &= [(1-m)S_0\ \ mS_0]^T
\end{aligned}
$$

where x_L, x_I, x_A are 2×1 block matrices. We replace ODE systems with vector systems to linearize the treatment model described in [42, 45].

$$\begin{aligned} x' &= \beta \Pi D y b x - V x, \\ y' &= -\beta D y b x \end{aligned} \tag{2.1.7}$$

where

$$D = \begin{bmatrix} 1 & 0 \\ 0 & \sigma_S \end{bmatrix}, \qquad \mathbf{\Pi} = \begin{bmatrix} 1 & 0 \\ 0 & 1 \\ 0 & 0 \\ 0 & 0 \\ 0 & 0 \\ 0 & 0 \end{bmatrix}, \qquad b = \begin{bmatrix} 0 & 0 & (1-q) & (1-q)\sigma_I & \delta & \delta\sigma_A \end{bmatrix}$$

The matrix V can be rewritten in terms of block matrices by

$$\mathbf{V} = \begin{pmatrix} V_L & 0 & 0 \\ -V_{LI} & V_I & 0 \\ -V_{LA} & 0 & V_A \end{pmatrix}$$

One can find the inverse of V as follows;

$$\mathbf{V^{-1}} = \begin{pmatrix} V_L^{-1} & 0 & 0 \\ V_I^{-1} V_{LI} V_L^{-1} & V_I^{-1} & 0 \\ V_A^{-1} V_{LA} V_L^{-1} & 0 & V_A^{-1} \end{pmatrix}$$

It can be derived from (2.1.3) in the system (2-2) as follows;

$$\begin{aligned} \int_0^\infty \frac{S'(t)}{S(t)} dt &= -\int_0^\infty \beta Q \\ \ln \frac{S(0)}{S_\infty} &= \beta \int_0^\infty Q \\ &= \beta b \hat{x} \\ &= \beta \left[(1-q)\hat{I} + (1-q)\sigma_I \hat{I_T} + \delta \hat{A} + \delta \sigma_A \hat{A_T} \right] \end{aligned} \tag{2.1.8}$$

$S_{T\infty}$ obtained from (2.1.4) is as follows.

$$\begin{aligned} ln\frac{S_T(0)}{S_{T\infty}} &= \sigma_S \beta b \hat{x} \\ &= \sigma_S \ \ln\frac{S(0)}{S_\infty} \\ S_{T\infty} &= S_T(0)\left(\frac{S_\infty}{S(0)}\right)^{\sigma_S} \end{aligned} \tag{2.1.9}$$

The system (2.1.7) is expressed as

$$\begin{aligned} x' + \Pi y' &= -Vx \\ \int_0^\infty (x' + \Pi y')dt &= \int_0^\infty -Vxdt \\ x_\infty - x(0) + \Pi(y_\infty - y(0)) &= -V\hat{x} \end{aligned}$$

Since x_∞=0 and V is non−singular matrix [44],

$$\begin{aligned} V\hat{x} &= x(0) + \Pi(y(0) - y_\infty) \\ \hat{x} &= V^{-1}x(0) + V^{-1}\Pi(y(0) - y_\infty) \\ &= V^{-1}(x(0) + \Pi(y(0) - y_\infty)) \end{aligned}$$

We put the matrix V^{-1} into the block form

$$\mathbf{V^{-1}} = \begin{pmatrix} W_L & 0 & 0 \\ W_{LI} & W_I & 0 \\ W_{LA} & 0 & W_A \end{pmatrix}$$

where $W_L, W_{LI}, W_I, W_{LA}, W_A$ are 2×2 block matrices. Then, the components of $\hat{x}$ can be written by

$$\hat{x} = \begin{bmatrix} x_L \\ x_I \\ x_A \end{bmatrix} = \begin{bmatrix} W_L & 0 & 0 \\ W_{LI} & W_I & 0 \\ W_{LA} & 0 & W_A \end{bmatrix} \begin{bmatrix} y(0) - y_\infty \\ M \\ 0 \end{bmatrix}$$

where M=$[I_0 \ \ 0]^T$. The components of $\hat{x}_I, \hat{x}_A$ are expressed as

$$\begin{aligned} \hat{x}_I &= W_{LI}\,(y(0) - y_\infty) + W_I M \\ \hat{x}_A &= W_{LA}\,(y(0) - y_\infty) \end{aligned}$$

where

$$\hat{x}_I = \begin{bmatrix} \hat{I} \\ \hat{I}_T \end{bmatrix} = W_{LI}(y(0) - y_\infty) + W_I \begin{bmatrix} I_0 \\ 0 \end{bmatrix}$$
$$= \begin{bmatrix} \dfrac{I_0}{(\alpha+\phi_I)} + \frac{p}{(\alpha+\phi_I)}(S(0) - S_\infty) \\ \dfrac{\phi_I I_0}{\alpha_T(\alpha+\phi_I)} + \dfrac{p\phi_I}{\alpha_T(\alpha+\phi_I)}(S(0) - S_\infty) + \dfrac{p\tau}{\alpha_T}(S_T(0) - S_{T\infty}) \end{bmatrix}$$

$$\hat{x}_A = \begin{bmatrix} \hat{A} \\ \hat{A}_T \end{bmatrix} = W_{LA}(y(0) - y_\infty)$$
$$= \begin{bmatrix} \dfrac{(1-p)}{(\eta+\phi_A)}(S(0) - S_\infty) \\ \dfrac{(1-p)\phi_A}{\eta_T(\eta+\phi_A)}(S(0) - S_\infty) + \dfrac{(1-p\tau)}{\eta_T}(S_T(0) - S_{T\infty}) \end{bmatrix}$$

The final size relation (2.1.10) given by (2.1.8) is

$$ln\frac{S(0)}{S_\infty} = (1-m)R_u\left(1 - \frac{S_\infty}{S(0)}\right) + \frac{m}{\sigma_S}R_v\left(1 - \frac{S_{T\infty}}{S_T(0)}\right) + \frac{\beta(1-q)I_0}{S_0(\alpha+\phi_I)} + \frac{\beta(1-q)\sigma_I\phi_I I_0}{S_0\alpha_T(\alpha+\phi_I)} \tag{2.1.10}$$

2.2 Stochastic modeling

The deterministic model is useful because it is easier to build and understand the outcomes than the stochastic model when the randomness or uncertainty is not important system. However, for the non-linear system, deterministic solution is not always equal to the mean of stochastic model. Fig.2-3 compares the deterministic solution with the results from stochastic model for the SLIAR model (2.1.2). Fig.2-3 (a) shows the deterministic solution and trajectories of stochastic model. One of the main reasons for the different trajectories is that the stochastic model involves the intrinsic fluctuation or randomness. The deterministic solutions do not correctly provide the approximation if the system involve the stochastic properties as an important role in the reaction events. Fig.2-3 (b) compares the deterministic solution with the mean as well as standard deviation of the stochastic model. The stochastic results are obtained by 10,000 realizations of the SSA. The time-evolution of two solutions is qualitatively similar, but there exists somewhat difference at the peak.

2.2.1 Stochastic master equation

We briefly describe the stochastic master equations described in [46, 47]. We consider a well-stirred mixture of s distinct compartments and r reactions $(R_1, \cdots, R_r)$. The number of

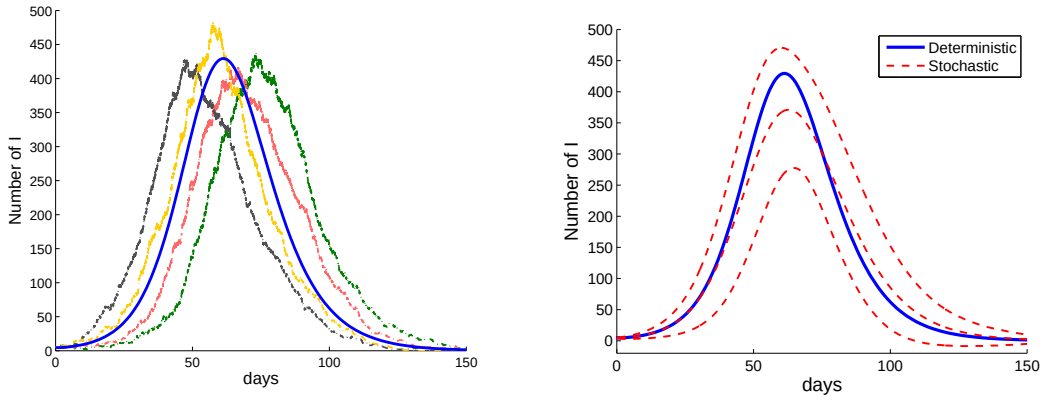

(a) (b)

Figure 2-3: Deterministic and Stochastic SLIAR models; (a) deterministic solution (blue solid) and stochastic realizations (black, red, green, yellow dashed) are displayed. (b) deterministic solution (blue solid) and the mean+standard deviation (upper red dashed), mean (middle red dashed), mean−standard deviation (lower red dashed) of the stochastic model are displayed. Initial conditions are $S(0) = 5000, I(0) = 5$, others are zero. Parameters are $p = 0.67, \delta = 0.5, \alpha = \eta = 1/7, \kappa = 1/1.4, f = 0.999$ and $\beta_0 = 0.3422$ (R_0=2.0). This results are shown in [1].

population is denoted by $\mathbf{X}(t) = (X_1(t), \cdots, X_s(t))$, where $X_i(t) \equiv$ the number of individuals in the i^{th} compartment at time t for $i = 1, \cdots, s$. For each reaction R_j, an a_j is referred to as the propensity function. The state-change vector v_j, which is j^{th} column of the stoichiometric matrix V is defined by the change in the number of individuals by the j^{th} reaction. v_{ij} is an (i, j) element of the matrix V. The propensity function a_j, given $\mathbf{X} = \mathbf{x}$, is well-defined by the law of mass action.

$$a_j(\mathbf{x}) = c_j h_j(\mathbf{x}),$$

where c_j is the probability rate constant. Then, $c_j\,\Delta t$ is the probability that a randomly chosen pair of j^{th} reaction reactant individuals will react during the time interval $(t, t + \Delta t)$. $h_j(\mathbf{x})$ is the number of distinct combinations of the j^{th} reaction reactant individuals in state $\mathbf{x}$. Thus, $a_j(\mathbf{x})dt$ is the probability that one R_j reaction will occur at the state $\mathbf{x}$ in the next time interval $[t, t + dt)$.

If $p(\mathbf{x}, t)$ denotes the probability that the number of population of compartments is $\mathbf{x}$ at time t, the probability of being in state $\mathbf{x}$ at the infinitesimal time $t + dt$ is described as

$$p(\mathbf{x}, t + dt) = \left(1 - \sum_{k=1}^{n} a_k(\mathbf{x})\right) p(\mathbf{x}, t) + \sum_{k=1}^{n} a_k(\mathbf{x} - V_k)dtp(\mathbf{x} - V_k, t) + o(dt) \quad (2.2.1)$$

Letting $dt \to 0$, then, the probability $p(\mathbf{x}, t)$ of $\mathbf{x}$ state at time t is given by the master equation

$$\frac{dp(\mathbf{x}, t)}{dt} = \sum_{k=1}^{n} [a_k(\mathbf{x} - V_k)p(\mathbf{x} - V_k, t) - a_k(\mathbf{x})p(\mathbf{x}, t)] \quad (2.2.2)$$

Considering over all possible states of $\mathbf{x}$, the governing equation (2.2.2) is written as the linear form

$$\frac{d\mathbf{p}}{dt} = K\mathbf{p}(t), \tag{2.2.3}$$

where $\mathbf{p}(t)$ is a column vector where $p_i(t)$ indicates the probability at i^{th} state at time t. The matrix K is the Markov chain generator that is determined by the transition rates among possible states. The solution of the system (2.2.3) is

$$\mathbf{p}(t) = e^{Kt}\mathbf{p}(0) \tag{2.2.4}$$

For example, stochastic form of the SEIR model (2.1.1) is described in Table 2-1.

Event	Process	Transition rate
Susceptible people infection	$S \to E$	βSI
Exposed people becoming infectious	$E \to I$	κE
Recovery of infectious people	$I \to R$	$f\alpha I$
Death of infectious people	$I \to D$	$(1-f)\alpha I$

Table 2-1: Event type and process and transition rate for SEIR model.

If we denote the number of susceptible (S), exposed (E), infectious (I), recovered (R) and dead (D) at time t by $\mathbf{x}(t) = (x_1(t), x_2(t), x_3(t), x_4(t), x_5(t))$, respectively, the stochastic governing equation of the model is given by

$$\begin{aligned}
&\frac{dp(x_1, x_2, x_3, x_4, x_5, t)}{dt} \\
= \;& c_1(x_1+1)x_3 p(x_1+1, x_2-1, x_3, x_4, x_5, t) \\
&+c_2(x_2+1)p(x_1, x_2+1, x_3-1, x_4, x_5, t) \\
&+c_3(x_3+1)p(x_1, x_2, x_3+1, x_4-1, x_5, t) \\
&+c_4(x_3+1)p(x_1, x_2, x_3+1, x_4, x_5-1, t) \\
&-(c_1x_1x_3 + c_2x_2 + c_3x_3 + c_4x_3)p(x_1, x_2, x_3, x_4, x_5, t).
\end{aligned}$$

where $c_1 = \beta, c_2 = \kappa, c_3 = f\alpha, c_4 = (1-f)\alpha$.

2.2.2 Stochastic simulation algorithm (SSA)

If the system has non-linear term or the high dimensionality, computational method is practical rather than solving the governing equation (2.2.2) as well as (2.2.3). The stochastic simulation algorithm (SSA) is well known as the exact stochastic algorithm [48]. The SSA computes the trajectories to solve indirectly the governing equation through the Monte-Carlo procedure. The

SSA is simply summarized. First, we set initial condition $\mathbf{x}(0) = \mathbf{x}_0$ and t=0, then we compute next three steps at time t;

Computational Procedure

Step 1. Calculate the propensity function $a_k(\mathbf{x})$ for each k^{th} reaction and $a_0 = \sum_{k=1}^{n} a_k(\mathbf{x})$
Step 2. Generate two random numbers r_1, r_2 from the uniform distributed in the interval $(0, 1)$. Set $\tau = -\frac{\log(r_1)}{a_0}$ and choose the next reaction index j such that $\sum_{k=1}^{j-1} a_k(\mathbf{x}) < r_2 a_0 \leq \sum_{k=1}^{j} a_k(\mathbf{x})$.
Step 3. Compute the number of individuals at time $t + \tau$.

Update the state vector and time as follows; $\mathbf{x} + V_j \to \mathbf{x}$, $t + \tau \to t$.

Steps 1-3 are repeated unless the time reaches the final time or there are no reactants in the system.

2.2.3 Moment closure method (MCM)

The SSA computes a single realization based on Markov property rather than the probability distribution. If the system has large population size or fast reactions, SSA requires the intensive computational cost. One of computational methods resolving this problem is the moment closure method (MCM). The MCM obtains the approximations of moment without Monte Carlo procedure. Here, we briefly summarize the way of MCM described rigorously in [20]. In section 2.1, SEIR type models have a second-order reaction, so that the function a_k is at most quadratic. If the system has the higher order of reaction, it can be explained as a consecutive reaction of second-order reaction. Now, we describe the formulation of recursive moment equations up to second order. The first moment for i^{th} compartment is denoted by $\mu_i = E[x_i]$ and the second and third central moment for i^{th} compartment is denoted by $\sigma_{i,j} = E[(x_i - \mu_i)(x_j - \mu_j)]$ and $\sigma_{i,j,k} = E[(x_i - \mu_i)(x_j - \mu_j)(x_k - \mu_k)]$, respectively.

First, one can derive ODE equations for the first moments (2.2.5) and second central moments (2.2.6) from the master equation (2.2.2) by using Taylor expansion for propensity functions $a_k(\mathbf{x})$ as follow.

$$\frac{d\mu_i}{dt} = \sum_k v_{ik}\Big(a_k(\mu) + \frac{1}{2}\sum_{l,m}\frac{\partial^2 a_k(\mu)}{\partial x_l \partial x_m}\sigma_{l,m}\Big) \tag{2.2.5}$$

$$\begin{aligned}\frac{d\sigma_{i,j}}{dt} = &\sum_k \Big[v_{ik}\sum_\ell \frac{\partial a_k(\mu)}{\partial x_\ell}\sigma_{j,\ell} + v_{jk}\sum_\ell \frac{\partial a_k(\mu)}{\partial x_\ell}\sigma_{i,\ell} \\ &+ v_{ik}v_{jk}\big(a_k(\mu) + \frac{1}{2}\sum_{\ell,m}\frac{\partial^2 a_k(\mu)}{\partial x_\ell \partial x_m}\sigma_{\ell,m}\big) + v_{ik}\frac{1}{2}\sum_{\ell,m}\frac{\partial^2 a_k(\mu)}{\partial x_\ell \partial x_m}\sigma_{j,\ell,m} \\ &+ v_{jk}\frac{1}{2}\sum_{\ell,m}\frac{\partial^2 a_k(\mu)}{\partial x_\ell \partial x_m}\sigma_{i,\ell,m}\Big],\end{aligned} \tag{2.2.6}$$

One can realize the moment equations include the higher-order moment term. Thus, the system of the moment equations (2.2.5), (2.2.6) is infinite dimensional, that is, the system is not closed. Therefore, the exact solution is rarely found. However, the third central moments become zero under the assumption of mutivariate normal distribution when there are sufficiently large population in the system [20, 49].

Second, the higher order moments such as the third order moment are truncated to make moment equations closed. Then, we obtain the recursive moment equations obtained by the truncation at the third moment as follows;

$$\frac{d\mu_i}{dt} = \sum_k v_{ik}\Big(a_k(\mu) + \frac{1}{2}\sum_{l,m}\frac{\partial^2 a_k(\mu)}{\partial x_l \partial x_m}\sigma_{l,m}\Big) \tag{2.2.7}$$

$$\begin{aligned}\frac{d\sigma_{i,j}}{dt} = \sum_k \Big[& v_{ik}\sum_\ell \frac{\partial a_k(\mu)}{\partial x_\ell}\sigma_{j,\ell} + v_{jk}\sum_\ell \frac{\partial a_k(\mu)}{\partial x_\ell}\sigma_{i,\ell} \\ & + v_{ik}v_{jk}\big(a_k(\mu) + \frac{1}{2}\sum_{\ell,m}\frac{\partial^2 a_k(\mu)}{\partial x_\ell \partial x_m}\sigma_{\ell,m}\big)\Big].\end{aligned} \tag{2.2.8}$$

Thus, infinite dimensional system of (2.2.5), (2.2.6) is changed to a finite dimensional system of (2.2.7), (2.2.8). As the same way, one can evaluate up to any number of moments with higher moments. In Lee [20], general n^{th} central moments are derived by letting the $(n+1)^{st}$ to be zero. Furthermore, this method guarantees numerical consistency.

As an example, we apply the system of moment equation (2.2.7) and (2.2.8) to the SEIR model with parameters from [50, 51]. For simplicity, the D compartment is removed since it is dependent variable. Fig.2-4 compares results obtained by SSA and MCM in terms of mean and standard deviation. The mean and standard deviation by SSA are almost same to the solution of the corresponding MCM. In terms of CPU time, the MCM takes about 0.5 seconds and the SSA takes more than 0.5 hours for 10000 realizations. The MCM has the good computational efficiency and its accuracy is good enough. Thus, we investigate the numerical results obtained by using the MCM to find the time-evolution solution of stochastic epidemic models instead of SSA in chapter 4 and chapter 5.

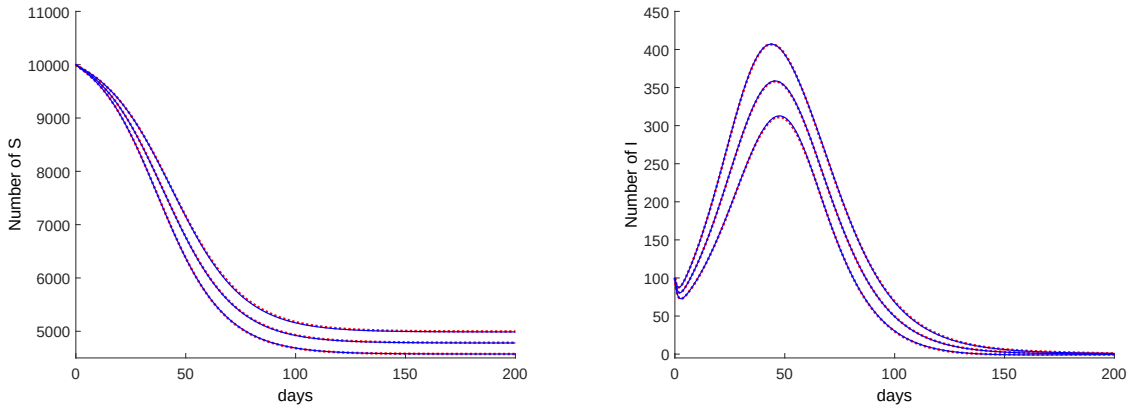

(a) (b)

Figure 2-4: Stochastic SEIR model; comparison of the results by SSA and MCM for (a) susceptible (S) and (b) infectious (I) varying time. The mean + standard deviation (upper curve), mean (middle curve) and mean − standard deviation (lower curve) by MCM (blue solid curves) and SSA (red dots) are displayed. The initial condition is $(S, E, I, R) = (10000, 0, 100, 0)$ and parameter values are $\kappa = 1/1.9, \alpha = 1/4.1,\ f = 0.98,\ \beta_0 = 0.3422$. This results are shown in [1].

The recursive moment equations of stochastic SEIR model are given by

$$
\begin{aligned}
\frac{d\mu_1}{dt} &= -c_1\mu_1\mu_3 - c_1\sigma_{1,3} \\
\frac{d\mu_2}{dt} &= -c_2\mu_2 + c_1\mu_1\mu_3 + c_1\sigma_{1,3} \\
\frac{d\mu_3}{dt} &= c_2\mu_2 - c_3\mu_3 - c_4\mu_3 \\
\frac{d\mu_4}{dt} &= c_3\mu_3 \\
\frac{d\sigma_{1,2}}{dt} &= -c_1\mu_1\mu_3 - c_2\sigma_{1,2} - c_1\mu_3\sigma_{1,2} - c_1\sigma_{1,3} + c_1\mu_1\sigma_{1,3} - c_1\mu_1\sigma_{2,3} + c_1\mu_3\sigma_{1,1} \\
\frac{d\sigma_{1,3}}{dt} &= c_2\sigma_{1,2} - c_3\sigma_{1,3} - c_4\sigma_{1,3} - c_1\mu_3\sigma_{1,3} - c_1\mu_1\sigma_{3,3} \\
\frac{d\sigma_{1,4}}{dt} &= -c_1\mu_1\sigma_{3,4} + c_3\sigma_{1,3} - c_1\mu_3\sigma_{1,4} \\
\frac{d\sigma_{2,3}}{dt} &= -c_2\mu_2 + c_1\mu_3\sigma_{1,3} - c_2\sigma_{2,3} - c_3\sigma_{2,3} - c_4\sigma_{2,3} + c_2\sigma_{2,2} + c_1\mu_1\sigma_{3,3} \\
\frac{d\sigma_{2,4}}{dt} &= c_1\mu_1\sigma_{3,4} + c_1\mu_3\sigma_{1,4} + c_3\sigma_{2,3} - c_2\sigma_{2,4} \\
\frac{d\sigma_{3,4}}{dt} &= -c_3\sigma_{3,4} - c_4\sigma_{3,4} + c_3\sigma_{3,3} - c_3\mu_3 + c_2\sigma_{2,4} \\
\frac{d\sigma_{1,1}}{dt} &= c_1\mu_1\mu_3 + c_1\sigma_{1,3} - 2c_1\mu_1\sigma_{1,3} - 2c_1\mu_3\sigma_{1,1} \\
\frac{d\sigma_{2,2}}{dt} &= c_2\mu_2 + c_1\mu_1\mu_3 + 2c_1\mu_3\sigma_{1,2} + c_1\sigma_{1,3} + 2c_1\mu_1\sigma_{2,3} - 2c_2\sigma_{2,2} \\
\frac{d\sigma_{3,3}}{dt} &= c_2\mu_2 + c_3\mu_3 + c_4\mu_3 + 2c_2\sigma_{2,3} - 2c_3\sigma_{3,3} - 2c_4\sigma_{3,3} \\
\frac{d\sigma_{4,4}}{dt} &= 2c_3\sigma_{3,4} + c_3\mu_3
\end{aligned}
$$

3

An Analytic Approach to a Stochastic Enzyme Kinetic Model*

We explicitly represent an analytic formula of the solution to the stochastic enzyme-substrate model with general initial conditions in terms of the block matrices of the Markov chain generator K.

3.1 Stochastic enzyme-substrate system

The stochastic models describe the time evolution of the probability of states. Here, we denote the number of molecules as $\mathbf{n}(t) = (n_1(t), n_2(t), \ldots, n_s(t))^T$ and each $n_i(t)$ denotes the number of molecules of i^{th} species at time t for $i = 1, \cdots, s$.

The time-dependent probability solution is given by the chemical master equation

$$\frac{\partial}{\partial t}p(\mathbf{n}, t) = \sum_{k=1}^{r} a_k(\mathbf{n} - V_k) \cdot p(\mathbf{n} - V_k, t) - \sum_{k} a_k(\mathbf{n}) \cdot p(\mathbf{n}, t), \tag{3.1.1}$$

where $p(\mathbf{n}, t)$ is the probability of the state $\mathbf{n}$ at time t, a_k is the propensity function for the k^{th} reaction, of $k = (1, 2, \cdots, r)$ and V_k is the k^{th} column vector of the stoichiometric matrix V. All possible states are defined by $\mathbf{X} := [\mathbf{x}_1, \mathbf{x}_2, \cdots]$ where $\mathbf{x}_i$ is the i^{th} state of $\mathbf{X}$. If the transition rates between all possible states are founded, the governing equation (3.1.1) is written in the linear expression.

$$\frac{d\mathbf{p}(t)}{dt} = K\mathbf{p}(t), \tag{3.1.2}$$

where $\mathbf{p}$ is the vector of probabilities of $\mathbf{X}$ at time t with the element p_i=Prob$[\mathbf{n}(t) = \mathbf{x}_i]$. K is

*This work was published as: H. Lee and CH Lee, ''An Analytic Approach to a Stochastic Enzyme Kinetic Model", MATCH-Communications in Mathematical and in Computer Chemistry, vol. 73, pp.691-704 (2015)

a Markov chain generator [47, 52]. The elements of K are given as

$$K_{ij} = \begin{cases} -\sum_{k=1}^{r} a_k(\mathbf{x}_i) & \text{for } i{=}j \\ a_k(\mathbf{x}_j) & \text{for all } i, \text{ if } \mathbf{x}_i = \mathbf{x}_j + V_k \\ 0 & \text{Otherwise} \end{cases}$$

One can find the solution of (3.1.2)

$$\mathbf{p}(t) = e^{Kt}\mathbf{p}(0). \tag{3.1.3}$$

Since the K in (3.1.3) is usually a large dimensional matrix in the stochastic models, it is very difficult to find the solution of (3.1.3) analytically or numerically. However, one can find the solution if there is a system which has relatively small number of species and reactions.

The enzyme-substrate reaction system is a standard and essential enzyme kinetic model. A model to describe an enzyme behavior has been first proposed by Michael and Menten [53]. Moreover, it works in general for most reactions of biochemical system including transcription and translation in gene regulatory networks [54, 55] and a phase transition in a cell cycle [56]. Several studies shows the evidence that have been made for finding the solution of the stochastic model [57, 58, 59]. An analytic solution for a single enzyme molecule was first presented in the stochastic enzyme-substrate model by Arányi and Tóth [60]. To our best knowledge, there has not yet presented the explicit formula of the solution to the stochastic enzyme-substrate model with general initial conditions.

The enzyme-substrate model has three types of reaction denoted by R_1, R_2, R_3: (1) binding of the enzyme E and the substrate S (R_1), (2) unbinding of the enzyme-substrate complex ES (R_2) and (3) creation of the product P (R_3). The reaction scheme for the stochastic enzyme-substrate reaction system is described by

$$E + S \underset{c_{-1}}{\overset{c_1}{\rightleftarrows}} ES \overset{c_2}{\to} E + P, \tag{3.1.4}$$

where c_1, c_{-1} and c_2 are probability reaction constants. We denote the number of molecules of E, S, ES, P at time t by $n_1(t), n_2(t), n_3(t), n_4(t)$ and let $\mathbf{n}(t) = (n_1(t), n_2(t), n_3(t), n_4(t))^T$. The stoichiometric matrix is given by

$$V = [\mathbf{v}_1|\mathbf{v}_2|\mathbf{v}_3] = \begin{bmatrix} -1 & 1 & 1 \\ -1 & 1 & 0 \\ 1 & -1 & -1 \\ 0 & 0 & 1 \end{bmatrix}.$$

3.2 Analytic solution of Stochastic enzyme-substrate system

The stochastic dynamics of this system can be completely described by a Markov chain. For example, if an initial condition is given as $\mathbf{n}(0) = (2, 3, 0, 0)$, Fig.3-1 represents the Markov chain.

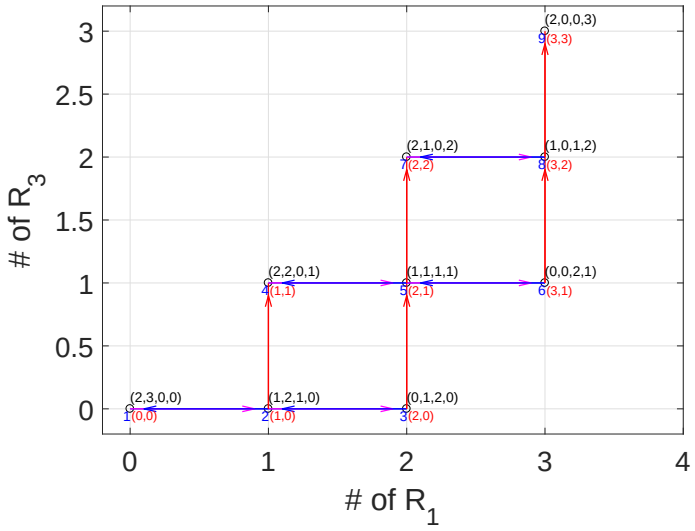

Figure 3-1: Markov chain for all possible states of stochastic enzyme-substrate system; blue numbers, $1\sim 9$ refer to any order-index of $\mathbf{X}$. Arrows represent the three reactions of R_1 (magenta), R_2 (blue), R_3 (red).

The governing equation is given by

$$\frac{d\mathbf{p}}{dt} = K\mathbf{p},$$

where the Markov chain generator K is determined by the transition rates between states.

$$K = \begin{bmatrix} K_1 & & & \\ K_{21} & K_2 & & \\ & K_{32} & K_3 & \\ & & K_{43} & K_4 \end{bmatrix}$$

and

$$K_1 = \begin{bmatrix} -6c_1 & c_{-1} & 0 \\ 6c_1 & -(2c_1 + c_{-1} + c_2) & 2c_{-1} \\ 0 & 2c_1 & -(2c_{-1} + 2c_2) \end{bmatrix},$$

$$K_2 = \begin{bmatrix} -4c_1 & c_{-1} & 0 \\ 4c_1 & -(c_1 + c_{-1} + c_2) & 2c_{-1} \\ 0 & c_1 & -(2c_{-1} + 2c_2) \end{bmatrix}, \quad K_3 = \begin{bmatrix} -2c_1 & c_{-1} \\ 2c_1 & -(c_{-1} + c_2) \end{bmatrix}, \quad K_4 = 0,$$

$$K_{21} = \begin{bmatrix} 0 & c_2 & 0 \\ 0 & 0 & 2c_2 \\ 0 & 0 & 0 \end{bmatrix}, \; K_{32} = \begin{bmatrix} 0 & c_2 & 0 \\ 0 & 0 & 2c_2 \end{bmatrix}, \text{ and } \; K_{43} = \begin{bmatrix} 0 & c_2 \end{bmatrix}.$$

For the initial condition $\mathbf{n}(0) = (e_0, s_0, 0, 0)^T$, D_i is defined as

$$D_i = \{\mathbf{n}(0) + a\mathbf{v}_1 + b\mathbf{v}_2 + (i-1)\mathbf{v}_3 \geq \mathbf{0}, a, b \;\text{ are positive integers}\},$$

for $i = 1, \ldots, N$ and N is the number of components of D_i. If the all elements of the vector are nonnegative, then the vector $\geq \mathbf{0}$. The state $S_j^{(i)}$ denote the j^{th} entry of i^{th} component D_i, $j = 1, \ldots, m_i$, where m_i is the number of states in D_i.

For example, the Markov chain in Fig.3-1 has $D_1 = \{S_1^{(1)} = (2,3,0,0), S_2^{(1)} = (1,2,1,0), S_3^{(1)} = (1,2,1,0)\}$, $D_2 = \{S_1^{(2)} = (2,2,0,1), S_2^{(2)} = (1,1,1,1), S_3^{(2)} = (0,0,2,1)\}$, $D_3 = \{S_1^{(3)} = (2,1,0,2), S_2^{(3)} = (1,0,1,2)\}$ and $D_4 = \{S_1^{(4)} = (2,0,0,3)\}$.
The number of components of D is $N = s_0 + 1$. Moreover, the number J of the total states is computed for the two cases (1) $e_0 \geq s_0$ and (2) $e_0 < s_0$ as follows;

(1) If $e_0 \geq s_0$, then

$$m_i = N + 1 - i, \quad i = 1, 2, \ldots, N$$

and $J = \frac{(s_0+1)(s_0+2)}{2}$.

(2) If $e_0 < s_0$, then

$$m_i = \begin{cases} e_0 + 1, & i = 1, \ldots, s_0 - e_0 + 1 \\ s_0 + 2 - i, & i = s_0 - e_0 + 2, \ldots, N \end{cases}$$

and $J = (s_0 - e_0 + 1)(e_0 + 1) + \frac{e_0(e_0+1)}{2}$.

The Markov chain generator K is given by

$$K = \begin{bmatrix} K_1 & & & & & \\ K_{2,1} & K_2 & & & & \\ & K_{3,2} & K_3 & & & \\ & & \ddots & \ddots & & \\ & & & \ddots & K_{n-1} & \\ & & & & K_{N,N-1} & K_N \end{bmatrix},$$

where $K_{i+1,i}$ is defined by transition rates from the states of component D_i to those of D_{i+1} with $m_{i+1} \times m_i$ block structure.

The matrix K is a block lower triangular matrix structure with diagonal blocks K_i and lower triangular blocks $K_{i+1,i}$. Thus, all eigenvalues of the matrix K consist of the eigenvalues of the diagonal block $K_i, i = 1, \ldots, N$. Moreover, since each diagonal block K_i is a real tridiagonal matrix such that $[K_i]_{j,j+1} \cdot [K_i]_{j+1,j} > 0$, the eigenvalues of K_i are real and distinct [61]. Therefore, the eigenvectors of K_i are linearly independent.

Remark 1. Since K_i is a tridiagonal matrix, the eigenvalues of K_i can be computed by recursive equations described in [61]. There are numerical methods such as Inverse iteration [62], Divide and Conquer method [63] and Multiple Relatively Robust Representations algorithm(MR^3) [64] to compute the eigenvectors of K_i.

We define Λ as the diagonal matrix of eigenvalues

$$\Lambda = diag\left(\Lambda^{(1)}, \Lambda^{(2)}, \cdots, \Lambda^{(N)}\right),$$

where $\Lambda^{(i)} = diag\left(\lambda_1^{(i)}, \cdots, \lambda_{m_i}^{(i)}\right),\ i = 1, \ldots, N$ and $\lambda_p^{(i)}$ are eigenvalues of $K_i,\ \ p = 1, \ldots, m_i$. The matrix of eigenvectors V of K is denoted by

$$V = \left[V^{(1)}|V^{(2)}|\cdots|V^{(N)}\right],$$

where $V^{(i)},\ i = 1, \ldots, N$ is a submatrix and the columns of $V^{(i)}$ are the eigenvectors $\mathbf{v}_p^{(i)}$ corresponding to eigenvalues $\lambda_p^{(i)}, p = 1, \ldots, m_i$, $\mathbf{v}_p^{(i)}$ is denoted by

$$\mathbf{v}_p^{(i)} = \begin{bmatrix} \mathbf{v}_p^{(1,i)} \\ \mathbf{v}_p^{(2,i)} \\ \vdots \\ \mathbf{v}_p^{(N,i)} \end{bmatrix},$$

where each $\mathbf{v}_p^{(j,i)}$ is the $m_j \times 1$ column vector, $j = 1, \ldots, N$. Now the lower triangular block matrix V is computed.

First, we find the eigenvectors $\mathbf{v}_p^{(1)}$ corresponding to the eigenvalue $\lambda_p^{(1)}$ of K_1 such that $K\mathbf{v}_p^{(1)} = \lambda_p^{(1)}\mathbf{v}_p^{(1)}$, $p = 1, \ldots, m_1$.

$$K_1\mathbf{v}_p^{(1,1)} = \lambda_p^{(1)}\mathbf{v}_p^{(1,1)}, \quad K_{i,i-1}\mathbf{v}_p^{(i-1,1)} + K_i\mathbf{v}_p^{(i,1)} = \lambda_p^{(1)}\mathbf{v}_p^{(i,1)},\ i = 2, \ldots, N \tag{3.2.1}$$

One can observe that the $\mathbf{v}_p^{(1,1)}$ are the eigenvectors of K_1 corresponding to $\lambda_p^{(1)}$, $p = 1, \ldots, m_1$. The recursive equations for $\mathbf{v}_p^{(i,1)}, i = 2, \ldots, N$ are derived from (3.2.1).

$$\left(K_i - \lambda_p^{(1)} I_{m_i}\right)\mathbf{v}_p^{(i,1)} = -K_{i,i-1}\mathbf{v}_p^{(i-1,1)}, \quad i = 2, \ldots, N. \tag{3.2.2}$$

Second, we find $\mathbf{v}_p^{(2)}$ corresponding to $\lambda_p^{(2)}$ of K_2 such that $K\mathbf{v}_p^{(2)} = \lambda_p^{(2)}\mathbf{v}_p^{(2)}$, $p = 1, \ldots, m_2$.

$$K_1\mathbf{v}_p^{(1,2)} = \lambda_p^{(2)}\mathbf{v}_p^{(1,2)},\ K_{i,i-1}\mathbf{v}_p^{(i-1,2)} + K_i\mathbf{v}_p^{(i,2)} = \lambda_p^{(2)}\mathbf{v}_p^{(i,2)},\ i = 2, \ldots, N. \tag{3.2.3}$$

$\mathbf{v}_p^{(1,2)}$ can be chosen as a zero vector. (3.2.3) is expressed as

$$K_2\mathbf{v}_p^{(2,2)} = \lambda_p^{(2)}\mathbf{v}_p^{(2,2)},\ \left(K_i - \lambda_p^{(2)}I_{m_i}\right)\mathbf{v}_p^{(i,2)} = -K_{i,i-1}\mathbf{v}_p^{(i-1,2)},\ i = 3, \ldots, N. \tag{3.2.4}$$

In (3.2.4), $\mathbf{v}_p^{(2,2)}$ is the eigenvector corresponding to the eigenvalue $\lambda_p^{(2)}$ of K_2. As the same way for $\lambda_p^{(j)}, j = 3, \ldots, N-1$, the eigenvector $\mathbf{v}_p^{(j)}$ of K corresponding to $\lambda_p^{(j)}$ can be written as

$$\mathbf{v}_p^{(j)} = \begin{bmatrix} \mathbf{0}_1 \\ \vdots \\ \mathbf{0}_{j-1} \\ \mathbf{v}_p^{(j,j)} \\ \vdots \\ \mathbf{v}_p^{(N,j)} \end{bmatrix},$$

where $\mathbf{0}_i$ is the $m_i \times 1$ zero vector, $i = 1, \cdots, j-1$ and $\mathbf{v}_p^{(j,j)}$ is the eigenvector of K_j corresponding to $\lambda_p^{(j)}$.

Third, the eigenvector $\mathbf{v}_p^{(i,j)}$ satisfies

$$\left(K_i - \lambda_p^{(j)}I_{m_i}\right)\mathbf{v}_p^{(i,j)} = -K_{i,i-1}\mathbf{v}_p^{(i-1,j)}. \tag{3.2.5}$$

where $i = j+1, \cdots, N$ and $p = 1, \ldots, m_j$. We choose $\mathbf{v}_1^{(N)}$ corresponding to the zero eigenvalue as the $m_N \times 1$ vector $(0, \ldots, 0, 1)^T$ since $K_N = 0$. We construct the eigenvectors V of K as follows;

$$V = \left[V^{(1)}|V^{(2)}|V^{(3)}|\cdots|V^{(N)}\right] = \left[\begin{array}{c|c|c|c|c} V^{(1,1)} & 0 & 0 & \cdots & 0 \\ V^{(2,1)} & V^{(2,2)} & 0 & \cdots & 0 \\ V^{(3,1)} & V^{(3,2)} & V^{(3,3)} & \ddots & 0 \\ \vdots & \vdots & \vdots & \ddots & 0 \\ V^{(N,1)} & V^{(N,2)} & \cdots & \cdots & V^{(N,N)} \end{array}\right],$$

where columns of $V^{(i,i)}$ are eigenvectors of $K_i, i = 1, \ldots, N$ such that $V^{(i,i)} = \left[\mathbf{v}_1^{(i,i)}|\cdots|\mathbf{v}_{m_i}^{(i,i)}\right]$, $i = 1, \ldots, N-1$ and $V^{(N,N)} = 1$, for $i \geq j = 1, \ldots, N-1$, $V^{(i,j)} = \left[\mathbf{v}_1^{(i,j)}|\cdots|\mathbf{v}_{m_j}^{(i,j)}\right]$.

Theorem 2. *The eigenvectors of K are linearly independent.*

We prove that the independence of eigenvectors of K in [65]. Theorem 2 plays an important role in finding the exact solution of (3.1.2). Theorem 2 implies that the eigenvector matrix V is invertible and the matrix K is diagonalizable. Thus, (3.1.3) can be diagonalized as

$$P(t) = e^{Kt} = Ve^{\Lambda t}V^{-1}. \tag{3.2.6}$$

The matrices $C^{(i,j)}$ are defined for computing V^{-1} more simply, $i \geq j = 1, \ldots, N$.

$$C^{(i,i)} = I_{m_i} \text{ and } C^{(i,j)} = (V^{(i,i)})^{-1}V^{(i,j)} \text{ for } i > j = 1, \ldots, N-1. \tag{3.2.7}$$

Here, $\mathbf{c}_p^{(i,j)}$ denotes the p^{th} column vector of $C^{(i,j)}$ and $C_{k,p}^{(i,j)}$ denotes the $(k,p)^{th}$ entry of $C^{(i,j)}$. (3.2.7) is rewritten as

$$\mathbf{v}_p^{(i,j)} = V^{(i,i)}\mathbf{c}_p^{(i,j)} = \sum_{k=1}^{m_i} C_{k,p}^{(i,j)}\mathbf{v}_k^{(i,i)} \text{ for } i > j. \tag{3.2.8}$$

The column vector $\mathbf{c}_p^{(i,j)}$ is computed by using (3.2.5) and (3.2.8) for $i = 2, \ldots, (N-1)$, $j = 1, \ldots, (i-1)$ and $p = 1, \ldots, m_j$.

$$\left(K_i - \lambda_p^{(j)} I_{m_i}\right)\left[V^{(i,i)}\right]\left[\mathbf{c}_p^{(i,j)}\right] = -K_{i,i-1}\mathbf{v}_p^{(i-1,j)}. \tag{3.2.9}$$

For $i = N$ and $j = 1, \ldots, N-1$,

$$\mathbf{c}_p^{(N,j)} = \frac{K_{N,N-1}\mathbf{v}_p^{(N-1,j)}}{\lambda_p^{(j)}}, \tag{3.2.10}$$

Finally, the matrices $C^{(i,j)}$, for $i > j$ can be computed by using (3.2.9) and (3.2.10). The inverse of V is also a block lower triangular matrix defined by

$$V^{-1} = \begin{bmatrix} W^{(1,1)} & & & & & \\ W^{(2,1)} & W^{(2,2)} & & & & \\ W^{(3,1)} & W^{(3,2)} & W^{(3,3)} & & & \\ \vdots & \vdots & \ddots & \ddots & & \\ W^{(N-1,1)} & W^{(N-1,2)} & & \ddots & W^{(N-1,N-1)} & \\ W^{(N,1)} & W^{(N,2)} & \cdots & & W^{(N,N-1)} & W^{(N,N)} \end{bmatrix}. \tag{3.2.11}$$

The blocks of V^{-1} can be computed by using $VV^{-1} = I$ for $i, j = 1, 2, \ldots, N$.

$$W^{(i,j)} = \begin{cases} \left(V^{(i,i)}\right)^{-1}, & \text{if } i = j \\ -C^{(i+1,i)}W^{(i,i)} & \text{if } i = j+1 \\ -\left[\sum_{k=j}^{i-1} C^{(i,k)}W^{(k,j)}\right] & \text{if } i > j+1 \end{cases} \tag{3.2.12}$$

Thus, we can write $P^{(i,j)}(t)$ such that the (i, j) block matrix of $P(t) = e^{Kt}$ for $i, j = 1, \ldots, N$.

$$P^{(i,j)}(t) = \left(e^{Kt}\right)^{(i,j)} = \begin{cases} V^{(i,i)}e^{\Lambda^{(i)}t}W^{(i,i)} & \textit{for } i = j \\ \sum_{k=j}^{i} V^{(i,k)}e^{\Lambda^{(k)}t}W^{(k,j)} & \textit{for } i > j \end{cases} \tag{3.2.13}$$

The entries of block matrix $P^{(i,j)}(t)$ are given as

$$P^{(i,j)}_{r,q}(t) = \sum_{k=j}^{i}\sum_{h=1}^{m_k}\sum_{g=1}^{m_i} C^{(i,k)}_{g,h}V^{(i,i)}_{r,g}W^{(k,j)}_{h,q}e^{\lambda^{(k)}_h t}, \tag{3.2.14}$$

where $P^{(i,j)}_{r,q}$, $C^{(i,j)}_{r,q}$, $W^{(i,j)}_{r,q}$ denote the $(r, q)^{th}$ entry of $P^{(i,j)}$, $C^{(i,j)}$ and $W^{(i,j)}$, respectively.

Generally, the initially $\mathbf{p}(0)$ is assumed as $\mathbf{p}(0) = (1, 0, 0, \cdots, 0)^T$, which is corresponding to the deterministic initial condition $\mathbf{n}(0) = (e_0, s_0, 0, 0)^T$. If the k^{th} state among all possible states refers to the ℓ^{th} state $S^{(i)}_\ell$ of i^{th} component where $k = \ell + \sum_{j=1}^{i-1} m_j$, then the exact probability of the k^{th} state at time t is computed by

$$p_k(t) = p^{(i)}_\ell(t) = \sum_{k=j}^{i}\sum_{h=1}^{m_k}\sum_{g=1}^{m_i} C^{(i,k)}_{g,h}V^{(i,i)}_{\ell,g}W^{(k,1)}_{h,1}e^{\lambda^{(k)}_h t}. \tag{3.2.15}$$

Moreover, the exact probability for any number of each species at any time can be computed as follows.

The probability of the number of the product P at time t for $i = 1, \ldots, s_0 + 1$ is defined by

$$P\left(n_4(t) = i - 1\right) = \sum_{\ell=1}^{m_i} p^{(i)}_\ell(t) = \sum_{\ell=1}^{m_i}\sum_{k=1}^{i}\sum_{h=1}^{m_k}\sum_{g=1}^{m_i} C^{(i,k)}_{g,h}V^{(i,i)}_{\ell,g}W^{(k,1)}_{h,1}e^{\lambda^{(k)}_h t}$$

The probability of the number of the substrate S at time t.

(1) if $e_0 \geq s_0$, then

$$P\left(n_2(t) = j\right) = \sum_{i=1}^{N-j} p_{\ell_i}(t), \quad \ell_i = \sum_{k=1}^{i} m_k - j \text{ and } j = 0, 1, \cdots, s_0.$$

(2) if $e_0 < s_0$, then

$$P\left(n_2(t)=j\right)=\begin{cases}\sum\limits_{i=1}^{e_0+1} p_{e_0+2-i+k(s_0-e_0+i-j)}(t) & \text{if } j=0,1,\cdots,s_0-e_0,\\ \sum\limits_{i=1}^{s_0+1-j} p_{s_0+2-i-j+k(i)}(t) & \text{if } j=s_0-e_0+1,\cdots,s_0,\end{cases}$$

where $k(a)=\sum\limits_{j=1}^{a-1} m_j$. The system has two conservation quantities $n_1+n_3+n_4=e_0$ and $n_2+n_3+n_4=s_0$. We can also compute the probability of the enzyme n_1 and enzyme-substrate complex n_3 from the probabilities for n_2 and n_4. In terms of the all possible states, we can derive the probability at the k^{th} state at time t from (3.2.14) for general initial condition $\mathbf{p}(0)$.

$$\begin{aligned}p_k(t)=p_\ell^{(i)}(t)&=\sum_{s=1}^{i}\sum_{n=1}^{m_s} P_{\ell,n}^{(i,s)}(t)\; p_{n+k(s)}(0)\\ &=\sum_{s=1}^{i}\sum_{n=1}^{m_s}\sum_{k=s}^{i}\sum_{h=1}^{m_k}\sum_{g=1}^{m_i} C_{g,h}^{(i,k)}V_{\ell,g}^{(i,i)}W_{h,n}^{(k,s)}e^{\lambda_h^{(k)}t}\; p_{n+k(s)}(0),\end{aligned}$$

3.3 Numerical computation procedure

We suggest the method for finding the exact probability solution of the stochastic enzyme-substrate model. The numerical efficiency and accuracy of the method are investigated.

Computational Procedure

Step 0 Construct the Markov chain generator K.
Define the block matrices $K_1,\cdots,K_n$ and $K_{2,1},\cdots,K_{N,N-1}$ as the transition rate.

Step 1. Compute the matrix $\Lambda^{(i)}$ of eigenvalues and the matrix $V^{(i,i)}$ of eigenvectors of K_i.

Step 2. Compute the matrix $C^{(i,j)}$ and $V^{(i,j)}$ by (3.2.8) – (3.2.10).
Compute $W^{(i,j)}$ by (3.2.12).

Step 3. Compute $P^{(i,j)}(t)$ using the explicit formula (3.2.13) or (3.2.14).
Compute the probability of the state by (3.2.15) for given the initial condition $\mathbf{n}(0)$.

We investigate the computational complexity for the two cases. First, if $e_0 \geq s_0$, the matrix exponential solution (3.2.6) has $O(J^3)=O(s_0^6)$, but the block form (3.2.13) has $O(s_0^4)$. If $e_0 < s_0$, then the matrix exponential solution (3.2.6) has $O(J^3)=O(e_0^3 s_0^3)$, but the block form (3.2.13) has $O(s_0^4)$. Moreover, solving (3.2.6) requires the intensive computational cost for most complex chemical systems due to the large dimension of state space. However, our exact block formula (3.2.13) has only $(s_0+1)^2$. In other words, our method is less dependent on the dimensionality.

We carry out numerical simulations for the two cases, $e_0 < s_0$ and $e_0 > s_0$. We use **expm** function of MATLAB to compute the matrix exponential solution. We compare the probability of the number of the substrate S at time t, $P(n_2(t) = i)$ from the matrix exponential solution (3.2.6)and our exact solution in block matrix form (3.2.13) in Fig.3-2, Fig.3-3 for each case.

Case 1. $e_0 < s_0$

We assume two initial conditions $\mathbf{n}(0) = (8, 10, 0, 0)$(the total number of states is $J = 63$) and $\mathbf{n}(0) = (10, 15, 0, 0)(J = 121)$, respectively

Case 2. $e_0 > s_0$

We assume two initial conditions $\mathbf{n}(0) = (30, 20, 0, 0)$ (thus $J = 231$) and $\mathbf{n}(0) = (40, 25, 0, 0)(J = 351)$, respectively.

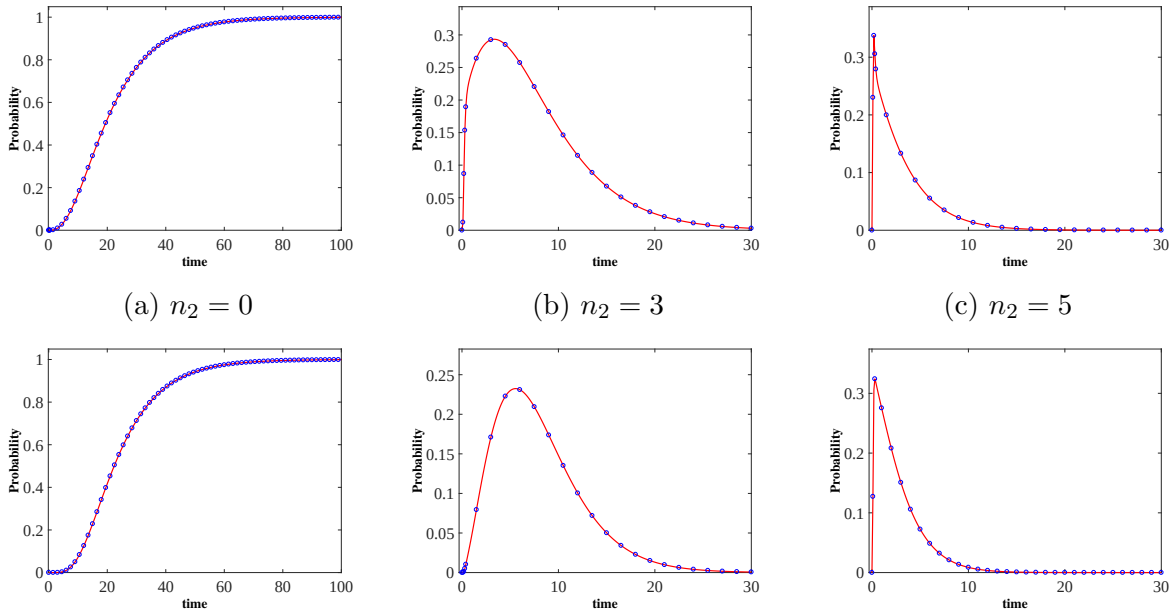

(a) $n_2 = 0$ (b) $n_2 = 3$ (c) $n_2 = 5$

(d) $n_2 = 0$ (e) $n_2 = 4$ (f) $n_2 = 7$

Figure 3-2: Case 1.$e_0 < s_0$: (a)-(c) the initial condition $\mathbf{n}(0) = (8, 10, 0, 0)$ and $J = 63$ (d)-(f) $\mathbf{n}(0) = (10, 15, 0, 0)$ and $J = 121$, comparison of the time evolution of the probability of substrate S at time t between the matrix exponential method(blue dots) and our exact block formula(red solid). The probability constants are $c_1 = 1, c_{-1} = 2, c_2 = 0.1$.

In Table 3-1, we compare CPU times taken by computations between the matrix exponential method and our exact method. As a result of Fig.3-2, Fig.3-3 and Table 3-1, our method is much faster than the matrix exponential method as the dimension of the system gets large. Thus, we conclude that our method is accurate and more efficient than the matrix exponential method.

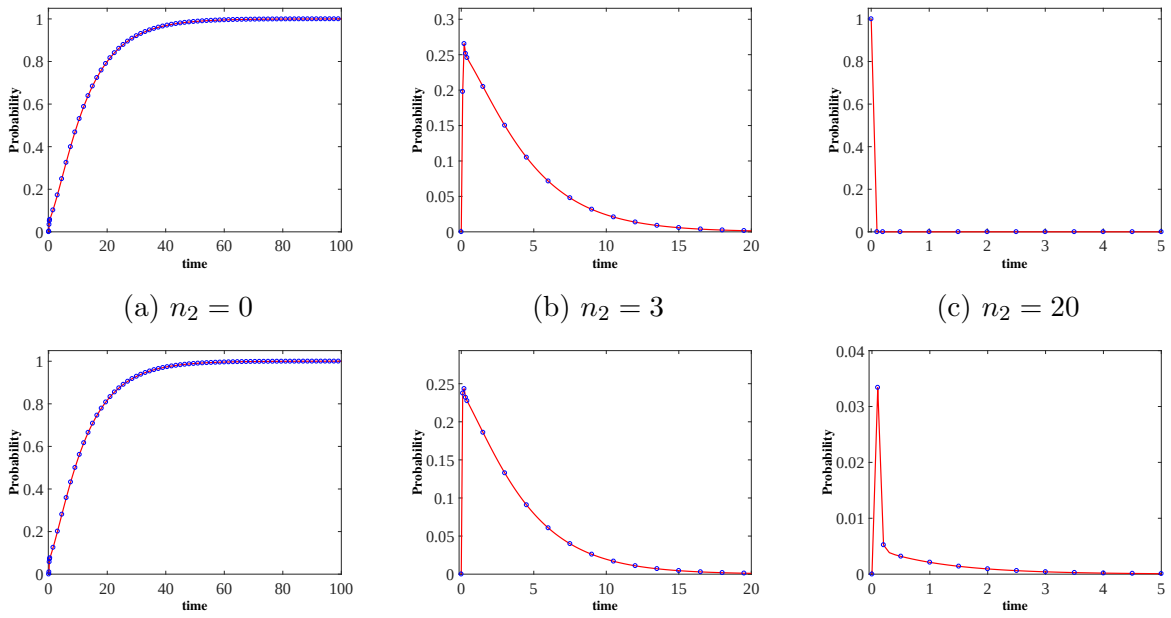

(a) $n_2 = 0$ (b) $n_2 = 3$ (c) $n_2 = 20$

(d) $n_2 = 0$ (e) $n_2 = 3$ (f) $n_2 = 7$

Figure 3-3: Case 2.$e_0 > s_0$: (a)-(c) the initial condition $\mathbf{n}(0) = (30, 20, 0, 0)$ and $J = 231$ and (d)-(f) $\mathbf{n}(0) = (40, 25, 0, 0)$ and $J = 351$, comparison of the time evolution of the probability of substrate S at time t between the matrix exponential method(blue dots) and our exact block formula(red solid). The probability constants are $c_1 = 1, c_{-1} = 2, c_2 = 0.1$.

Cases	$e_0 < s_0$		$e_0 > s_0$	
Number of states J	63	121	231	351
Exact formula	0.79	1.61	3.03	4.99
Matrix exponential	0.96	3.26	17.74	58.37

Table 3-1: Comparison of CPU time (in seconds) elapsed by the exact formula and the matrix exponential.

4

Stochastic Methods for Epidemic Models: An Application to the 2009 H1N1 Influenza Outbreak in Korea**

4.1 Mathematical model of H1N1 influenza with interventions

In section 2.1.2, the SLIAR with treatment model based on [42] has been described. The model takes an account for treatments including the vaccination and the antiviral treatment without the vaccination during the epidemic. The focus has been made on the impact of control interventions on the spread of H1N1 influenza prevailed in Korea from 2009 through 2010. We investigate more realistic scenarios for the 2009 Korean influenza pandemic. The vaccination was implemented during the epidemic not at the beginning of the outbreak because the vaccine was available after 6 months from the first detection. We add the factor γ considering the vaccination during the epidemic for susceptible individuals into the previous model (2.1.5). We denote the number of individuals in the treated susceptible (or vaccinated susceptible), treated latent, treated infectious and treated asymptomatic classes by $S_T(t), L_T(t), I_T(t)$ and $A_T(t)$, respectively. The flow diagram is described in Fig.4-1.

**This work was published as: H.Lee, S. Lee and CH Lee, ''Stochastic methods for epidemic models: An application to the 2009 H1N1 influenza outbreak in Korea", Applied Mathematics and Computation, vol. 286, pp.232-249 (2016)

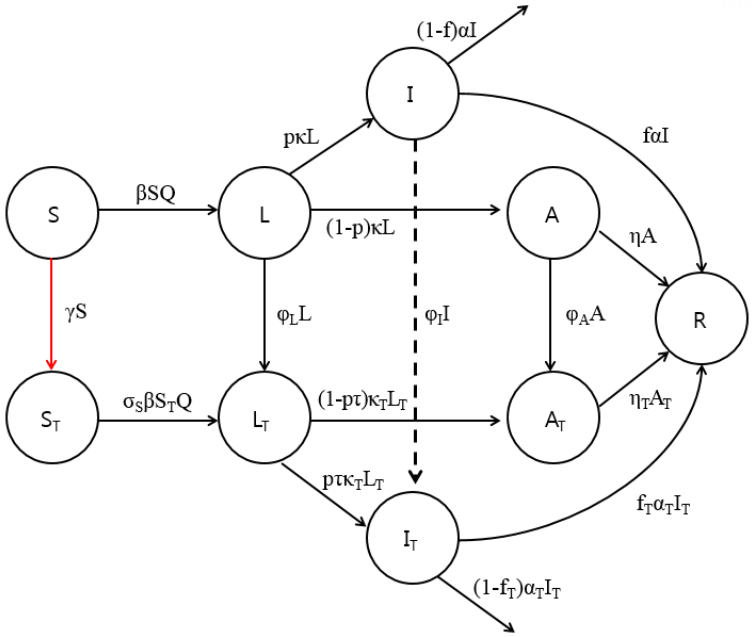

Figure 4-1: SLIAR with Treatment model

The above model lead to the following equations:

$$
\begin{aligned}
\frac{dS}{dt} &= -\beta SQ - \gamma S \\
\frac{dS_T}{dt} &= -\sigma_s \beta S_T Q + \gamma S \\
\frac{dL}{dt} &= \beta SQ - \kappa L \\
\frac{dL_T}{dt} &= \sigma_s \beta S_T Q - \kappa_T L_T \\
\frac{dI}{dt} &= p\kappa L - \alpha I - \phi_I I \\
\frac{dI_T}{dt} &= p\tau\kappa_T L_T - \alpha_T I_T + \phi_I I \\
\frac{dA}{dt} &= (1-p)\kappa L - \eta A - \phi_A A \\
\frac{dA_T}{dt} &= (1-p\tau)\kappa_T L_T - \eta_T A_T + \phi_A A \\
\frac{dR}{dt} &= f\alpha I + f_T \alpha_T I_T + \eta A + \eta_T A_T \\
\frac{dD}{dt} &= (1-f)\alpha I + (1-f_T)\alpha_T I_T \\
Q &= (1-q)I + (1-q)\sigma_I I_T + \delta A + \delta\sigma_A A_T,
\end{aligned}
\tag{4.1.1}
$$

where $S(0) = S_0 > 0, S_T(0) = 0, I(0) = I_0 > 0, L(0) = L_T(0) = A(0) = A_T(0) = I_T(0) = R(0) = D(0) = 0$. All constant parameters are summarized in Table 4-1.

Parameter	Description	Value	Reference
p	Fraction of L that progress to I	0.67	[66]
$(1-f)$	Fatality fraction for I	0.001	[66]
$(1-f_T)$	Fatality fraction for I_T	0	[66]
α	Recovery rate for I	0.2/day	[51]
η	Recovery rate for A	0.2/day	[51]
κ	Rate of departure from L	0.59/day	[51]
α_T	Recovery rate for I_T	0.22/day	[51]
η_T	Recovery rate for A_T	0.22/day	[51]
κ_T	Rate of departure from L_T	0.59/day	[51]
τ	Fraction of progression rate for L_T	0.38	[51]
δ	Infectivity reduction constant for A, A_T	0.5	[51]
q	Contact reduction constant for I, I_T	0.3	[66]
σ_S	Reduction constant for susceptibility of S_T	0.2	[66]
σ_I, σ_A	Infectivity reduction constant for I_T, A_T	0.2	[42]

Table 4-1: Parameters for the 2009 H1N1 Influenza model in Korea.

4.2 Stochastic influenza model

We present a stochastic model for the H1N1 influenza pandemic. Let us denote the numbers of $S, S_T, L, L_T, I, I_T, A, A_T, R, D$ at time t by $\mathbf{x}(t) = (x_1(t), x_2(t), \cdots, x_9(t), x_{10}(t))$, respectively. The stochastic governing equation of the model is obtained in (4.2.1). Since we consider the dynamics of H1N1 influenza in Korea, this system is highly populated and relatively reactive. The SSA requires heavy computational loads. The MCM is much more efficient than SSA as mentioned in section 2.2. Moreover, we focus on the time-evolution of epidemic outcomes to investigate the effectiveness of various intervention scenarios. In that case, the MCM is much more efficient than the SSA to obtain the stochastic outcomes fast. Thus, we employ the MCM to solve the stochastic model (4.2.1) instead of the SSA. Furthermore, we derive the moment equations up to second order moments and truncate them at the third moments where the first moments $\mu_i = E[x_i]$ and second moments $\sigma_{i,j} = E[(x_i - \mu_i)(x_j - \mu_j)]$. There are 65 moment equations for the stochastic SLIAR with treatment model given in Appendix A.

$$
\begin{aligned}
& \frac{dp(\mathbf{x},t)}{dt} \qquad (4.2.1)\\
= \;& \big(c_1(x_1+1)x_5 + c_2(x_1+1)x_6 + c_3(x_1+1)x_7 + c_4(x_1+1)x_8\big)\\
& \cdot p(\mathbf{x}+\mathbf{e}_1-\mathbf{e}_3,t)\\
+ \;& \big(c_5(x_2+1)x_5 + c_6(x_2+1)x_6 + c_7(x_2+1)x_7 + c_8(x_2+1)x_8\big)\\
& \cdot p(\mathbf{x}+\mathbf{e}_2-\mathbf{e}_4,t)\\
+ \;& c_9(x_3+1)p(\mathbf{x}+\mathbf{e}_3-\mathbf{e}_5,t) + c_{10}(x_3+1)p(\mathbf{x}+\mathbf{e}_3-\mathbf{e}_7,t)\\
+ \;& c_{11}(x_4+1)p(\mathbf{x}+\mathbf{e}_4-\mathbf{e}_6,t) + c_{12}(x_4+1)p(\mathbf{x}+\mathbf{e}_4-\mathbf{e}_8,t)\\
+ \;& c_{13}(x_5+1)p(\mathbf{x}+\mathbf{e}_5-\mathbf{e}_6,t) + c_{14}(x_5+1)p(\mathbf{x}+\mathbf{e}_5-\mathbf{e}_9,t)\\
+ \;& c_{15}(x_5+1)p(\mathbf{x}+\mathbf{e}_5-\mathbf{e}_{10},t) + c_{16}(x_6+1)p(\mathbf{x}+\mathbf{e}_6-\mathbf{e}_9,t)\\
+ \;& c_{17}(x_6+1)p(\mathbf{x}+\mathbf{e}_6-\mathbf{e}_{10},t) + c_{18}(x_7+1)p(\mathbf{x}+\mathbf{e}_7-\mathbf{e}_8,t)\\
+ \;& c_{19}(x_7+1)p(\mathbf{x}+\mathbf{e}_7-\mathbf{e}_9,t) + c_{20}(x_8+1)p(\mathbf{x}+\mathbf{e}_8-\mathbf{e}_9,t)\\
+ \;& c_{21}(x_1+1)p(\mathbf{x}+\mathbf{e}_1-\mathbf{e}_2,t)\\
- \;& \big(c_1x_1x_5 + c_2x_1x_6 + c_3x_1x_7 + c_4x_1x_8 + c_5x_2x_5 + c_6x_2x_6 + c_7x_2x_7\\
& + c_8x_2x_8 + c_9x_3 + c_{10}x_3 + c_{11}x_4 + c_{12}x_4 + c_{13}x_5 + c_{14}x_5\\
& + c_{15}x_5 + c_{16}x_6 + c_{17}x_6 + c_{18}x_7 + c_{19}x_7 + c_{20}x_8 + c_{21}x_1\big)p(\mathbf{x},t)
\end{aligned}
$$

where each $\mathbf{e}_i,\ i = 1,\ldots,10$ denotes the 10 dimensional unit vector containing 1 at the i^{th} entry and 0 elsewhere and parameters are as follows;

$$
\begin{aligned}
& c_1 = \beta(1-q), \quad c_2 = \beta(1-q)\sigma_I, \quad c_3 = \beta\delta, \quad c_4 = \beta\delta\sigma_A, \quad c_5 = \sigma_S\beta(1-q),\\
& c_6 = \sigma_S\sigma_I\beta(1-q), \quad c_7 = \sigma_S\beta\delta, \quad c_8 = \sigma_S\beta\delta\sigma_A, \quad c_9 = p\kappa, \quad c_{10} = (1-p)\kappa,\\
& c_{11} = p\tau\kappa_T, \quad c_{12} = (1-p\tau)\kappa_T, \quad c_{13} = \phi_I, c_{14} = f\alpha, \quad c_{15} = (1-f)\alpha,\\
& c_{16} = f_T\alpha_T, \quad c_{17} = (1-f_T)\alpha_T, \quad c_{18} = \phi_A, \quad c_{19} = \eta, \quad c_{20} = \eta_T, \quad c_{21} = \gamma.
\end{aligned}
$$

4.3 Epidemiological parameters for control strategies in Korea

The control measures include non-pharmaceutical and pharmaceutical interventions. First, non-pharmaceutical interventions refer to administrative controls considering the isolation of detected individuals and quarantine of suspected individuals. Second, pharmaceutical interventions involve the antiviral treatment and vaccination. The vaccination has an effect on the reduction of the susceptibility to the influenza. Also, the antiviral treatment such as Tamiflu reduce the force of infection for the influenza. When the outbreak is initiated, generally no vaccine is available. So the antiviral treatment plays an important role in mitigating the spread of influenza. There are intervention strategies involved in our model as follows;

(i) The isolation and quarantine reduce the contact rate by a control parameter x, i.e. the contact rate is $\beta(1-x)$.

(ii) The parameters ϕ_I and ϕ_A are assumed as the function $-\ln(1-r_a)/d_a$ where r_a and d_a are the rate and the duration of the antiviral treatment, respectively [66, 67].

(iii) The parameter γ for the vaccination is also assumed as $-\ln(1-r_v)/d_v$, where r_v and d_v are the rate and the duration of vaccination, respectively.

Control parameters for numerical simulations

The first diagnosed case was a women returning from Mexico on May 2, 2009, so we set that day as day 0. We carry out numerical simulations from day 0 to day 400 for deterministic and stochastic models by applying intervention strategies. The total population size of Korea in 2009 is 47,800,896 estimated from [68] and the initial infective people is assumed as 10 [66]. The epidemic duration is divided into four different periods, day 0 $\sim$ 79 (period P_1), day 80 $\sim$ 110 (P_2), day 111 $\sim$ 176 (P_3) and day 177 $\sim$ 400 (P_4). Korean government implemented the following countermeasures in the four periods [51, 66, 69].

(i) P_1: **Prevent the propagation of the disease**
Infected people voluntarily restrict their activities out of school or work that cause the infection to spread. It means that the contact rate is reduced by 60%. The confirmed cases received the antiviral treatment by 60%. Asymptomatic infectious who contact with a confirmed case also received antiviral treatment for prophylaxis by 30%.

(ii) P_2: **Minimize the outbreak**
One of purpose of the policy was to minimize the outbreak of serious cases and mortalities for reducing socioeconomic costs. The government recommended the public behavioral responses such as washing hands or using hand sanitizer more frequently and wearing a mask. It has the effect on the reduction of the contact rate by 20%. Only confirmed cases received antiviral drugs.

(iii) P_3: **Antiviral drugs were widely available**
The antiviral treatment rates were increased. The vaccination was not available during the periods P_1, P_2 and P_3, i.e., γ =0.

(iiii) P_4: **Vaccination policy started implementing**
According to the KCDC [70], the vaccination rate between day 177 and day 400 is estimated as 0.28. We assume that the vaccine was provided within 20 days for most people. i.e., the duration of vaccination d_v is 20 days.

The control parameters in the four periods implemented by government are summarized in Table 4-2.

Period	Response strategies	Control Parameter
P_1	• The contact rate of I is reduced by 60%, i.e. $q = 0.6$. • Antiviral treatment for I and A are given as 60% and 30%.	$\beta_0 = 0.7390$ $\phi_I = \frac{-ln(1-0.6)}{d_1}$, $\phi_A = \frac{-ln(1-0.3)}{d_1}$
P_2	• The contact rate is reduced by 20% by washing hands and wearing a mask • Antiviral treatment for I is given as 20%.	$\beta_0 = 0.4038$ $\phi_I = \frac{-ln(1-0.2)}{d_2}$
P_3	• Antiviral treatment for I and A is given as 40%, 20%.	$\phi_I = \frac{-ln(1-0.4)}{d_3}$, $\phi_A = \frac{-ln(1-0.2)}{d_3}$
P_4	• Antiviral treatment for I and A is given as 20%, 20%. • The vaccination was implemented from Oct. 27, 2009.	$\phi_I = \frac{-ln(1-0.2)}{d_4}$, $\phi_A = \frac{-ln(1-0.2)}{d_4}$ $\gamma = \frac{-ln(1-0.28)}{20}$

Table 4-2: Summary of Response to the 2009 H1N1 Influenza in Korea. Here d_i denotes the duration of the P_i period.

4.4 Results

We compare the time-evolution dynamics for deterministic and stochastic model by applying intervention strategies described in Table 4-2. The influenza outcomes involve the peak time, the peak size and the final attack ratio. The peak size refers to the maximum value of the incidence during the epidemic. The peak time represents the time when the peak size occurs. The final attack ratio is defined as $1 - \lim_{t\to\infty}(S(t) + S_T(t))/N$. The control reproduction number, R_c is defined as the number of secondary infections by a single infectious individual in only susceptible population with the control measures. The R_c is derived in section 2.1.3 when γ =0. The control reproduction number R_c is equal to the basic reproduction number R_0 in absence of control measures with $\phi_A = \phi_I = 0$. Based on the parameters given in Table 4-1 and Table 4-2, for example, the control reproduction number is $R_c = 1.55$ and the basic reproduction number is $R_0 = 3.09$ in the first period P_1. We investigate how much difference occurs between solutions of two models for different infectives initially such as $10, 50$ and 250. Fig.4-2 and Table 4-3 shows the difference between the solutions of the two models decreases as the initial number of the infectives increases. Especially when the infective individuals are just 10 initially in Fig.4-2 (a), one can see a significant discrepancy between solutions and that the deterministic solution is even out of the interval of mean $\pm$ standard deviation of the stochastic solution in the time interval between 200 and 230 days. Fig.4-2 (b) and (c) show the difference between two solutions gets smaller as the initial infectives get larger as 50 and 250. Thus, when the initial number of the infectives is small enough, if the deterministic model is used to estimate the dynamics of incidence, then it is highly likely that the model would generate a significant error. Kurtz [71, 72] and Ethier [73] proved convergence of the stochastic model

to the ODE-based mean-field approximation for the continuous-time stochastic SIR process by using approximation theorems for the operator semigroup and martingale theory. Simon [74] described the summary of existing proofs based on stochastic theory and PDE-based approach and presented the new elementary approach based on the ODE arguments.

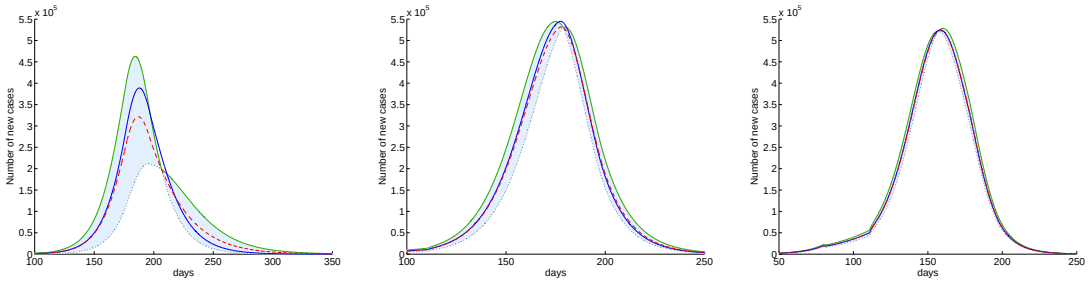

(a) I(0)=10 (b) I(0)=50 (c) I(0)=250

Figure 4-2: Comparison of deterministic and stochastic models for the incidence: deterministic solution (blue solid) and the mean + standard deviation (green dash-dot), mean(red dash) and mean − standard deviation (black dotted) of the stochastic model.

Model	Epidemic outcomes	Initial infectives ($I(0)$)		
		10	50	250
Deterministic	Peak time	187.94	177.49	158.44
	Peak size	388810	544922	524894
	Final attack ratio	0.3963334	0.5219399	0.5828409
Stochastic	Peak time	187.02	177.78	158.59
	Peak size	321812	531516	522856
	Final attack ratio	0.3735441	0.5173449	0.5825586
	Relative L^2 Error	0.1810354	0.0274155	0.0060483

Table 4-3: Comparison of deterministic and stochastic models for the incidence: under different initial numbers $I(0)$, given total population size (N) is fixed. The relative L^2 error is defined as $\sqrt{\sum_t (x(t)-y(t))^2}/\sqrt{\sum_t x(t)^2}$, where $x(t), y(t)$ are the solutions of the MCM and ODE at time t, respectively.

Vaccination date	Baseline (Day 177)	day 167	day 147	day 117	day 87
Peak time	187.02	181.60	168.30	142.60	99.00
Peak size	321812	221464	78080	9593	1121
Final attack ratio	0.3735441	0.2468626	0.0842707	0.0108695	0.0015369

Table 4-4: Under starting dates of vaccination, the peak time, the peak size and the final attack ratio are calculated.

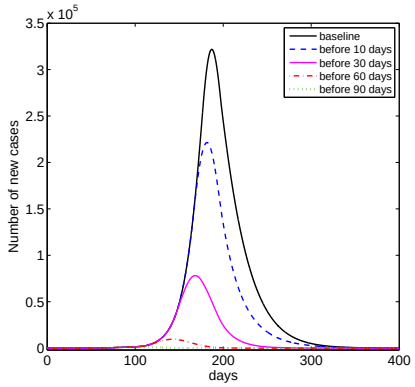

Figure 4-3: Incidence curves under starting dates of vaccination.

From here, we investigate the impact of three control scenarios on the influenza outcomes only for the stochastic model by using the stochastic method (MCM). The baseline curve (black solid) is time-evolution of infectives for stochastic model based on the parameter in Table 4-1 and Table 4-2 given $I(0)$=10. First, we investigate how much the spread of disease could be controlled if the vaccination would start earlier than the actual first date of the vaccination done in Korea. Fig.4-3 shows the impact of early vaccination on the influenza outcomes. The vaccination starting date configures day 167, day 147, day 117, day 87, which are 10 days, 30 days, 60 days and 90 days earlier than the actual initial date, respectively. In Table 4-4, if the vaccination is implemented 10 days earlier, the peak sizes are decreased by 31.2%. Moreover, 30 days, 60 days and 90 days earlier vaccination have an effect on the reduction of the peak size by 75.7%, 97% and 99.7%, respectively. As the results, the earlier the vaccination is available, the smaller the incidence curves will be.

Second, the impact of amounts of antiviral treatment on the influenza outcomes is explored. Fig.4-4 describes how the influenza outcomes are influenced when the antiviral treatment for infectious individuals are increased 50% more than the amount of baseline spent in each period. As we expected, the infectives are reduced due to the elevated rate of antiviral treatment in any periods. One can observe that it is most effective to increase the antiviral treatment for the periods P_1 or P_3 in Table 4-5. The peak size decreases by 19.7% (63,400 cases) with a delay of 2.5 days at the peak and 8.2% (26,400 cases) with a delay of a day at the peak as the results corresponding to the periods P_1 and P_3, respectively. Amount of antiviral treatment of baseline in the period P_1 is more than that in the period P_3, i.e., ϕ_I in $P_1 > \phi_I$ in P_3.

Furthermore, the impact of antiviral treatment for infectious individuals on the third period (P_3) only is investigated in Fig.4-5 and Table 4-6. If the amount of antiviral treatment of the infectives, ϕ_I in the period P_3 is increased by 20%, 50% and 100% more than the actual amount, then, one can observe that the peak sizes are reduced by 3%, 8.2% and 20.7% compared to the baseline, respectively.

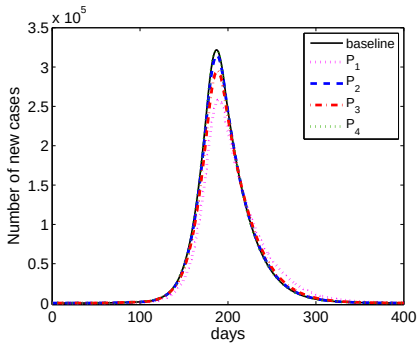

Figure 4-4: Antiviral treatment rate: the incidence curves when the antiviral treatment rate ϕ_I is increased 50% times more than the baseline amount implemented by the government for each period.

Period	P_1	P_2	P_3	P_4
Peak time	189.48	187.35	188.06	186.99
Peak size	258437	314946	295393	320793
Final attack ratio	0.3369820	0.3694439	0.3596954	0.3723046

Table 4-5: Antiviral treatment rate: the peak time, the peak size and the final attack ratio are calculated for the results of Fig.4-4.

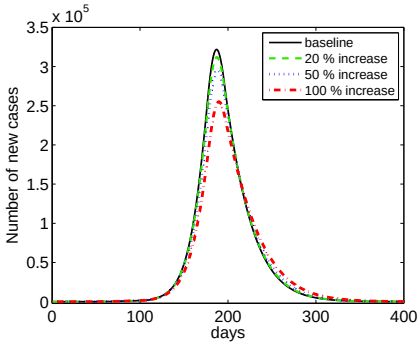

Figure 4-5: Antiviral treatment rate in P_3: incidence curves under treatment rates ϕ_I for the third period (P_3).

Increased amount	20% increase	50% increase	100% increase
Peak time	187.40	188.06	189.71
Peak size	312037	295393	255180
Final attack ratio	0.3685485	0.3596954	0.3381703

Table 4-6: Antiviral treatment rate in P_3: the peak time, the peak size and the final attack ratio are calculated for the results in Fig.4-5.

5

Mathematical Modeling and Computation of Dengue Fever caused by Climate Changes in Korea

Dengue fever is a mosquito-borne viral disease occurring in tropical regions. Dengue virus has serotypes 1-4 (DENV 1-4), where especially only DENV 2, DENV 3 are prevalently identified in tropical countries [75]. Infected people with one serotype obtain permanent immunity to that serotype but temporary cross immunity to other serotypes. People re-infected by the other serotype have the risk of developing severe diseases such as dengue hemorrhagic fever (DHF) and dengue shock syndrome (DSS) caused by the ADE.

Thus, it is reasonable to consider the two-strain model for the primary infection as well as the secondary infection. The population involved in the transmission in the model is divided into human hosts, aquatic stage mosquito (egg, larva, pupae) and adult female mosquito. We incorporate the temperature-dependent entomological parameters into the model described by [31] to investigate the effect of climate changes. All infected people reported in Korea are travelers who visited endemic areas. As the number of international travelers has increased, the risk of dengue outbreaks has been elevated, so we incorporate the inflow rate of international travelers into the model.

In this chapter, first, we investigate the relation between the dengue outbreak and seasonality based on the RCP climate change scenarios. Second, we also investigate the impact of international travelers on the transmission dynamics of dengue outbreaks. Finally, there are small number of cases at the initial stage of the epidemic. In that case, we compare quantitatively

5.1 Deterministic dengue transmission model

5.1.1 Vector-host model for primary infection

The primary infection model is the most common model which is caused by one strain [76]. The dengue transmission model for primary infection including the effect of the temperature has been developed without regarding to the international visitors and virus incubation state of human host [27]. They have investigated the impact of the temperature variation on the dengue transmission dynamics regarding the life cycle of mosquitoes for a relatively short time (less than one year). Based on the previous model [27], we add an E compartment related to the virus incubation or human latency period. Since dengue virus can be transferred through vertical infection, the aquatic stage mosquito is divided into susceptible(S_e) and infectious(I_e) classes. The adult mosquito populations are divided into susceptible(S_v), infected but not infectious(E_v), and infectious(I_v), so that the total adult mosquito population is $N_v \equiv S_v + E_v + I_v$. The human populations are divided into susceptible(S_h), infected but not infections(E_h), infectious(I_h), and recovered(R_h), so that the total human population is $N_h \equiv S_h + E_h + I_h + R_h$. The diagram of this model is shown in Fig.5-1. The system consists of the SEI mosquito population and the SEIR human population. The nonlinear ordinary differential equations are described in (5.1.1).

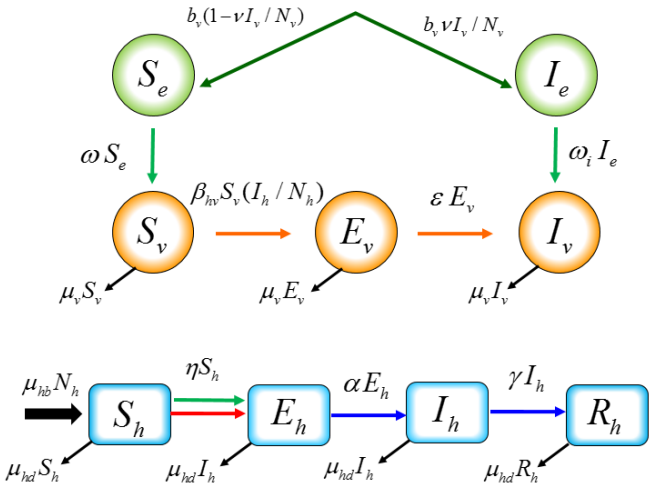

Figure 5-1: Dengue transmission model for the primary infection

$$
\begin{aligned}
\frac{dS_e}{dt} &= b_v\,(1-\nu I_v/N_v) - \omega S_e \\
\frac{dI_e}{dt} &= b_v \nu I_v/N_v - \omega I_e \\
\frac{dS_v}{dt} &= \omega S_e - \beta_{hv} S_v I_h/N_h - \mu_v S_v \\
\frac{dE_v}{dt} &= \beta_{hv} S_v I_h/N_h - \varepsilon E_v - \mu_v E_v \\
\frac{dI_v}{dt} &= \varepsilon E_v + \omega I_e - \mu_v I_v \\
\frac{dS_h}{dt} &= \mu_{hb} N_h - \beta_{vh} S_h I_v/N_h - \eta S_h - \mu_{hd} S_h \\
\frac{dE_h}{dt} &= \beta_{vh} S_h I_v/N_h + \eta S_h - \alpha E_h - \mu_{hd} E_h \\
\frac{dI_h}{dt} &= \alpha E_h - \gamma I_h - \mu_{hd} I_h \\
\frac{dR_h}{dt} &= \gamma I_h - \mu_{hd} R_h
\end{aligned}
\tag{5.1.1}
$$

The parameters related to mosquito include the oviposition rate (b_v), the pre-adult mosquito maturation rate (ω), and the mortality rate of adult mosquitoes (μ_v). Moreover, $1/\varepsilon$ refers to the extrinsic incubation period. The vertical infection rate (ν) represents the infection rate transferred from infected mosquitoes to eggs. For the transmission process, a mosquito bites the human and transmits the dengue virus. The daily biting rate (b), probability of infection (human to mosquito) per bite (b_m) and the probability of infection (mosquito to human) per bite (b_h) are included. The parameter $\beta_{hv} := x_1 b b_m$ is transmissible biting rate from human to vector and $\beta_{vh} := x_2 b b_h$ is the transmissible rate from vector to human. x_1 and x_2 are the transmission factors which are obtained by fitting the model to the data. The parameters μ_{hb} and μ_{hd} represent the human birth rate and death rate, respectively. The parameter $1/\alpha$ and $1/\gamma$ are the latent period and infectious period for human, respectively. The inflow rate of infection due to the international travelers is defined by η.

5.1.2 Secondary infection model

DHF and DSS are associated with individuals re-infected with a second serotype due to the effects of ADE which has been attributed to the presence of preexisting dengue antibodies at sub-neutralizing levels [77]. Additional infection such as tertiary and quaternary infections had hardly been reported. Secondary infection takes into account the formulation only in human population. A mathematical model of dengue fever with two strains is developed to investigate the transmission dynamics. We distinguish the two strains as the major strain 1 and minor strain 2. The subscript i=1, 2 denotes the primary and ij, $j = 3 - i$ denotes the secondary infection. Human population at time t, denoted by N_h, is divided into the 12 subpopulations; S_h is susceptible population that has not been infected. E_{hi} is the exposed population that has

been infected but not infectious. I_{hi} is the infectious population for the primary infection by strain i.

Moreover, in case of secondary infection, R_{hi} denotes the susceptible population with an experienced previous dengue infection by strain i. E_{hij} and I_{hij} are the exposed and infectious population recovered from strain i and currently infected by strain j, respectively. R is finally recovered and life-long immune population against the two different strains, so that $N_h = S_h + E_{h1} + E_{h2} + I_{h1} + I_{h2} + R_{h1} + R_{h2} + E_{h12} + E_{h21} + I_{h12} + I_{h21} + R$. Female mosquito population, denoted by N_v, is divided into 8 subpopulations; susceptible S_v, infected but not infectious E_{vi}, infectious I_{vi} for the infection by strain i, where $N_v = S_v + E_{v1} + E_{v2} + I_{v1} + I_{v2}$. The full diagram for the dengue transmission model with two strains is shown in Fig.5-2.

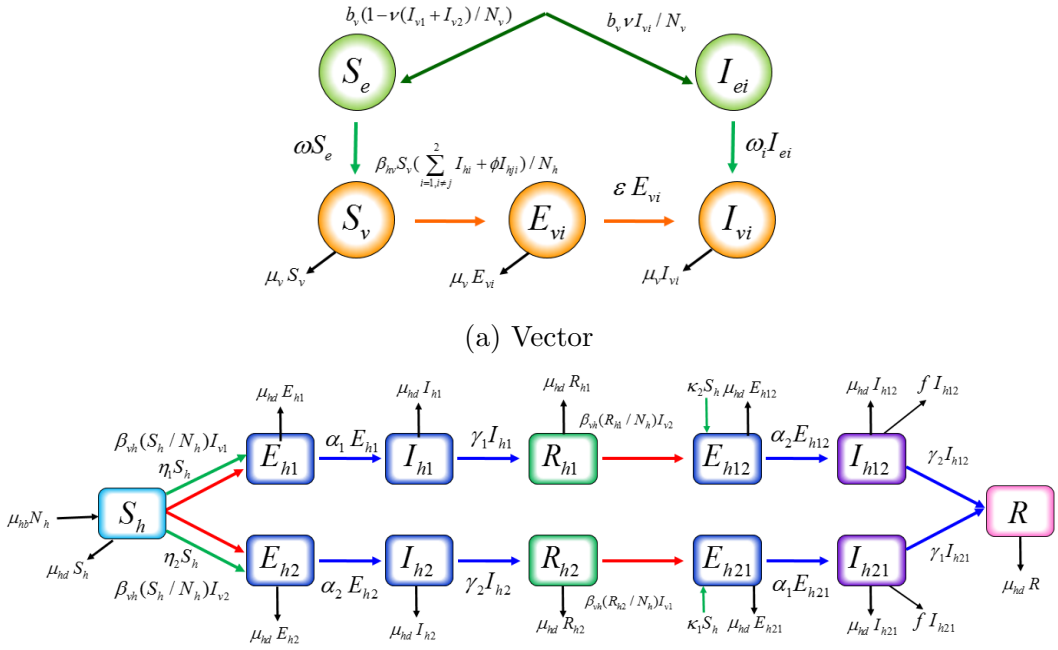

(b) Host

Figure 5-2: Dengue transmission model for the secondary infection

The system consists of 21 differential equations with the fatality class described in (5.1.2) and (5.1.3). The parameter $1/\alpha_i$ and $1/\gamma_i$ are the latent period and infectious period for human with strain i, respectively. There are additional parameters in the model of secondary infection. The ADE factor ϕ is the rate contributing to the force of secondary infection. For $\phi > 1$, individuals in the secondary infection transmit the disease more than the individuals in the primary infection. ω_i denotes the maturation rate of the pre-adult mosquito for each strain i, where $\omega_1 + \omega_2 = \omega$. We assume $\omega_i = 0.5\omega$. The inflow rates of imported cases by international travel for primary infection and secondary infection are denoted by η_i and κ_i for strain i, respectively. f is the fatality rate due to the sever disease caused by secondary infection.

Vector

$$\begin{aligned}
\frac{dS_e}{dt} &= b_v\left(1-\nu\sum_{i=1}^{2} I_{vi}/N_v\right)-(\omega_1+\omega_2)S_e \\
\frac{dI_{ei}}{dt} &= b_v\nu\frac{I_{vi}}{N_v}-\omega_i I_{ei} \\
\frac{dS_v}{dt} &= (\omega_1+\omega_2)S_e - S_v\sum_{i=1,i\neq j}^{2}\beta_{hv}(I_{hi}+\phi I_{hji})/N_h-\mu_v S_v \\
\frac{dE_{vi}}{dt} &= \beta_{hv}S_v\left(I_{hi}+\phi I_{hji}\right)/N_h-\varepsilon E_{vi}-\mu_v E_{vi} \\
\frac{dI_{vi}}{dt} &= \omega_i I_{ei}+\varepsilon E_{vi}-\mu_v I_{vi}
\end{aligned} \tag{5.1.2}$$

Host

$$\begin{aligned}
\frac{dS_h}{dt} &= \mu_{hb}N_h - S_h\sum_{i=1}^{2}\beta_{vh}I_{vi}/N_h-\sum_{i=1}^{2}(\eta_i+\kappa_i)S_h-\mu_{hd}S_h \\
\frac{dE_{hi}}{dt} &= \beta_{vh}S_h I_{vi}/N_h+\eta_i S_h-(\alpha_i+\mu_{hd})E_{hi} \\
\frac{dI_{hi}}{dt} &= \alpha_i E_{hi}-\gamma_i I_{hi}-\mu_{hd}I_{hi} \\
\frac{dR_{hi}}{dt} &= \gamma_i I_{hi}-\beta_{vh}R_{hi}I_{vj}/N_h-\mu_{hd}R_{hi} \\
\frac{dE_{hij}}{dt} &= \beta_{vh}R_{hi}I_{vj}/N_h+\kappa_j S_h-\alpha_j E_{hij}-\mu_{hd}E_{hij} \\
\frac{dI_{hij}}{dt} &= \alpha_j E_{hij}-\left(\gamma_j+\mu_{hd}+f\right)I_{hij} \\
\frac{dR}{dt} &= (\gamma_2 I_{h12}+\gamma_1 I_{h21})-\mu_{hd}R \\
\frac{dD}{dt} &= f(I_{h12}+I_{h21})
\end{aligned} \tag{5.1.3}$$

5.2 Seasonal reproduction number

The seasonal reproduction number, R_s is an alternative form of the basic reproduction number, R_0 [31]. The R_0 is calculated as the spectral radius of next generation matrix at the disease free equilibrium [39]. In a similar way, we can derive the R_s which includes the time-dependent parameters. In computing the R_s for primary infection model and secondary infection model, the inflow rate of imported dengue cases by international travel is assumed to be zero.

5.2.1 Seasonal reproduction number R_s for primary infection model

The system (5.1.1) has the disease-free state $x_0 = (S_e, 0, S_v, 0, 0, S_h, 0, 0, 0)$ with η=0.

$$\begin{aligned}
\frac{dI_e}{dt} &= b_v v \frac{I_v}{N_v} - \omega I_e \\
\frac{dE_v}{dt} &= \beta_{hv} \frac{I_h}{N_h} S_v - \varepsilon E_v - \mu_v E_v \\
\frac{dI_v}{dt} &= \varepsilon E_v + \omega I_e - \mu_v I_v \\
\frac{dE_h}{dt} &= \beta_{vh} \frac{S_h}{N_h} I_v - \alpha E_h - \mu_{hd} E_h \\
\frac{dI_h}{dt} &= \alpha E_h - \gamma I_h - \mu_{hd} I_h
\end{aligned} \tag{5.2.1}$$

Let $\mathbf{x} = (I_e, E_v, I_v, E_h, I_h)^T$, the system (5.2.1) is rewritten as $\mathbf{x}' = \mathcal{F} - \mathcal{V}$.
$\mathcal{F}(\mathbf{x})$ represents all of the new infections. The net transition rates of the corresponding compartments are represented by $\mathcal{V}(\mathbf{x})$, where

$$\mathcal{F}(\mathbf{x}) = \begin{pmatrix} b_v v \frac{I_v}{N_v} \\ \beta_{hv} \frac{I_h}{N_h} S_v \\ 0 \\ \beta_{vh} \frac{S_h}{N_h} I_v \\ 0 \end{pmatrix}, \mathcal{V}(\mathbf{x}) = \begin{pmatrix} \omega I_e \\ (\varepsilon + \mu_v) E_v \\ -\varepsilon E_v - \omega I_e + \mu_v I_v \\ (\alpha + \mu_{hd}) E_h \\ -\alpha E_h + (\gamma + \mu_{hd}) I_h \end{pmatrix}$$

F and V are 5× 5 matrices given by $F = [\frac{\partial \mathcal{F}}{\partial x_j}(x_0)]$ and $V = [\frac{\partial \mathcal{V}}{\partial x_j}(x_0)]$

$$F = \begin{bmatrix} 0 & 0 & b_v \nu / N_v & 0 & 0 \\ 0 & 0 & 0 & 0 & \beta_{hv} S_v / N_h \\ 0 & 0 & 0 & 0 & 0 \\ 0 & 0 & \beta_{vh} S_h / N_h & 0 & 0 \\ 0 & 0 & 0 & 0 & 0 \end{bmatrix}$$

$$V = \begin{bmatrix} \omega & 0 & 0 & 0 & 0 \\ 0 & (\varepsilon+\mu_v) & 0 & 0 & 0 \\ -\omega & -\varepsilon & \mu_v & 0 & 0 \\ 0 & 0 & 0 & (\alpha+\mu_{hd}) & 0 \\ 0 & 0 & 0 & -\alpha & (\gamma+\mu_{hd}) \end{bmatrix}$$

and

$$V^{-1} = \begin{bmatrix} \omega^{-1} & 0 & 0 & 0 & 0 \\ 0 & (\varepsilon+\mu_v)^{-1} & 0 & 0 & 0 \\ {\mu_v}^{-1} & \frac{\varepsilon}{\mu_v(\varepsilon+\mu_v)} & {\mu_v}^{-1} & 0 & 0 \\ 0 & 0 & 0 & (\alpha+\mu_{hd})^{-1} & 0 \\ 0 & 0 & 0 & \frac{\alpha}{(\alpha+\mu_{hd})(\mu_{hd}+\gamma)} & (\gamma+\mu_{hd})^{-1} \end{bmatrix}$$

FV^{-1} be the next generation matrix of system (5.1.1).

$$FV^{-1} = \begin{bmatrix} \frac{b_v\nu}{\mu_v N_v} & \frac{b_v\varepsilon\nu}{\mu_v N_v(\varepsilon+\mu_v)} & \frac{b_v\nu}{\mu_v N_v} & 0 & 0 \\ 0 & 0 & 0 & \frac{\alpha\beta_{hv}S_v}{N_h(\mu_{hd}+\gamma)(\mu_{hd}+\alpha)} & \frac{\beta_{hv}S_v}{N_h(\mu_{hd}+\gamma)} \\ 0 & 0 & 0 & 0 & 0 \\ \frac{\beta_{vh}S_h}{\mu_v N_h} & \frac{\beta_{vh}\varepsilon S_h}{\mu_v N_h(\varepsilon+\mu_v)} & \frac{\beta_{vh}S_h}{\mu_v N_h} & 0 & 0 \\ 0 & 0 & 0 & 0 & 0 \end{bmatrix}$$

Thus, the seasonal reproduction number of the system (5.1.1) at time t in absence of the inflow rate of international travelers (i.e., $\eta = 0$) is given by the spectral radius of matrix FV^{-1} as follows:

$$R_s = \frac{A}{2} + \frac{1}{2}\sqrt{A^2+4\Lambda} \tag{5.2.2}$$

$$A = \frac{b_v(t)\nu}{\mu_v(t)N_v(t)}, \tag{5.2.3}$$

$$\Lambda = \frac{\alpha\beta_{hv}(t)\beta_{vh}(t)\varepsilon(t)S_h(t)S_v(t)}{(\alpha+\mu_{hd})\mu_v(t)(\varepsilon(t)+\mu_v(t))(\mu_{hd}+\gamma)N_h(t)^2}$$

Fig.5-3 shows the relationship between the seasonal reproduction number, temperature, and the number of infectious human in primary infection model for six years. Fig.5-3 (a) indicates the dengue prevalence increases when the high-temperature ranges of above $15.5°C$, which is the average temperature during the six years. Fig.5-3 (b) shows the time to peak of R_s and temperature occurs in early August.

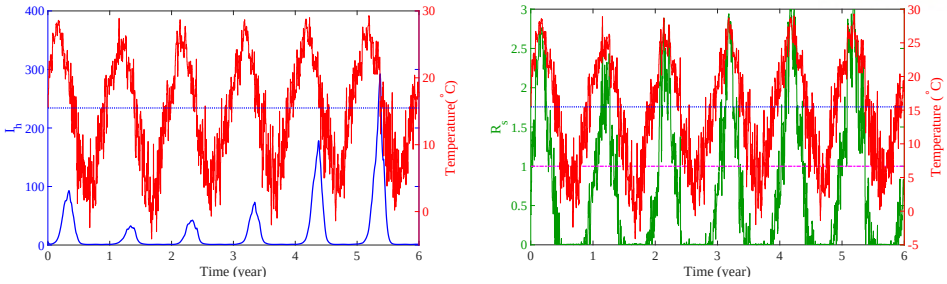

(a) Temperature and I_h (b) Temperature and R_s

Figure 5-3: Daily temperature based on scenario RCP 8.5 (red dashed) and the seasonal reproduction number, R_s (green dashed) and infectious human (blue solid) are displayed during six years with initial conditions of $I_h(0)$=5, $I_v(0)$=0, N_h=608313, N_v=2×608313; blue dotted line represents the average temperature ($15.5°C$) during 6 years and magenta dash-dotted line represents the R_s=1.

5.2.2 Seasonal reproduction number R_s for secondary infection model

When inflow rate of imported dengue cases by international travel is absent, we consider the disease free state x_0 consisting of a 21 × 1 zero vector except for S_e, S_v, S_h.

Vector

$$
\begin{aligned}
\frac{dI_{e1}}{dt} &= b_v v \frac{I_{v1}}{N_v} - \omega_1 I_{e1} \\
\frac{dI_{e2}}{dt} &= b_v v \frac{I_{v2}}{N_v} - \omega_2 I_{e2} \\
\frac{dE_{v1}}{dt} &= \beta_{hv} \left(\frac{I_{h1} + \phi I_{h21}}{N_h} \right) S_v - \varepsilon E_{v1} - \mu_v E_{v1} \\
\frac{dE_{v2}}{dt} &= \beta_{hv} \left(\frac{I_{h2} + \phi I_{h12}}{N_h} \right) S_v - \varepsilon E_{v2} - \mu_v E_{v2} \\
\frac{dI_{v1}}{dt} &= \omega_1 I_{e1} + \varepsilon E_{v1} - \mu_v I_{v1} \\
\frac{dI_{v2}}{dt} &= \omega_2 I_{e2} + \varepsilon E_{v2} - \mu_v I_{v2}
\end{aligned}
\tag{5.2.4}
$$

Host

$$
\begin{aligned}
\frac{dE_{h1}}{dt} &= S_h\left(\beta_{vh}\frac{I_{v1}}{N_h}\right) + \eta_1 S_h - (\alpha_1+\mu_{hd})E_{h1} \\
\frac{dE_{h2}}{dt} &= S_h\left(\beta_{vh}\frac{I_{v2}}{N_h}\right) + \eta_2 S_h - (\alpha_2+\mu_{hd})E_{h2} \\
\frac{dI_{h1}}{dt} &= \alpha_1 E_{h1} - \gamma_1 I_{h1} - \mu_{hd} I_{h1} \\
\frac{dI_{h2}}{dt} &= \alpha_2 E_{h2} - \gamma_2 I_{h2} - \mu_{hd} I_{h2} \\
\frac{dE_{h12}}{dt} &= R_{h1}\beta_{vh}\left(\frac{I_{v2}}{N_h}\right) + \kappa_2 S_h - \alpha_2 E_{h12} - \mu_{hd} E_{h12} \\
\frac{dE_{h21}}{dt} &= R_{h2}\beta_{vh}\left(\frac{I_{v1}}{N_h}\right) + \kappa_1 S_h - \alpha_1 E_{h21} - \mu_{hd} E_{h21} \\
\frac{dI_{h12}}{dt} &= \alpha_2 E_{h12} - (\gamma_2+\mu_{hd}+f)\, I_{h12} \\
\frac{dI_{h21}}{dt} &= \alpha_1 E_{h21} - (\gamma_1+\mu_{hd}+f)\, I_{h21}
\end{aligned}
\tag{5.2.5}
$$

Let $\mathbf{x} = (I_{ei}, E_{vi}, I_{vi}, E_{hi}, I_{hi})^T$, the system (5.2.4) and (5.2.5) are rewritten as $\mathbf{x}' = \mathcal{F} - \mathcal{V}$. $\mathcal{F}(\mathbf{x})$ represents all of the new infections. The net transition rates of the corresponding compartment are represented by $\mathcal{V}(\mathbf{x})$, where

$$
\mathcal{F}(\mathbf{x}) = \begin{pmatrix}
b_v v\frac{I_{v1}}{N_v} \\
b_v v\frac{I_{v2}}{N_v} \\
\beta_{hv}\left(\frac{I_{h1}+\phi I_{h21}}{N_h}\right) S_v \\
\beta_{hv}\left(\frac{I_{h2}+\phi I_{h12}}{N_h}\right) S_v \\
0 \\ 0 \\
S_h\left(\beta_{vh}\frac{I_{v1}}{N_h}\right) \\
S_h\left(\beta_{vh}\frac{I_{v2}}{N_h}\right) \\
0 \\ 0 \\
\beta_{vh}R_{h1}\frac{I_{v2}}{N_h} \\
\beta_{vh}R_{h2}\frac{I_{v1}}{N_h} \\
0 \\ 0
\end{pmatrix}, \mathcal{V}(\mathbf{x}) = \begin{pmatrix}
\omega_1 I_{e1} \\
\omega_2 I_{e2} \\
(\varepsilon+\mu_v)E_{v1} \\
(\varepsilon+\mu_v)E_{v2} \\
-\omega_1 I_{e1} - \varepsilon E_{v1} + \mu_v I_{v1} \\
-\omega_2 I_{e2} - \varepsilon E_{v2} + \mu_v I_{v2} \\
(\alpha_1+\mu_{hd})E_{h1} \\
(\alpha_2+\mu_{hd})E_{h2} \\
-\alpha_1 E_{h1} + (\gamma_1+\mu_{hd})I_{h1} \\
-\alpha_2 E_{h2} + (\gamma_2+\mu_{hd})I_{h2} \\
(\alpha_2+\mu_{hd})E_{h12} \\
(\alpha_1+\mu_{hd})E_{h21} \\
-\alpha_2 E_{h12} + (\gamma_2+\mu_{hd}+f)\, I_{h12} \\
-\alpha_1 E_{h21} + (\gamma_1+\mu_{hd}+f)\, I_{h21}
\end{pmatrix}
$$

F and V are 14× 14 matrices at x_0 given by

$$F = \begin{bmatrix}
0 & 0 & 0 & 0 & f_{1,5} & 0 & 0 & 0 & 0 & 0 & 0 & 0 & 0 & 0 \\
0 & 0 & 0 & 0 & 0 & f_{2,6} & 0 & 0 & 0 & 0 & 0 & 0 & 0 & 0 \\
0 & 0 & 0 & 0 & 0 & 0 & 0 & 0 & f_{3,9} & 0 & 0 & 0 & 0 & f_{3,14} \\
0 & 0 & 0 & 0 & 0 & 0 & 0 & 0 & 0 & f_{4,10} & 0 & 0 & f_{4,13} & 0 \\
0 & 0 & 0 & 0 & 0 & 0 & 0 & 0 & 0 & 0 & 0 & 0 & 0 & 0 \\
0 & 0 & 0 & 0 & 0 & 0 & 0 & 0 & 0 & 0 & 0 & 0 & 0 & 0 \\
0 & 0 & 0 & 0 & f_{7,5} & 0 & 0 & 0 & 0 & 0 & 0 & 0 & 0 & 0 \\
0 & 0 & 0 & 0 & 0 & f_{8,6} & 0 & 0 & 0 & 0 & 0 & 0 & 0 & 0 \\
0 & 0 & 0 & 0 & 0 & 0 & 0 & 0 & 0 & 0 & 0 & 0 & 0 & 0 \\
0 & 0 & 0 & 0 & 0 & 0 & 0 & 0 & 0 & 0 & 0 & 0 & 0 & 0 \\
0 & 0 & 0 & 0 & 0 & 0 & 0 & 0 & 0 & 0 & 0 & 0 & 0 & 0 \\
0 & 0 & 0 & 0 & 0 & 0 & 0 & 0 & 0 & 0 & 0 & 0 & 0 & 0 \\
0 & 0 & 0 & 0 & 0 & 0 & 0 & 0 & 0 & 0 & 0 & 0 & 0 & 0 \\
0 & 0 & 0 & 0 & 0 & 0 & 0 & 0 & 0 & 0 & 0 & 0 & 0 & 0
\end{bmatrix}$$

$$f_{1,5} = \frac{b_v \nu}{N_v} \quad f_{2,6} = \frac{b_v \nu}{N_v} \quad f_{3,9} = \frac{\beta_{hv} S_v}{N_h} \quad f_{3,14} = \frac{\beta_{hv} \phi S_v}{N_h}$$
$$f_{4,10} = \frac{\beta_{hv} S_v}{N_h} \quad f_{4,13} = \frac{\beta_{hv} \phi S_v}{N_h} \quad f_{7,5} = \frac{\beta_{vh} S_h}{N_h} \quad f_{8,6} = \frac{\beta_{vh} S_h}{N_h}$$

and

$$V = \begin{bmatrix}
v_{1,1} & 0 & 0 & 0 & 0 & 0 & 0 & 0 & 0 & 0 & 0 & 0 & 0 & 0 \\
0 & v_{2,2} & 0 & 0 & 0 & 0 & 0 & 0 & 0 & 0 & 0 & 0 & 0 & 0 \\
0 & 0 & v_{3,3} & 0 & 0 & 0 & 0 & 0 & 0 & 0 & 0 & 0 & 0 & 0 \\
0 & 0 & 0 & v_{4,4} & 0 & 0 & 0 & 0 & 0 & 0 & 0 & 0 & 0 & 0 \\
v_{5,1} & 0 & v_{5,3} & 0 & v_{5,5} & 0 & 0 & 0 & 0 & 0 & 0 & 0 & 0 & 0 \\
0 & v_{6,2} & 0 & v_{6,4} & 0 & v_{6,6} & 0 & 0 & 0 & 0 & 0 & 0 & 0 & 0 \\
0 & 0 & 0 & 0 & 0 & 0 & v_{7,7} & 0 & 0 & 0 & 0 & 0 & 0 & 0 \\
0 & 0 & 0 & 0 & 0 & 0 & 0 & v_{8,8} & 0 & 0 & 0 & 0 & 0 & 0 \\
0 & 0 & 0 & 0 & 0 & 0 & v_{9,7} & 0 & v_{9,9} & 0 & 0 & 0 & 0 & 0 \\
0 & 0 & 0 & 0 & 0 & 0 & 0 & v_{10,8} & 0 & v_{10,10} & 0 & 0 & 0 & 0 \\
0 & 0 & 0 & 0 & 0 & 0 & 0 & 0 & 0 & 0 & v_{11,11} & 0 & 0 & 0 \\
0 & 0 & 0 & 0 & 0 & 0 & 0 & 0 & 0 & 0 & 0 & v_{12,12} & 0 & 0 \\
0 & 0 & 0 & 0 & 0 & 0 & 0 & 0 & 0 & 0 & v_{13,11} & 0 & v_{13,13} & 0 \\
0 & 0 & 0 & 0 & 0 & 0 & 0 & 0 & 0 & 0 & 0 & v_{14,12} & 0 & v_{14,14}
\end{bmatrix}$$

$$
\begin{array}{cccc}
v_{1,1}=\omega_1 & v_{2,2}=\omega_2 & v_{3,3}=(\varepsilon+\mu_v) & v_{4,4}=(\varepsilon+\mu_v) \\
v_{5,5}=\mu_v & v_{6,6}=\mu_v & v_{7,7}=(\alpha_1+\mu_{hd}) & v_{8,8}=(\alpha_2+\mu_{hd}) \\
v_{9,9}=(\gamma_1+\mu_{hd}) & v_{10,10}=(\gamma_2+\mu_{hd}) & v_{11,11}=(\alpha_2+\mu_{hd}) & v_{12,12}=(\alpha_1+\mu_{hd}) \\
v_{13,13}=(\gamma_2+\mu_{hd}+f) & v_{14,14}=(\gamma_1+\mu_{hd}+f) & v_{5,1}=-\omega_1 & v_{5,3}=-\varepsilon \\
v_{6,2}=-\omega_2 & v_{6,4}=-\varepsilon & v_{9,7}=-\alpha_1 & v_{10,8}=-\alpha_2 \\
v_{13,11}=-\alpha_2 & v_{14,12}=-\alpha_1 & &
\end{array}
$$

FV^{-1} be the next generation matrix of system (5.1.2) and (5.1.3). Thus, the seasonal reproduction number of system (5.1.2) and (5.1.3) in absence of the inflow rate of international travelers (i.e., $\eta_i = \kappa_i = 0$) is given by the spectral radius of matrix FV^{-1} as follows:

$$
\begin{aligned}
R_s &= max(R_{s1}, R_{s2}) \\
R_{s1} &= \frac{A}{2} + \frac{1}{2}\sqrt{A^2 + 4\Lambda_1}, \quad R_{s2} = \frac{A}{2} + \frac{1}{2}\sqrt{A^2 + 4\Lambda_2} \\
\text{where} \quad A &= \frac{b_v(t)\nu}{\mu_v(t)N_v(t)}, \quad \Lambda_i = \frac{\alpha_i\beta_{hv}(t)\beta_{vh}(t)\varepsilon(t)S_h(t)S_v(t)}{(\alpha_i+\mu_{hd})\mu_v(t)(\varepsilon(t)+\mu_v(t))(\mu_{hd}+\gamma_i)N_h(t)^2}
\end{aligned}
$$

In Fig.5-4, the relation between R_s and primarily infectious human as well as secondarily infectious human is investigated. The primarily and secondarily infectious individuals increase when either $R_s > 1$ or the temperature is higher than the $15.5°C$. It is consistent with the results of the primary infection model in Fig.5-3. Thus, the dengue prevalence also increases when the R_s is larger than 1. Temperature is associated positively with dengue outbreaks at a time-lag. There is evidence that the temperature influences the mosquito population size indirectly.

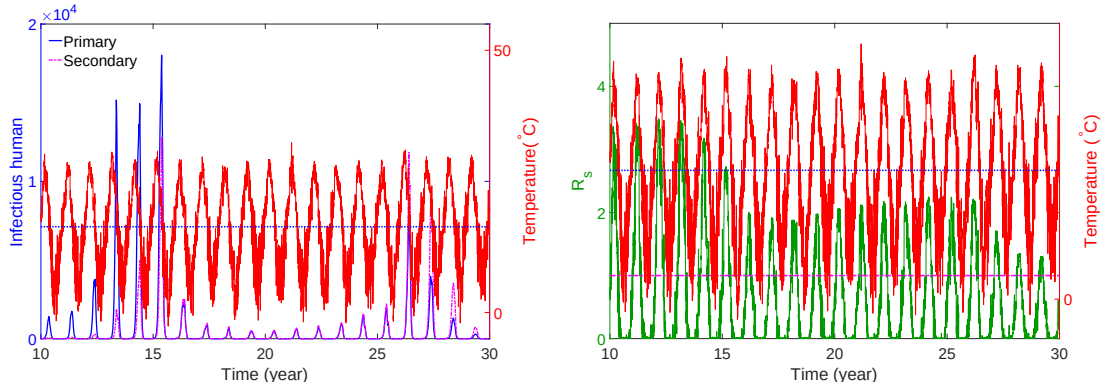

(a) I_{hi},I_{hij} and temperature (b) I_{hi},I_{hij} and R_s

Figure 5-4: The relationship between dengue cases and daily temperature based on RCP 8.5 data is investigated. Blue dotted line represents the average temperature during 20 years from year 10 to year 30; (a) temperature (red dashed) and primarily infectious human (blue solid) and secondarily infectious human (magenta dash-dotted) are displayed during 20 years. (b) temperature (red dashed) and R_s (green dashed) are displayed. Magenta dash-dotted line represents the R_s=1. Initial conditions are $I_{h1}(0)$=5, $I_{h2}(0)$=2, $I_{v1}(0) = I_{v2}(0)$=0, $N_h(0)$=608313, $N_v(0)$=2×608313.

5.3 Parameter estimation

5.3.1 Temperature-dependent parameters

There are several vector parameters that are temperature sensitive. Liu and Alto [78, 79] found that temperature plays an important role in influencing the dengue transmission and the *Aedes* mosquito population. Thus, we consider the dengue transmission parameters and mosquito's life cycle parameters as temperature dependent.

Parameters for extended temperature range

Dengue transmission parameters involve (1) b, the biting rate of a *Aedes* mosquito, (2) b_m, the probability of infection from human to mosquito per bite and (3) b_h, the probability of infection from mosquito to human per bite, which are all derived in [31]. Mosquito's life cycle parameters involve (4) μ_v, the mortality rates of the mosquitoes, and (5) ω, the pre-adult maturation rate in relation to temperature (T) determined from [32]. Since these functions are described over the temperature range of $10°C \leq T \leq 33°C$, these functions are extended in order to estimate the dengue epidemics in Korea with lower temperature during the winters, and defined below with respect to temperature ($\circ C$).

(1) **The biting rate (b)**.

$$b(T) = 0.0943 + 0.0043T$$

(2) **The probability of infection from mosquito to human per bite (b_h)**. This parameter is defined for $T \geq 12.286°C$. In case of $T < 12.286°C$, the value can be inferred as zero.

$$b_h(T) = \begin{cases} 0.001044T(T - 12.286)\sqrt{32.461 - T} & (12.286°C \leq T \leq 32.461°C) \\ 0 & (T < 12.286°C, T > 32.461°C) \end{cases}$$

(3) **The probability of infection from human to mosquito per bite (b_m)**. This parameter is defined for $12.4°C$ to $32.5°C$. For $T < 12.4°C$ or $T > 32.5°C$, the value can be inferred as zero compared with $b_h(T)$.

$$b_m(T) = \begin{cases} -0.9037 + 0.0729T & (12.4°C \leq T < 26.1°C) \\ 1 & (26.1°C \leq T \leq 32.5°C) \\ 0 & (T < 12.4°C, T > 32.5°C) \end{cases}$$

(4) **Mortality rate of the adult mosquito (μ_v)**. This parameter is defined for $10.54°C <$

$T < 33.4°C$. We assume that μ_v cannot be larger than 1.

$$\begin{aligned}\mu_v(T) &= 8.692 \times 10^{-1} - 1.590 \times 10^{-1}T + 1.116 \times 10^{-2}T^2 \\ &- 3.408 \times 10^{-4}T^3 + 3.809 \times 10^{-6}T^4\end{aligned}$$

(5) **Pre-adult maturation rate (ω)**. For T≤10°C, the value must be fixed to zero because a larva cannot develop to a mosquito [32].

$$\begin{aligned}\omega(T) &= 0.1310 - 0.05723T + 0.01164T^2 - 0.001341T^3 + 0.8723 \times 10^{-4}T^4 \\ &-0.3017 \times 10^{-5}T^5 + 0.5153 \times 10^{-7}x^6 + 0.342 \times 10^{-6}x^7\end{aligned}$$

Fig.5-5 shows the values of the temperature-dependent functions defined in [31, 32, 78] as black dots. Fig.5-5 contains the extended fitting functions over wider range of temperature as red and blue dashed lines for lower and higher temperatures respectively. In Fig.5-5 (c), since x_1=0.4455 and x_2=1, which are obtained from data fitting, β_{hv} is larger than β_{vh} [25].

Virus incubation rate (ε) derived from experimental data

Virus incubation rate (ε) is based on the experimental data of the extrinsic incubation period at temperatures 13°C ∼ 35°C [80], defined as a 4^{th} order polynomial function to fit the data. For T ≤ 10.3°C, the negative values must be fixed to zero. Fig.5-6 shows the virus incubation rate depending on temperature.

$$\varepsilon(T) = -1.678 + 0.344T - 2.422 \times 10^{-2}T^2 + 7.252 \times 10^{-4}T^3 - 7.713 \times 10^{-6}T^4$$

Furthermore, we assume that mosquito population is constant for a day because mosquitoes lay eggs only during the day. Oviposition rate (b_v) of mosquitoes is defined as $b_v = \mu_v N_v$, which is updated daily [81].

5.3.2 RCP scenarios and research area

For its Fifth Assessment Report in 2014, the Intergovernmental Panel on Climate Change (IPCC) had developed four greenhouse gas concentration trajectories called "Representative Concentration Pathways (RCPs)" to facilitate future assessment of climate change including emissions mitigation. The four RCP scenarios which range up to year 2100, are defined, according to the radiative forcing levels from 2.6 to 8.5 W/m^2 as in Table 5-1 : the lowest forcing level scenario (RCP 2.6), two medium stabilization scenarios (RCP 4.5/RCP 6.0), and the high-end baseline emission scenario (RCP 8.5). The Korea Meterological Administration (KMA) provides future climate data generated from RCP scenarios. We compare the dynamics of dengue

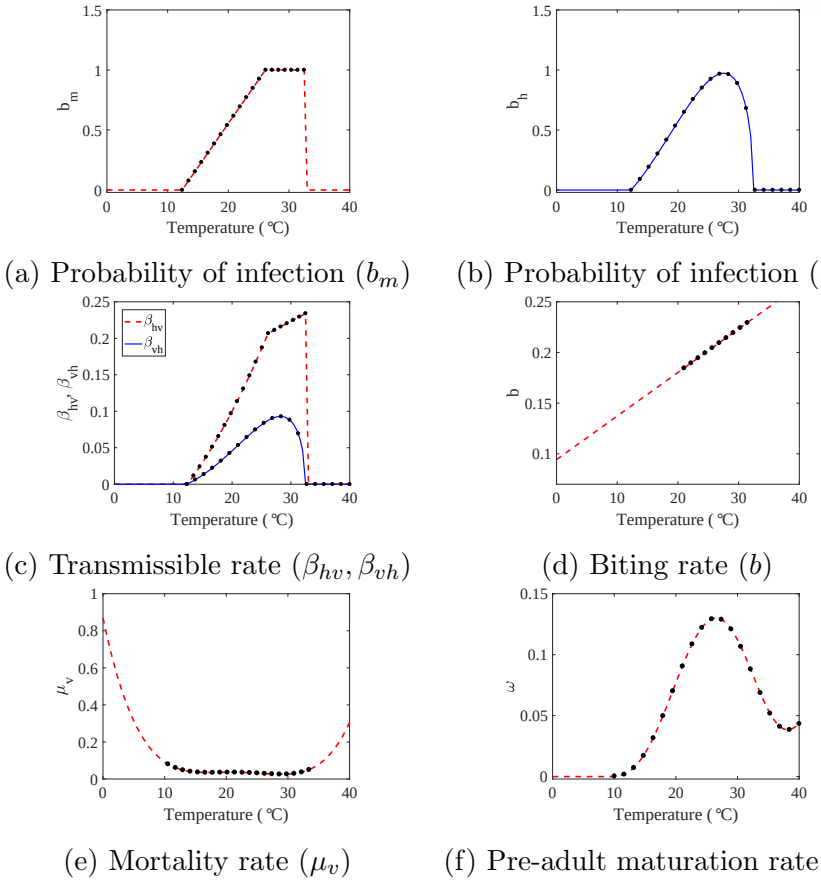

(a) Probability of infection (b_m) (b) Probability of infection (b_h)

(c) Transmissible rate (β_{hv}, β_{vh}) (d) Biting rate (b)

(e) Mortality rate (μ_v) (f) Pre-adult maturation rate (ω)

Figure 5-5: Temperature dependent entomological parameters are displayed under varying temperature with the range of $0°C$ to $40°C$; red dashed and blue solid lines represent the extended parameters for wide-temperature range, and black dots are values of fitting functions over the given temperature range from the experimental data.

prevalence between the two types of climate change scenarios – RCP 4.5 and RCP 8.5 – to investigate the effect of climate change on the dengue outbreaks. Fig.5-7 (a) describes that the average temperature for every ten year from 2020 to 2089. According to the RCP 4.5 and RCP 8.5 scenarios, it is expected that the average temperature in Jeju Island of Korea will increase by $1.5°C$ in RCP 4.5 and $3.5°C$ in RCP 8.5 for 70 years. Fig.5-7 (b) describes the daily average temperature of every five year from 2020 to 2024.

No indigenous dengue case has been reported in Korea. All of diagnosed people in Korea returned after visiting the endemic areas. Dengue virus invades into the new areas with potential of an outbreak. Global warming by climate change and globalization such as increased international travel, trade, and transportation can influence the spread of dengue outbreak [36, 82, 83]. Jeju Island is located at the southern end of the Korean Peninsula, which has subtropical climate. The larvae of the Asian tiger mosquito have been found in Jeju Island in 2010. The discovery suggests that the Jeju Island is potentially under risk of dengue fever outbreak. Increased international travel and climate changes are important factors in the future spread of dengue fever in Jeju Island. Moreover, dengue transmission has been expected

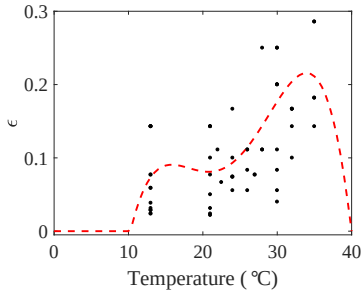

Figure 5-6: Virus incubation rate is displayed under varying temperature with the range of $0°C$ to $40°C$; red dashed line represents the fitting equation by using experimental data (black dots).

Scenarios	Description	CO_2 (ppm)
RCP 2.6	Peak in radiative forcing at $\sim 3W/m$ before 2100 year and decline	420
RCP 4.5	Stabilization without overshoot pathway to $\sim 4.5W/m$ at stabilization after 2100 year	540
RCP 6.0	Stabilization without overshoot pathway to $\sim 6W/m$ at stabilization after 2100 year	670
RCP 8.5	Rising radiative forcing pathway leading to 8.5 W/m in 2100 year	940

Table 5-1: Representative concentration pathways (RCPs) scenario (IPCC)

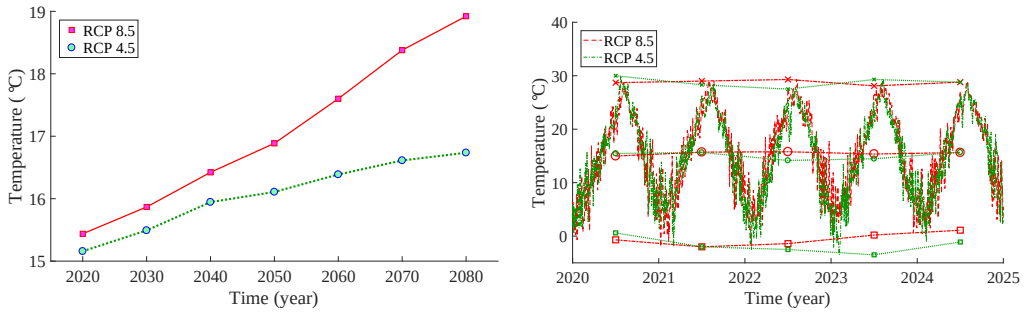

(a) Decennial mean temperature (b) Average daily temperature

Figure 5-7: Temperature based on RCP 4.5 and RCP 8.5 climate change scenarios in Jeju Island is displayed; (a) the average temperature during 10 years is expressed as red square (RCP 8.5) and blue circle (RCP 4.5) during 70 years from year 2020 to year 2089. (b) the daily average temperature of five years since 2020. Symbols $\times, \circ, \square$ represent the maximum, mean and minimum temperature for each year, respectively.

to expand to Korea. Due to international travels to endemic area and inhabitation of *Aedes* mosquitoes, the country is no longer safe from the dengue fever outbreak. The Korea Centers for Disease Control and Prevention (KCDC) provides monthly reported cases of dengue fever [84] in Korea. We interpolate the monthly data of international travel in Table 5-2 to obtain

the daily inflow rate for a whole year. The daily inflow rate over time is denoted by η in the primary infection model (5.1.1) while η_i and κ_i in the secondary infection model (5.1.3). Let $\eta_i = \theta_i\eta, \kappa_i = \tau_i\eta$ where θ_i, τ_i are the weights satisfying $\sum_{i=1}^{2}(\theta_i + \tau_i) = 1$ and $\eta = \sum_{i=1}^{2}(\eta_i + \kappa_i)$. We assume the $\theta_i = 0.35$ and $\tau_i = 0.15$ to be $\theta_i > \tau_i$ for i, j=1, 2. The demographic parameters for human in Jeju Island which refers the birth rate (μ_{hb}) and the death rate (μ_{hd}) are obtained from Statistics Korea [85]. Table 5-3 summarizes the constant parameters.

Jan	Feb	Mar	Apr	May	Jun	Jul	Aug	Sep	Oct	Nov	Dec	Total
11	12	15	10	15	10	22	36	24	41	39	20	255

Table 5-2: Reported targeted cases of dengue fever by month in 2015 (unit: case)

5.3.3 Data fitting by using least square method

In this section, we compare the dengue incidence data in Taiwan with the results of numerical simulation in absence of imported dengue cases to confirm the validity of parameters in the model; then, we determine x_1 and x_2 through data fitting. Fig.5-8 shows the monthly confirmed dengue cases and monthly average temperature data in Taiwan from January 2012 to May 2016. The range of temperature is from $15°C$ to $28°C$. We observe that the temperature is strongly related with dengue outbreaks in 2014–2015. We consider dengue cases including dengue fever (DF), DHF, and DSS as a single object called 'dengue fever cases'. This type of data was not available from year 2012 to year 2016. Taiwan experienced a large dengue fever outbreak in 2014 and another consecutively larger dengue fever outbreak in 2015, resulting in a total of 51579 cases.

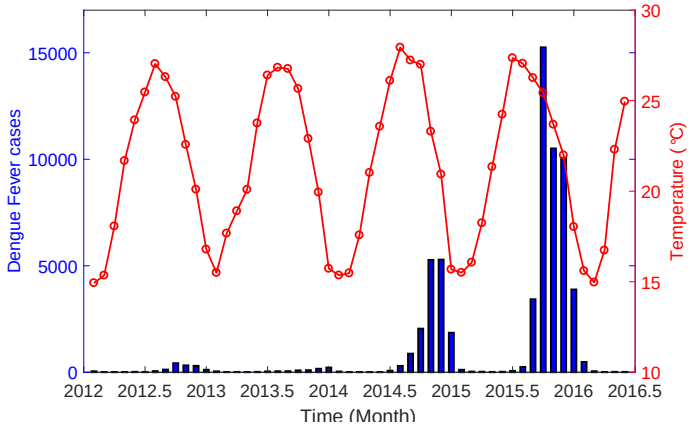

Figure 5-8: Monthly dengue cases (blue bar) and average temperature data (red dots) from January 2012 to May 2016 in Taiwan.

According to Taiwans Centers for Disease Control (Taiwan CDC), in 2014, 96% of the infected cases occurred in Kaohsiung city, which is located in the south of Taiwan. Kaohsiung

Symbol	Meaning	Value	Reference
ν	Vertical infection rate of *Aedes albopictus* mosquitoes	0.004	[81]
α	Host incubation rate (per day)	1/5	[86]
γ	Recovery rate for human (per day)	1/7	[23, 27, 81]
α_i	Host incubation rate with strain i (per day)	1/5	[86]
γ_i	Recovery rate for human with strain i (per day)	1/7	[23, 27, 81]
ϕ	Effect of antibody-dependent enhancement	1.5	[25]
f	Disease-induced mortality rate	0.005	[23, 87]
μ_{hb}	Human birth rate	0.000029	[85]
μ_{hd}	Human death rate	0.000016	[85]
$N_v(0)$	Total number of mosquitoes	608313×2	[27, 85]
$N_h(0)$	Total number of human	608313	[85]
x_1	Transmission mosquito-human probability	0.4455	data fitting
x_2	Transmission mosquito-human probability	1	data fitting
b	Biting rate per day	-	[31]
b_h	Probability of transmission of the virus per bite (v→h)	-	[76]
b_m	Probability of transmission of the virus per bite (h→v)	-	[76]
β_{vh}	Transmissible rate (v→h)	$x_1 b b_h$	[76]
β_{hv}	Transmissible rate (h→v)	$x_2 b b_m$	[76]
η	New infection rate by immigration	-	[84]
η_i	New primary infection rate by immigration for strain i	-	[84]
κ_i	New secondary infection rate i by immigration for strain	-	[84]

Table 5-3: Parameter; the symbol – refers to the time-dependent parameter.

is a petrochemical industrial city, with many pipelines running under the streets. Wang [88, 89] explains why dengue cases increased significantly in 2014 and 2015. An underground gas explosion was significantly correlated with the large dengue fever outbreaks in 2014. The holes caused by explosion and subsequently continuous heavy rains may have resulted in an increase in stagnant water which formed a good breeding habitat for mosquitoes. The mosquito population was expected to increase. Moreover, dengue fever outbreaks in 2014 and 2015 had predominant strains DENV1 and DENV2, respectively. There was a significant number of subsequently infected cases with the sever dengue symptoms in 2015. It is possible that dengue fever cases increased in 2015 due to the previously infected cases as well as the subsequently infected cases. In addition, the average temperatures in 2015 was $25.2°C$, which was $1.6°C$ higher than

that in 2014. The dengue incidence data has been applied to the control strategies. However, our models focus on the dengue transmission dynamics with seasonality in absence of control. We focus on the 2014 dengue fever outbreaks to fit our models to the data without control because the control strategies had not been implemented before the dengue major outbreak was initiated. The *Aedes aegypti* mosquitoes are predominant in subtropical and tropical regions including Taiwan. The vertical infection rate (ν) is 0.028 [81]. Population size in Taiwan in 2014 was 23434000 with the births and deaths 210383 and 163929, respectively. In other words, the birth rate (μ_{hb}) and death rate (μ_{hd}) per day were 0.000025 and 0.000019, respectively in Taiwan.

The transmission probability x_1 and x_2 are obtained from data fitting. We carry out numerical simulation on from week 0 (2013.12.29 − 2014.1.4) to week 80 (2015.5.3 − 2015.5.9). We set the number of initial infected human as 7 dengue cases on week 0 and the mosquito population size to be two times larger than the initial human population size.

Data fitting procedure

Step 1. We generate the daily temperature and dengue incidence data.

All weekly confirmed dengue cases are provided by Taiwan Center of Disease Control (Taiwan CDC), and there are 15997 reported dengue cases during week 0 − week 80. Monthly temperature is provided by Central Weather Bureau in Taiwan. The data of temperature and dengue confirmed cases have different time scales, and temperature-dependent parameters are based on daily unit time. We generate the daily temperature data and dengue incidence by using cubic spline interpolation.

Step 2. The daily incidence and weekly incidence are computed for the primary infection model.

The incidence at day t is defined by $\alpha E_h(t)$. The weekly incidence during seven days from day t_1 to day t_2 is computed as $\int_{t_1}^{t_2} \alpha E_h(t)dt$. The weekly incidence obtained from numerical simulations is the numerical result to fit the dengue incidence data.

Step 3. We carry out data fitting with least squares.

We use **LSQcurvefit** function from Matlab which implements data fitting with nonliear least squares methods. Since predominant strains are DENV1 and DENV2 in 2014 and 2015, respectively, we consider two time intervals to fit the data. One period denoted by T_1 is from week 0 (2013.12.29 − 2014.1.4) to week 52 (2014.12.21 − 2014.12.27), and the other period denoted by T_2 is from week 53 (2014.12.28 − 2015.1.3) to week 80 (2015.5.3 − 2015.5.9). As a result, x_1 and x_2 are 0.4455 and 1 on period T_1 in 2014. x_1 and x_2 are 0.0613 and 1 on period T_2 in 2015. Therefore, x_1 and x_2 are determined to be 0.4455 and 1, respectively, as the baseline value. Fig.5-9 indicates that the primary infection model provides good fit to the weekly incidence of dengue cases.

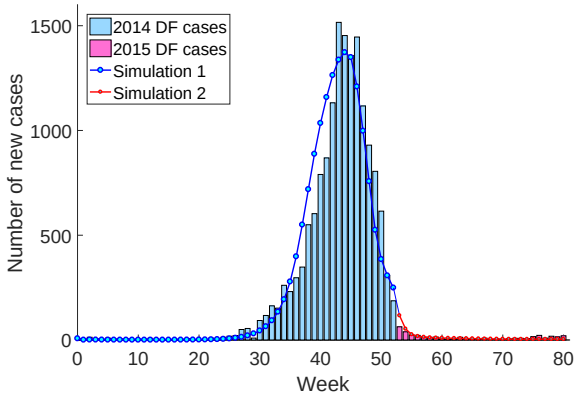

Figure 5-9: Comparison between numerical results and weekly dengue incidence data in Taiwan; Numerical results are obtained from primary infection model with the initial conditions of $I_h(0)$=7, which is the number of dengue cases on week 0, $I_v(0)$=14. The total population size is $N_h(0)$= 23434000, $N_v(0) = 2 \times N_h(0)$.

5.4 Stochastic dengue transmission model

5.4.1 The stochastic primary infection model

In the primary infection model (5.1.1), we denote the number of population of $(S_e, I_e, S_v, E_v, I_v, S_h, E_h, I_h, R_h)$ by $\mathbf{x} = (x_1, x_2, x_3, x_4, x_5, x_6, x_7, x_8, x_9)$ at time t, respectively. We write the stochastic governing equation of the model.

$$
\begin{aligned}
& \frac{dp(\mathbf{x},t)}{dt} \\
= \;& c_1(1 - c_{11}x_5/(x_3+x_4+x_5))\; p(\mathbf{x}-\mathbf{e}_1,t) + c_1c_{11}x_5/(x_3+x_4+x_5)\; p(\mathbf{x}-\mathbf{e}_2,t) \\
+ \;& c_2(x_1+1)\; p(\mathbf{x}+\mathbf{e}_1-\mathbf{e}_3,t) + c_2(x_2+1)\; p(\mathbf{x}+\mathbf{e}_2-\mathbf{e}_5,t) \\
+ \;& c_3(x_3+1)x_8/(x_6+x_7+x_8+x_9)\; p(\mathbf{x}+\mathbf{e}_3-\mathbf{e}_4,t) + c_5(x_4+1)\; p(\mathbf{x}+\mathbf{e}_4-\mathbf{e}_5,t) \\
+ \;& c_6(x_3+1)\; p(\mathbf{x}+\mathbf{e}_3,t) + c_6(x_4+1)\; p(\mathbf{x}+\mathbf{e}_4,t) \\
+ \;& c_6(x_5+1)\; p(\mathbf{x}+\mathbf{e}_5,t) + c_4x_5(x_6+1)/(x_6+x_7+x_8+x_9)\; p(\mathbf{x}+\mathbf{e}_6-\mathbf{e}_7,t) \\
+ \;& c_7(x_6+1)\; p(\mathbf{x}+\mathbf{e}_6-\mathbf{e}_7,t) + c_{12}(x_7+1)\; p(\mathbf{x}+\mathbf{e}_7-\mathbf{e}_8,t) \\
+ \;& c_8(x_8+1)\; p(\mathbf{x}+\mathbf{e}_8-\mathbf{e}_9,t) + c_9(x_6+x_7+x_8+x_9-1)\; p(\mathbf{x}-\mathbf{e}_6,t) \\
+ \;& c_{10}(x_6+1)\; p(\mathbf{x}+\mathbf{e}_6,t) + c_{10}(x_7+1)\; p(\mathbf{x}+\mathbf{e}_7,t) \\
+ \;& c_{10}(x_8+1)\; p(\mathbf{x}+\mathbf{e}_8,t) + c_{10}(x_9+1)\; p(\mathbf{x}+\mathbf{e}_9,t) \\
- \;& \big(c_1(1 - c_{11}x_5/(x_3+x_4+x_5)) + c_1c_{11}x_5/(x_3+x_4+x_5) + c_2x_1 \\
+ \;& c_2x_2 + c_3x_3x_8/(x_6+x_7+x_8+x_9) + c_5x_4 + c_6x_3 + c_6x_4 \\
+ \;& c_6x_5 + c_4x_5x_6/(x_6+x_7+x_8+x_9) + c_7x_6 + c_{12}x_7 + c_8x_8 \\
+ \;& c_9(x_6+x_7+x_8+x_9) + c_{10}x_6 + c_{10}x_7 + c_{10}x_8 + c_{10}x_9\big)\; p(\mathbf{x},t)
\end{aligned}
$$

where each $\mathbf{e}_i,\ i = 1, \ldots, 9$ denotes the 9 dimensional unit vector containing 1 at the i^{th} entry and 0. The probability constants are defined by

$$\begin{array}{cccc} c_1 = b_v & c_2 = \omega & c_3 = \beta_{hv} & c_4 = \beta_{vh} \\ c_5 = \varepsilon & c_6 = \mu_v & c_7 = \eta & c_8 = \gamma \\ c_9 = \mu_{hb} & c_{10} = \mu_{hd} & c_{11} = \nu & c_{12} = \alpha \end{array}$$

Table 5-4 shows the reactions and transition rates for primary infection model. By using MCM, we get 54 recursive moment equations in Appendix B.

Event	Process	Transition rate
Vector		
Oviposition of susceptible vector	$\phi \to S_e$	$b_v(1 - \nu I_v/N_v)$
Oviposition of infectious vector	$\phi \to I_e$	$b_v \nu I_v/N_v$
Maturation of susceptible pre-adult vector	$S_e \to S_v$	$(\omega_1 + \omega_2)S_e$
Maturation of infectious pre-adult vector	$I_e \to I_v$	$(\omega_1 + \omega_2)I_e$
Susceptible vector infection	$S_v \to E_v$	$\beta_{hv} S_v I_h/N_h$
Exposed vector becoming infectious	$E_v \to I_v$	εE_v
Death of susceptible vector	$S_v \to \phi$	$\mu_v S_v$
Death of exposed vector	$E_v \to \phi$	$\mu_v E_v$
Death of infectious vector	$I_v \to \phi$	$\mu_v I_v$
Human for primary infection		
Susceptible human infection by vector	$S_h \to E_h$	$\beta_{vh} I_v S_h/N_h$
Susceptible human infection through travel	$S_h \to E_h$	ηS_h
Exposed human becoming infectious	$E_h \to I_h$	αE_h
Recovery of infectious human	$I_h \to R_h$	γI_h
Birth of susceptible human	$\phi \to S_h$	$\mu_{hb} N_h$
Death of susceptible human	$S_h \to \phi$	$\mu_{hd} S_h$
Death of exposed human	$E_h \to \phi$	$\mu_{hd} E_h$
Death of infectious human	$I_h \to \phi$	$\mu_{hd} I_h$
Death of recovered human	$R_h \to \phi$	$\mu_{hd} R_h$

Table 5-4: Event type and process and transition rate for primary infection model.

5.4.2 The stochastic secondary infection model

In the secondary infection model from (5.1.2) to (5.1.3), we denote the number of population of $(S_e, I_{e1}, I_{e2}, S_v, E_{v1}, E_{v2}, I_{v1}, I_{v2}, S_h, E_{h1}, E_{h2}, I_{h1}, I_{h2}, R_{h1}, R_{h2}, E_{h12}, E_{h21}, I_{h12}, I_{h21}, R, D)$ by $\mathbf{x} = (x_1, x_2, \cdots, x_{20}, x_{21})$ at time t, respectively. We write the stochastic governing equation of

the model. To simplify the equation, define $\Sigma_v := \sum_{i=4}^{8} x_i$ and $\Sigma_h := \sum_{i=9}^{20} x_i$.

$$
\begin{aligned}
&\frac{dp(\mathbf{x},t)}{dt} \\
=\ & c_1(1-c_{16}(x_7+x_8)/\Sigma_v)\ p(\mathbf{x}-\mathbf{e}_1,t) + c_1c_{16}x_7/\Sigma_v\ p(\mathbf{x}-\mathbf{e}_2,t) + c_1c_{16}x_8/\Sigma_v\ p(\mathbf{x}-\mathbf{e}_3,t) \\
+\ & (c_2+c_3)(x_1+1)\ p(\mathbf{x}+\mathbf{e}_1-\mathbf{e}_4,t) + c_2(x_2+1)\ p(\mathbf{x}+\mathbf{e}_2-\mathbf{e}_7,t) \\
+\ & c_3(x_3+1)\ p(\mathbf{x}+\mathbf{e}_3-\mathbf{e}_8,t) + c_4(x_{12}+c_{19}x_{19})(x_4+1)/\Sigma_h\ p(\mathbf{x}+\mathbf{e}_4-\mathbf{e}_5,t) \\
+\ & c_4(x_{13}+c_{19}x_{18})(x_4+1)/\Sigma_h\ p(\mathbf{x}+\mathbf{e}_4-\mathbf{e}_6,t) + c_6(x_5+1)\ p(\mathbf{x}+\mathbf{e}_5-\mathbf{e}_7,t) \\
+\ & c_6(x_6+1)\ p(\mathbf{x}+\mathbf{e}_6-\mathbf{e}_8,t) + c_7(x_4+1)\ p(\mathbf{x}+\mathbf{e}_4,t) + c_7(x_5+1)\ p(\mathbf{x}+\mathbf{e}_5,t) \\
+\ & c_7(x_6+1)\ p(\mathbf{x}+\mathbf{e}_6,t) + c_7(x_7+1)\ p(\mathbf{x}+\mathbf{e}_7,t) + c_7(x_8+1)\ p(\mathbf{x}+\mathbf{e}_8,t) \\
+\ & c_5x_7(x_9+1)/\Sigma_h\ p(\mathbf{x}+\mathbf{e}_9-\mathbf{e}_{10},t) + c_5x_8(x_9+1)/\Sigma_h\ p(\mathbf{x}+\mathbf{e}_9-\mathbf{e}_{11},t) \\
+\ & c_8(x_9+1)\ p(\mathbf{x}+\mathbf{e}_9-\mathbf{e}_{10},t) + c_9(x_9+1)\ p(\mathbf{x}+\mathbf{e}_9-\mathbf{e}_{11},t) \\
+\ & c_{17}(x_{10}+1)\ p(\mathbf{x}+\mathbf{e}_{10}-\mathbf{e}_{12},t) + c_{18}(x_{11}+1)\ p(\mathbf{x}+\mathbf{e}_{11}-\mathbf{e}_{13},t) \\
\\
+\ & c_{12}(x_{12}+1)\ p(\mathbf{x}+\mathbf{e}_{12}-\mathbf{e}_{14},t) + c_{13}(x_{13}+1)\ p(\mathbf{x}+\mathbf{e}_{13}-\mathbf{e}_{15},t) \\
+\ & c_{14}(\Sigma_h-1)\ p(\mathbf{x}-\mathbf{e}_9,t) + c_{15}(x_9+1)\ p(\mathbf{x}+\mathbf{e}_9,t) + c_{15}(x_{10}+1)\ p(\mathbf{x}+\mathbf{e}_{10},t) \\
+\ & c_{15}(x_{11}+1)\ p(\mathbf{x}+\mathbf{e}_{11},t) + c_{15}(x_{12}+1)\ p(\mathbf{x}+\mathbf{e}_{12},t) + c_{15}(x_{13}+1)\ p(\mathbf{x}+\mathbf{e}_{13},t) \\
+\ & c_5x_8(x_{14}+1)/\Sigma_h\ p(\mathbf{x}+\mathbf{e}_{14}-\mathbf{e}_{16},t) + c_5x_7(x_{15}+1)/\Sigma_h\ p(\mathbf{x}+\mathbf{e}_{15}-\mathbf{e}_{17},t) \\
+\ & c_{18}(x_{16}+1)\ p(\mathbf{x}+\mathbf{e}_{16}-\mathbf{e}_{18},t) + c_{17}(x_{17}+1)\ p(\mathbf{x}+\mathbf{e}_{17}-\mathbf{e}_{19},t) \\
+\ & c_{13}(x_{18}+1)\ p(\mathbf{x}+\mathbf{e}_{18}-\mathbf{e}_{20},t) + c_{12}(x_{19}+1)\ p(\mathbf{x}+\mathbf{e}_{19}-\mathbf{e}_{20},t) \\
+\ & c_{11}(x_9+1)\ p(\mathbf{x}+\mathbf{e}_9-\mathbf{e}_{16},t) + c_{10}(x_9+1)\ p(\mathbf{x}+\mathbf{e}_9-\mathbf{e}_{17},t) + c_{15}(x_{14}+1)\ p(\mathbf{x}+\mathbf{e}_{14},t) \\
+\ & c_{15}(x_{15}+1)\ p(\mathbf{x}+\mathbf{e}_{15},t) + c_{15}(x_{16}+1)\ p(\mathbf{x}+\mathbf{e}_{16},t) + c_{15}(x_{17}+1)\ p(\mathbf{x}+\mathbf{e}_{17},t) \\
+\ & c_{15}(x_{18}+1)\ p(\mathbf{x}+\mathbf{e}_{18},t) + c_{15}(x_{19}+1)\ p(\mathbf{x}+\mathbf{e}_{19},t) + c_{20}(x_{18}+1)\ p(\mathbf{x}+\mathbf{e}_{18}-\mathbf{e}_{21},t) \\
+\ & c_{20}(x_{19}+1)\ p(\mathbf{x}+\mathbf{e}_{19}-\mathbf{e}_{21},t) + c_{15}(x_{20}+1)\ p(\mathbf{x}+\mathbf{e}_{20},t) - \big(c_1(1-c_{16}(x_7+x_8)/\Sigma_v) \\
+\ & c_1c_{16}x_7/\Sigma_v + c_1c_{16}x_8/\Sigma_v + (c_2+c_3)x_1 + c_2x_2 + c_3x_3 + c_4(x_{12}+c_{19}x_{19})x_4/\Sigma_h \\
+\ & c_4(x_{13}+c_{19}x_{18})x_4/\Sigma_h + c_6x_5 + c_6x_6 + c_7x_4 + c_7x_5 + c_7x_6 + c_7x_7 + c_7x_8 + c_5x_7x_9/\Sigma_h \\
+\ & c_5x_8x_9/\Sigma_h + c_8x_9 + c_9x_9 + c_{17}x_{10} + c_{18}x_{11} + c_{12}x_{12} + c_{13}x_{13} + c_{14}\Sigma_h + c_{15}x_9 \\
+\ & c_{15}x_{10} + c_{15}x_{11} + c_{15}x_{12} + c_{15}x_{13} + c_5x_8x_{14}/\Sigma_h + c_5x_7x_{15}/\Sigma_h + c_{18}x_{16} + c_{17}x_{17} \\
+\ & c_{13}x_{18} + c_{12}x_{19} + c_{11}x_9 + c_{10}x_9 + c_{15}x_{14} + c_{15}x_{15} + c_{15}x_{16} + c_{15}x_{17} + c_{15}x_{18} + c_{15}x_{19} \\
+\ & c_{20}x_{18} + c_{20}x_{19} + c_{15}x_{20}\big)\ p(\mathbf{x},t)
\end{aligned}
$$

where each $\mathbf{e}_i,\ i = 1,\ldots,21$ denotes the 21 dimensional unit vector containing 1 at the i^{th} entry and 0.

$$
\begin{array}{lllll}
c_1 = b_v & c_2 = \omega_1 & c_3 = \omega_2 & c_4 = \beta_{hv} & c_5 = \beta_{vh} \\
c_6 = \varepsilon & c_7 = \mu_v & c_8 = \eta_1 & c_9 = \eta_2 & c_{10} = \kappa_1 \\
c_{11} = \kappa_2 & c_{12} = \gamma_1 & c_{13} = \gamma_2 & c_{14} = \mu_{hb} & c_{15} = \mu_{hd} \\
c_{16} = \nu & c_{17} = \alpha_1 & c_{18} = \alpha_2 & c_{19} = \phi & c_{20} = f
\end{array}
$$

Table 5-5 shows the reactions and transition rates for secondary infection model in terms of three types of reactions for vector, human for primary infection and human for secondary infection. By using MCM, we get 21 first moments and 231 second central moments for secondary infection model.

5.5 Results

The simulation results predict the climate dependent behavior of the dengue prevalence for human and mosquito population in Jeju Island, Korea. Temperature changes are estimated by RCP 4.5 and RCP 8.5 climate change scenarios. We assume that the first case is confirmed on June 1, 2017 in Jeju Island. The total population size of the island is 608313, estimated from [90]. The Birth rate and death rate per day are 0.000029 and 0.000016, respectively [85]. The initial population size of human and mosquito is given by $N_h = 608313, N_v = 608313 \times 2$ because the mosquito population size is larger than the human population size [25].

5.5.1 Dengue transmission dynamics for deterministic model based on RCP 4.5 and 8.5 scenarios

Fig.5-10 shows the time evolution of the dengue outbreaks of deterministic model for the primary infection from 2017 to 2067 for 50 years. The initial infected individuals are given as $I_h = 5$ and $I_v = 0$. The dengue outbreaks for human and mosquitoes have the periodic patterns which mimic the re-emerging dengue fever. Infected individuals reach a peak by the early of August. We investigate how the dengue outbreaks are influenced by the temperature data. In the RCP 8.5 scenario, the dengue outbreak starts earlier with larger and more frequent peaks compared to RCP 4.5 scenario. Dengue epidemics occur with an approximate 10-year period for major outbreak and 5-year period for minor outbreak for both RCP 4.5 and RCP 8.5 data in Jeju Island over 50 years. In tropical area such as Bangkok, Thailand, dengue outbreaks have been the 3-year period pattern [25].

Fig.5-11 shows the time evolution of the dengue outbreaks of deterministic model for secondary infection from 2017 to 2067 for 50 years. The initial infected individuals are given as I_{h1}=5, I_{h2}=2, and I_{v1}=0, I_{v2}=0. The first major outbreak of dengue cases is distributed from year 5 to year 15 based on RCP 8.5 scenario and is distributed from year 10 to year 20 based

Event	Process	Transition rate
Vector		
Oviposition of susceptible vector	$\phi \rightarrow S_e$	$b_v\big(1-\nu(I_{v1}+I_{v2})/N_v\big)$
Oviposition of infectious vector with strain i	$\phi \rightarrow I_{ei}$	$b_v\nu I_{vi}/N_v$
Maturation of susceptible pre-adult vector	$S_e \rightarrow S_v$	$(\omega_1+\omega_2)S_e$
Maturation of infectious pre-adult vector with strain i	$I_{ei} \rightarrow I_{vi}$	$\omega_i I_{ei}$
Susceptible vector infection for strain i	$S_v \rightarrow E_{vi}$	$\beta_{hv}S_v(I_{hi}+\phi I_{hji})/N_h$
Exposed vector becoming infectious for strain i	$E_{vi} \rightarrow I_{vi}$	εE_{vi}
Death of susceptible vector	$S_v \rightarrow \phi$	$\mu_v S_v$
Death of exposed vector with strain i	$E_{vi} \rightarrow \phi$	$\mu_v E_{vi}$
Death of infectious vector with strain i	$I_{vi} \rightarrow \phi$	$\mu_v I_{vi}$
Human for primary infection		
Susceptible human infection by vector with strain i	$S_h \rightarrow E_{hi}$	$\beta_{vh}I_{vi}S_h/N_h$
Susceptible human infection by strain i through travel	$S_h \rightarrow E_{hi}$	$\eta_i S_h$
Exposed human becoming infectious by strain i	$E_{hi} \rightarrow I_{hi}$	$\alpha_i E_{hi}$
Recovery of infectious human by strain i	$I_{hi} \rightarrow R_{hi}$	$\gamma_i I_{hi}$
Birth of susceptible human	$\phi \rightarrow S_h$	$\mu_{hb}N_h$
Death of susceptible human	$S_h \rightarrow \phi$	$\mu_{hd}S_h$
Death of exposed human with strain i	$E_{hi} \rightarrow \phi$	$\mu_{hd}E_{hi}$
Death of infectious human with strain i	$I_{hi} \rightarrow \phi$	$\mu_{hd}I_{hi}$
Human for secondary infection		
Susceptible human for strain j who is recovered from strain i	$R_{hi} \rightarrow E_{hij}$	$\beta_{vh}I_{vj}R_{hi}/N_h$
Secondarily exposed human becoming infectious for strain j	$E_{hij} \rightarrow I_{hij}$	$\alpha_j E_{ij}$
Recovery of secondarily infectious human by strain j	$I_{hij} \rightarrow R$	$\gamma_j I_{hij}$
Inflow rate of secondary infection by international travel	$S_h \rightarrow E_{hij}$	$\kappa_j S_h$
Death of recovered human by strain i	$R_{hi} \rightarrow \phi$	$\mu_{hd}R_{hi}$
Death of re-infected human who is exposed by strain j	$E_{hij} \rightarrow \phi$	$\mu_{hd}E_{hij}$
Death of re-infected human who is infectious by strain j	$I_{hij} \rightarrow \phi$	$\mu_{hd}I_{hij}$
Fatality of re-infected human who is infectious by strain j	$I_{hij} \rightarrow D$	fI_{hij}
Recovery of re-infected human who is infectious by strain j	$R \rightarrow \phi$	$\mu_{hd}R$

Table 5-5: Event type and process and transition rate for secondary infection model.

on RCP 4.5. Primarily infectious human occurs consistently with the relatively small peak size after the first major outbreak. Secondarily infectious human occurs with the 10-year period pattern of the major outbreak starting after year 10. Fig.5-11 (d) describes that there are more cumulative fatality cases after 50 years based on RCP 8.5 scenario than the results based on

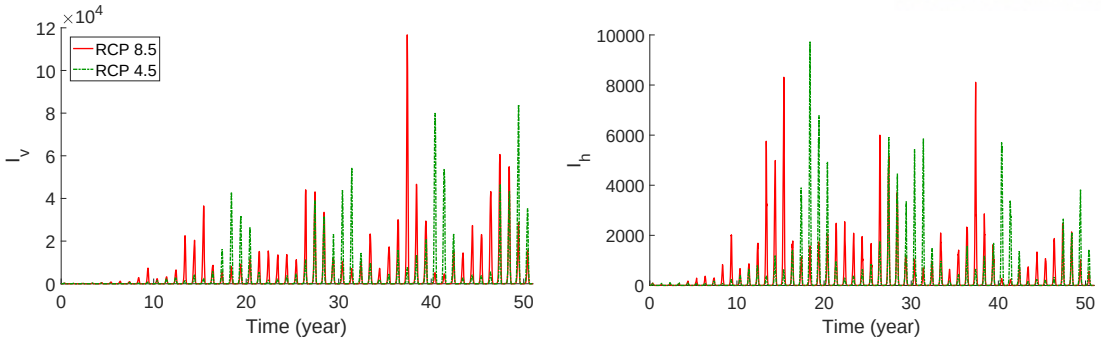

(a) Infectious mosquito (b) Infectious human

Figure 5-10: Primary infection: the infectious mosquito and infectious human are displayed during 50 years based on RCP 4.5 (green dashed line) and RCP 8.5 (red solid line). The initial conditions are set as $I_h(0)$=5, $I_v(0)$=0, $N_h(0)$=608313, $N_v(0)$=2×608313.

RCP 4.5 data.

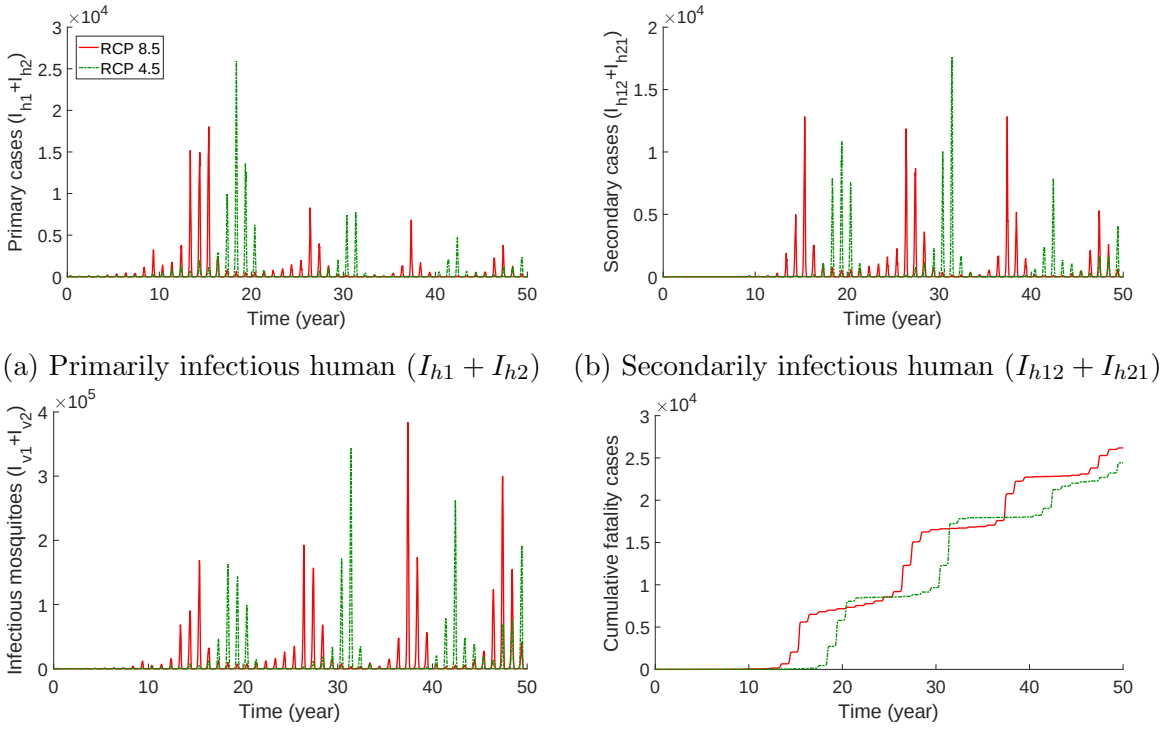

(a) Primarily infectious human ($I_{h1} + I_{h2}$) (b) Secondarily infectious human ($I_{h12} + I_{h21}$)

(c) Infectious mosquitoes ($I_{v1} + I_{v2}$) (d) Cumulative fatality cases

Figure 5-11: Secondary infection: the infectious mosquito, infectious human and cumulative fatality cases and are displayed during 50 years based on RCP 4.5 (green dashed line) and RCP 8.5 (red solid line). The initial conditions are set as $I_{v1}(0) = I_{v2}(0) = 0, I_{h1}(0) = 5, I_{h2}(0) = 2$, $N_h(0)$=608313, $N_v(0)$=2×608313.

5.5.2 Comparison of deterministic and stochastic models based on RCP 8.5

Primary infection model

We consider the stochastic system including the climate changes and international travel rate. Fig.5-12 compares the time evolution of the mean and standard deviation of infectious human (I_h) and infectious mosquito (I_v) between the SSA and the MCM. The MCM can accurately reconstruct the means as well as the standard deviations. For 1000 realizations of SSA runs, the computation time takes 19 hours. However, the MCM takes only one second without the Monte-Carlo procedure. Now, we apply the MCM instead of the SSA to solve the stochastic models for dengue transmission dynamics of the large population size in terms of computational efficiency. We compare the dynamics of the primary infection model between the results of stochastic and deterministic models when the number of initial infectious people is small enough as 5 and the number of infected mosquitoes is zero in Fig.5-13. The dynamical behaviors of the two models are similar, but there is a significant difference near the peak from year 14 to year 19. Fig.5-14 shows that the quantitative discrepancies between the deterministic and stochastic models becomes small when the initial number of infected individuals is sufficiently large as 2% of the total human population size.

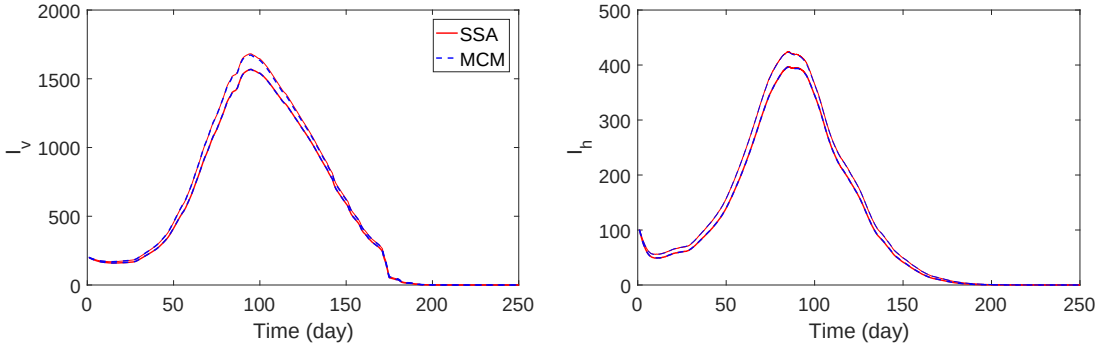

(a) Infectious mosquito (I_v) (b) Infectious human (I_h)

Figure 5-12: Comparison of the mean (lower curves) and mean + standard deviation (upper curves) for SSA (red lines) and MCM (blue dashed lines) for the stochastic primary infection model. The initial conditions are $I_h(0)$=100, $I_v(0)$=200, N_h=5000, N_v=10000. The results of SSA are based on 1000 realizations.

Secondary infection model

Fig.5-15 compares the time evolution of the mean and standard deviation for primarily infectious human I_{hi} and secondarily infectious human I_{hij} between the SSA and MCM. The solution of MCM seems to track well with the SSA. Moreover, it takes approximately only 8 seconds to find the solution by using MCM. The SSA runs 1000 realizations and the computation time takes 8 hours if we consider the climate changes based on RCP 8.5 and international travel rate. We compare the time evolution dynamics of secondary infection model between

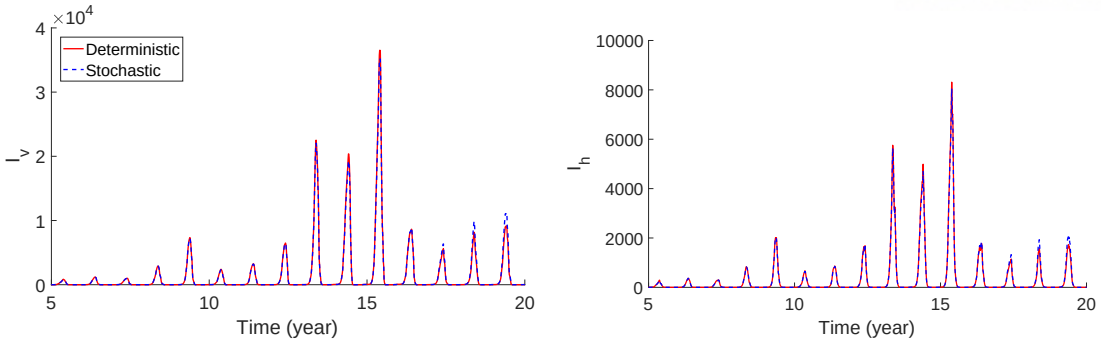

(a) Infectious mosquito (I_v) (b) Infectious human (I_h)

Figure 5-13: Comparison of the mean of stochastic model (blue dashed line) and the solution of the deterministic model (red solid line) for the primary infection model. The initial conditions are $I_h(0)$=5, $I_v(0)$=0, $N_h(0)$=608313, $N_v(0)$=2×608313.

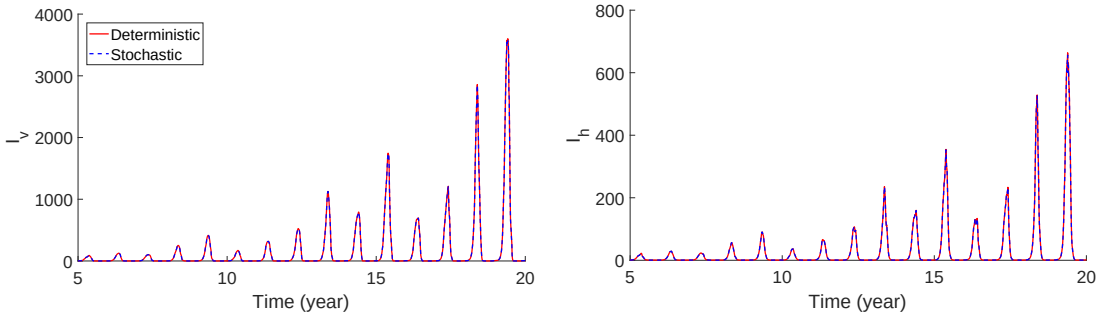

(a) Infectious mosquito (I_v) (b) Infectious human (I_h)

Figure 5-14: Comparison of the mean of stochastic model (blue dashed line) and the solution of the deterministic model (red solid line) for the primary infection model. The initial conditions are $I_h(0)$=2500, $I_v(0)$=5000, $N_h(0)$=608313, $N_v(0)$=2×608313.

the results of stochastic and deterministic models when the initial infectious human is small as I_{h1}=5 and I_{h2}=2, $I_{v1} = I_{v2}$=0 in Fig.5-16. The dynamics of two models are similar, but there exists significant discrepancy from year 13 to year 19 at the peak. The cumulative fatality cases increase rapidly from year 13 to year 16. Fig.5-17 represents the mean of stochastic model concurs to the solution of the deterministic model when the number of initial infected individuals for human and mosquitoes of dengue infection was large enough as 6.5% of the total human population size.

5.5.3 The effect of the inflow rate of dengue cases by international travel

We investigate how the inflow rate of imported infection by travelers influences on the dynamics of infected individuals. For the primary infection model, η is replaced with $\eta(1-u)$. Likewise, in case of secondary infection model, η_i and κ_i are the imported dengue factors by international travel for strain i, where u is the reduced inflow rate by control strategies.

As the result of primary infection model, one can see that the peak size increases as u is smaller, which refers to the reduction of control interventions in Fig.5-18. Therefore, the inflow

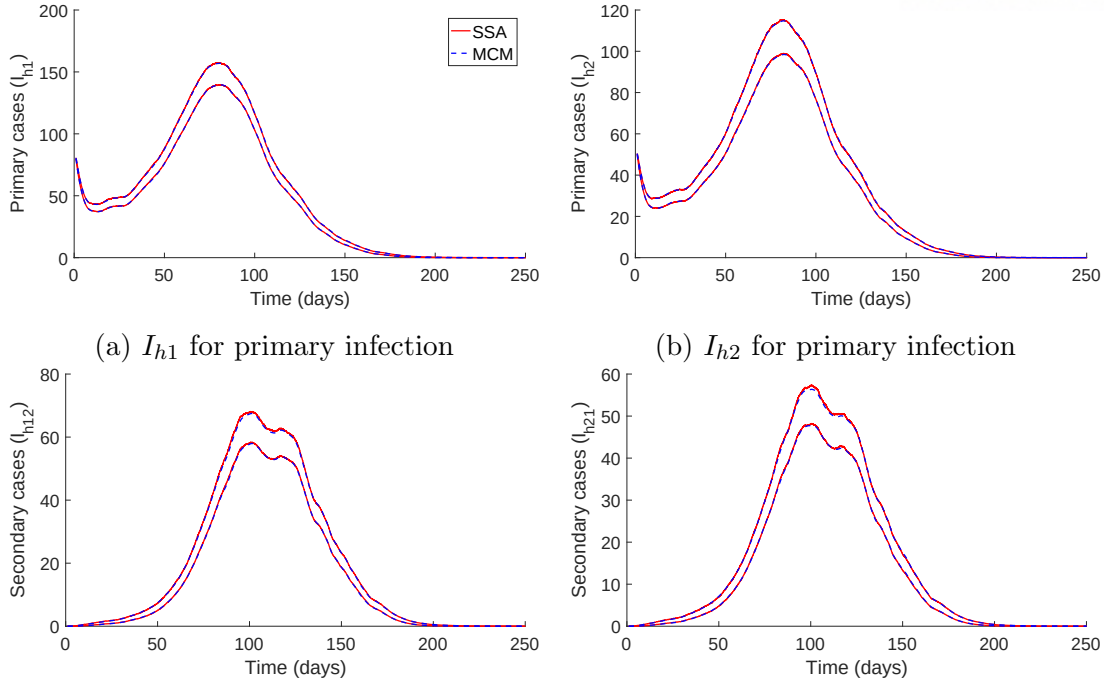

(a) I_{h1} for primary infection

(b) I_{h2} for primary infection

(c) I_{h12} for secondary infection

(d) I_{h21} for secondary infection

Figure 5-15: Comparison of the mean (lower curves) and mean + standard deviation (upper curves) for SSA (red lines) and MCM (blue dashed lines) for the stochastic secondary infection model. The initial conditions are $I_{h1}(0)$=80, $I_{h2}(0)$=50, $I_{v1}(0)$=150, $I_{v2}(0)$=100, $N_h(0)$=3000, $N_v(0)$=5000. The results of SSA are based on 1000 realizations taking about 8 hours.

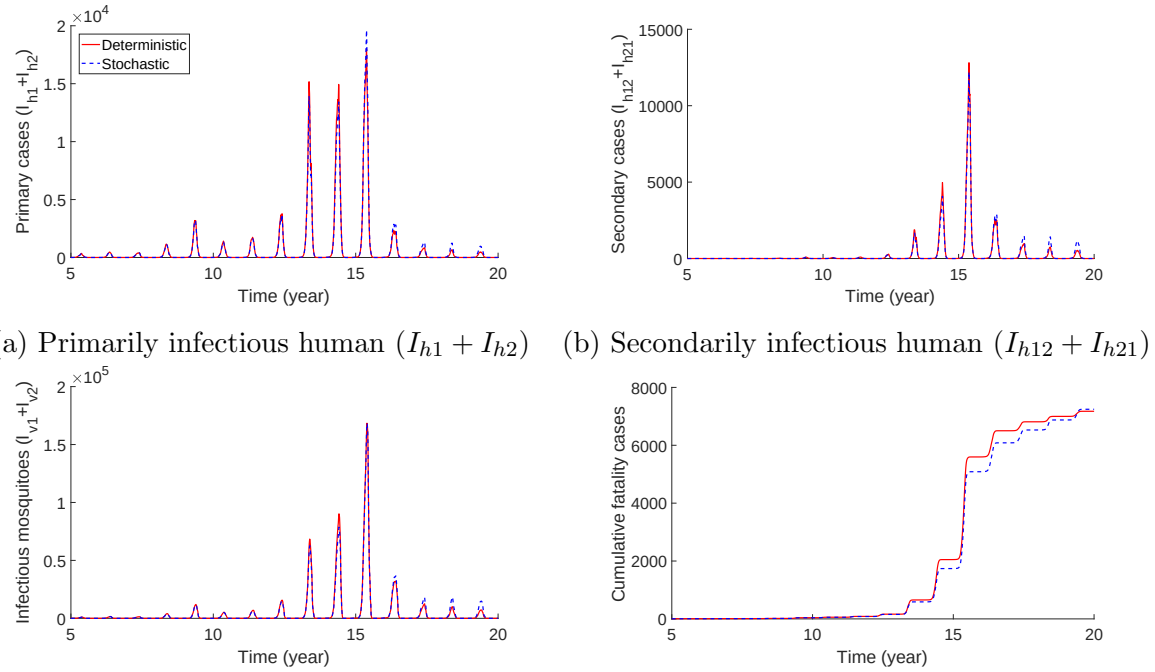

(a) Primarily infectious human ($I_{h1} + I_{h2}$)

(b) Secondarily infectious human ($I_{h12} + I_{h21}$)

(c) Infectious mosquitoes ($I_{v1} + I_{v2}$)

(d) Cumulative fatality cases

Figure 5-16: Comparison of the mean of stochastic model (blue dashed line) and the solution of the deterministic model (red solid line) for the secondary infection model. The initial conditions are $I_{v1}(0) = I_{v2}(0) = 0, I_{h1}(0) = 5, I_{h2}(0) = 2$, $N_h(0)$=608313, $N_v(0)$=2×608313.

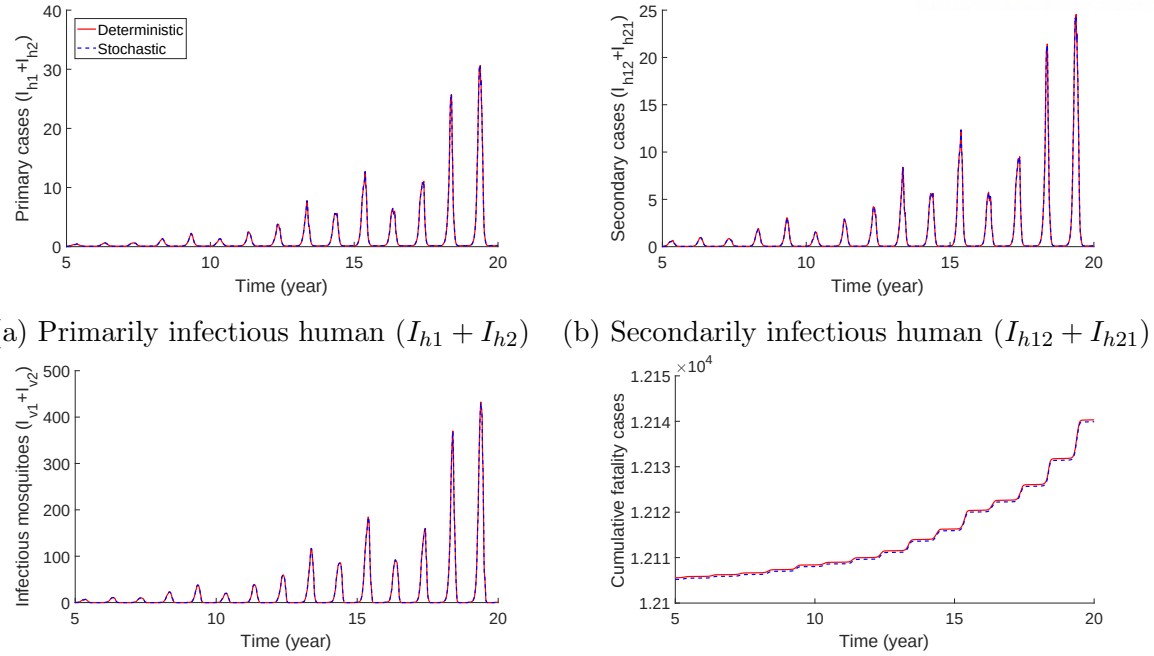

(a) Primarily infectious human $(I_{h1} + I_{h2})$ (b) Secondarily infectious human $(I_{h12} + I_{h21})$

(c) Infectious mosquitoes $(I_{v1} + I_{v2})$ (d) Cumulative fatality cases

Figure 5-17: Comparison of the mean of stochastic model (blue dashed line) and the solution of the deterministic model (red solid line) for the secondary infection model. The initial conditions are $I_{v1}(0) = 50000, I_{v2}(0) = 30000, I_{h1}(0) = 25000, I_{h2}(0) = 15000$, $N_h(0)$=608313, $N_v(0)$=2×608313.

rate by travelers increases the number of dengue incidence.

Now, we wonder how the amount of difference of the peak size between deterministic and stochastic models depends on u. Fig.5-19 (a) shows the difference of the peak in year 9 for infectious human (I_h) between deterministic and stochastic model depending on u. The difference of the peak is defined as $(x(u) - y(u))$, where $x(u)$, $y(u)$ are the peak size of ODE and MCM at time $t \in [9, 10]$ depending on u. Normalization is an attempt to realize the relative difference since the peak size scales correspondingly to various values of u. The Normalization of each peak size is based on the ODE solution for each values of u. The relative difference is defined as $(x(u) - y(u))/x(u)$, where $x(u)$ and $y(u)$ are the peak size of ODE and MCM at time $t \in [9, 10]$. In Fig.5-19 (b), u and the peak size are negatively correlated, and the relative discrepancy between the two models increases as u grows larger. Therefore, Fig.5-18 and Fig.5-19 show that as u decreases, the intensity of control strategies is reduced, which consequently increases the inflow rate of international travel. Finally, the solution of stochastic model converges to the solution of deterministic model.

For the result of secondary infection model, Fig.5-20 shows that the peak size increases as u decreases for both primary cases $(I_{h1}+I_{h2})$ and secondary cases $(I_{h12}+I_{h21})$. The control of the reduction for the inflow rate is sufficiently effective to prevent the dengue epidemic, especially for the long time scale. We compare the difference of the peak size between deterministic and stochastic models in accordance with the control level of u. Here, we focus on the primary cases rather than the secondary cases. In Fig.5-21 (a), if the control for the imported dengue

cases become stronger (i.e., u increases), then the difference of peak size between two models is smaller quantitatively due to the decrease in imported cases. Fig.5-21 (b) indicates the normalized difference of peak size. If the control is stronger, the discrepancy of peak size between the two models increases quantitatively.

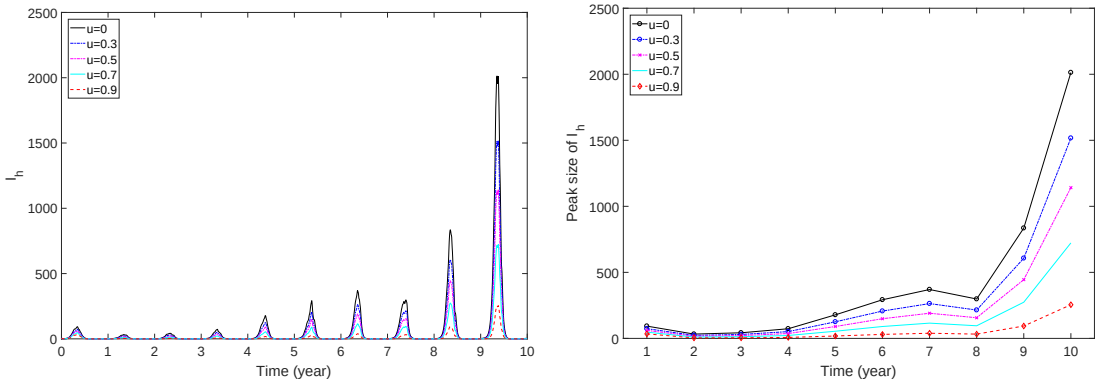

(a) Infectious human (I_h) (b) Peak size of I_h

Figure 5-18: Primary infection: the number of the infectious human is displayed during 10 years depending on u to control the inflow rate of travelers. Inflow rate with control is defined as $\eta(1-u)$; (a) I_h with control u and (b) the peak size of I_h for each year with control u. The initial conditions are set as $I_h(0)$=5, $I_v(0)$=0, $N_h(0)$=608313, $N_v(0)$=2×608313.

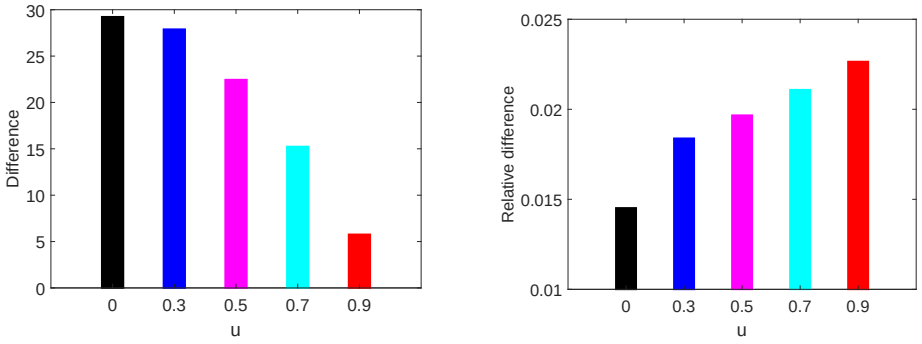

(a) Difference of peak size of I_h (b) Relative difference of peak size of I_h

Figure 5-19: Primary infection: the difference of peak size of infectious human is displayed between deterministic and stochastic model at year 9. Inflow rate with control is defined as $\eta(1-u)$; (a) $(x(u)-y(u))$ and (b) $(x(u)-y(u))/x(u)$, where $x(u)$ and $y(u)$ are the peak size of ODE and MCM at time $t \in [9, 10]$.

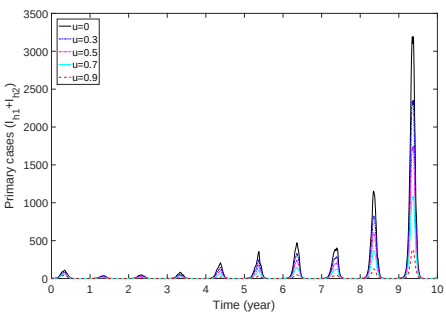

(a) Primarily infectious human $(I_{h1} + I_{h2})$

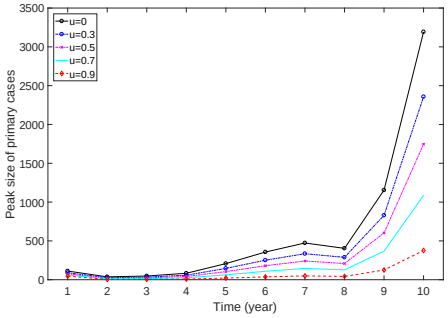

(b) Peak size of primary cases

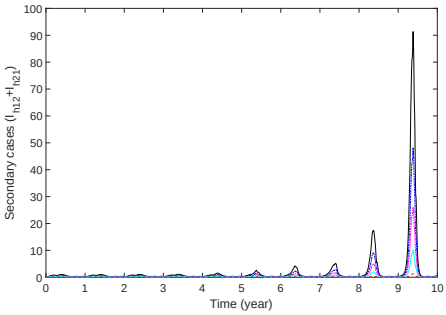

(c) Secondarily infectious human $(I_{h12} + I_{h21})$

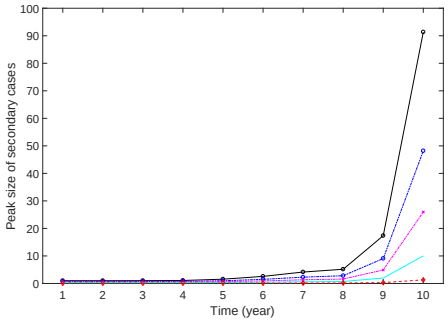

(d) Peak size of secondary cases

Figure 5-20: Secondary infection: the numbers of the primarily infectious human $(I_{h1} + I_{h2})$ and secondarily infectious human $(I_{h12} + I_{h21})$ are displayed for 10 years depending on u to control the inflow rate of travelers. Inflow rates with control for primary infection and secondary infection are defined as $\eta_i(1-u), \kappa_i(1-u)$ for strain i, respectively; (a)-(b) primarily infectious human $(I_{h1}+I_{h2})$ with control u and (c)-(d) secondarily infectious human $(I_{h12} + I_{h21})$ with control u. The initial conditions are $I_{v1}(0) = I_{v2}(0) = 0, I_{h1}(0) = 5, I_{h2}(0) = 2$, $N_h(0)$=608313, $N_v(0)$=2×608313.

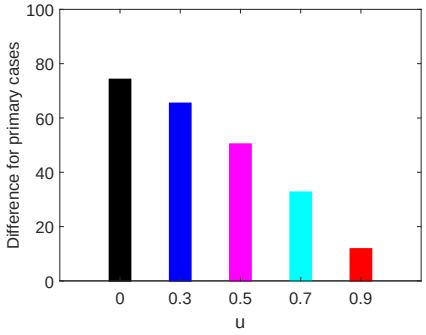

(a) Difference of peak size

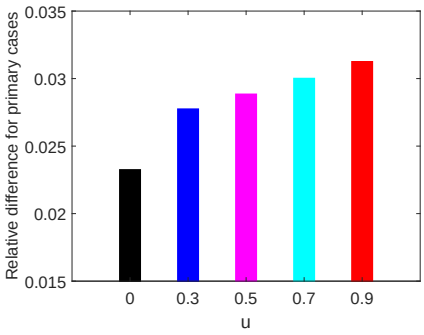

(b) Relative difference of peak size

Figure 5-21: Secondary infection: the difference of peak size of primarily infectious human $(I_{h1} + I_{h2})$ is displayed between deterministic and stochastic model at year 9. Inflow rates with control for primary infection and secondary infection are defined as $\eta_i(1-u), \kappa_i(1-u)$ for strain i, respectively; (a) $(x(u) - y(u))$ and (b) $(x(u) - y(u))/x(u)$, where x(u), y(u) are the peak size of ODE and MCM at time $t \in [9, 10]$.

5.5.4 Sensitivity analysis

The infection dynamics of a deterministic model is determined by parameters. The sensitivity analysis describes how influential each parameter is to the spread of disease. Sensitivity analysis results help us to choose the highly sensitive parameters. On the other hand, an insensitive parameter does not have to be carefully estimated. We carry out sensitivity analysis considering constant parameters and temperature dependent parameters. Rodrigues described the normalized forward sensitivity index of R_0 in [91]. We defined the normalized forward sensitivity index of cumulative incidence (CI), which depends on a parameter p in a differentiable manner.

$$r_p^{(CI)} = \frac{\partial(CI)}{\partial p} \times \frac{p}{(CI)}.$$

Sensitivity analysis helps us to identify the highly sensitive parameters which require caution and effort to estimate. On the other hand, insensitive parameters do not require as much effort as the highly sensitive parameters to be estimated. 100 sets are randomly selected from a uniform distribution between the range of $\pm$ 20% of the baseline of constant parameters given by Table 5-3. Fig.5-22 shows the elasticities of CI with respect to each parameter for 100 sets of randomly sampled parameter values from a uniform distribution. We set day 1 on Jan. 1, 2017 and compute the CI of infectious human from day 1 to day 400. Fig.5-22 (a) shows the elasticity for cumulative incidence in primary infection model. The cumulative incidence from day t_1 to day t_2 is defined as $\int_{t_1}^{t_2} \alpha E_h(t)dt$, where $t_1 = 1, t_2 = 400$. The elasticity of the recovery rate (γ) has the large width of the box (Inter Quartile Range, IQR) which indicates the important parameter to disease transmission. α is the weakly positive influential parameter. However, γ is the strongly negative influential parameter. Fig.5-22 (b) shows the elasticity for cumulative incidence in secondary infection model. The cumulative incidence from day t_1 to day t_2 is defined as $\int_{t_1}^{t_2} (\alpha_1 E_{h1}(t) + \alpha_2 E_{h2}(t) + \alpha_1 E_{h21}(t) + \alpha_2 E_{h12}(t))\, dt$. Therefore, α_i, ϕ are the weakly positive influential parameter. Moreover, γ_i is the highest influence on the CI among all constant parameters. If γ_i is increased by 10%, then the CI decreases by 12%.

Sensitivity analysis of temperature dependent parameters

Now, we investigate how much parameters regarding the change of the temperature influence the seasonal reproduction number (R_s). Temperature dependent parameters are defined in section 5.3.1. We derived seasonal reproduction numbers for the primary infection model in section 5.2.1 and the secondary infection model in section 5.3.1. The seasonal reproduction number of

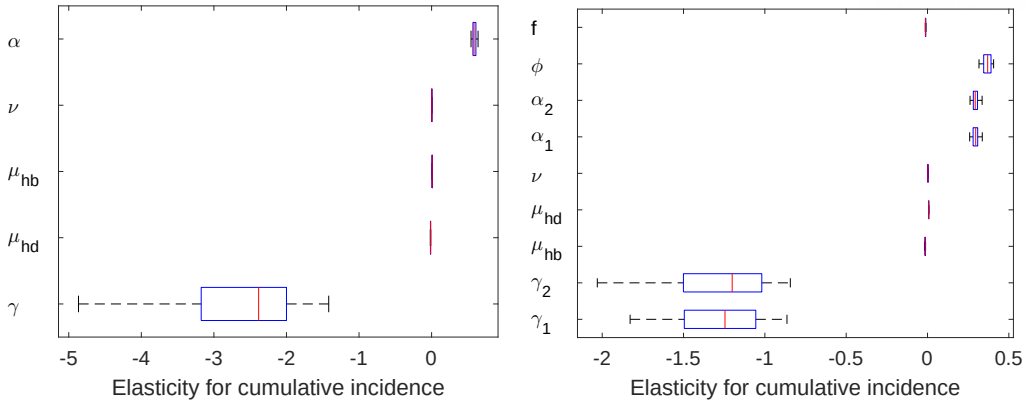

(a) Primary infection model (b) Secondary infection model

Figure 5-22: Elasticity on cumulative incidence of infectious human; (a) primary infection model under the initial conditions as $I_h(0)$=5, $I_v(0)$=0, $N_h(0)$=608313, $N_v(0)$=2×608313. (b) secondary infection model under the initial conditions as $I_{v1}(0) = I_{v2}(0) = 0, I_{h1}(0) = 5, I_{h2}(0) = 2$, $N_h(0)$=608313, $N_v(0)$=2×608313.

the primary infection model is computed as

$$\begin{aligned} R_s &= \frac{A}{2} + \frac{1}{2}\sqrt{A^2 + 4\Lambda} \\ A &= \frac{b_v(t)\nu}{\mu_v(t)N_v(t)}, \\ \Lambda &= \frac{\alpha\beta_{hv}(t)\beta_{vh}(t)\varepsilon(t)S_h(t)S_v(t)}{(\alpha+\mu_{hd})\mu_v(t)(\varepsilon(t)+\mu_v(t))(\mu_{hd}+\gamma)N_h(t)^2} \end{aligned} \tag{5.5.1}$$

The seasonal reproduction number of the secondary infection model is computed as

$$\begin{aligned} R_s &= max(R_{s1}, R_{s2}) \\ R_{s1} &= \frac{A}{2} + \frac{1}{2}\sqrt{A^2 + 4\Lambda_1}, \\ R_{s2} &= \frac{A}{2} + \frac{1}{2}\sqrt{A^2 + 4\Lambda_2} \\ \text{where} \quad A &= \frac{b_v(t)\nu}{\mu_v(t)N_v(t)}, \quad \Lambda_i = \frac{\alpha_i\beta_{hv}(t)\beta_{vh}(t)\varepsilon(t)S_h(t)S_v(t)}{(\alpha_i+\mu_{hd})\mu_v(t)(\varepsilon(t)+\mu_v(t))(\mu_{hd}+\gamma_i)N_h(t)^2} \end{aligned} \tag{5.5.2}$$

Fig.5-23 shows the values of temperature dependent parameters under the RCP 8.5 scenario varying time starting on Jan.1, 2017. The maturation rate (ω), virus incubation rate (ε) and transmissible rates (β_{hv}, β_{vh}) are maintained highly between day 150 to day 250 which refers to the summer season. On the other hand, the mortality rate of mosquitoes (μ_v) is close to zero in this time interval. From here, we focus on the primary infection model. The results of secondary infection model are similar to those of primary infection model because the impact of the secondary infection on the dynamics is relatively small within a short time period. In Fig.5-24, the infectious human (I_h) and the seasonal reproduction number (R_s) are investigated. The number of infectious human increases between day 150 and day 250 when the R_s is larger

than 1. The outline of procedure to perform the sensitivity analysis for temperature dependent parameters is summarized by the following three steps.

Outline of procedure

Step 1. A random sampling is used to generate 100 values randomly selected from the uniform distribution between the range of ±0.5% of Kelvin daily temperature. Then, kelvin (K) is converted to celsius ($^{\circ}C$) by adding 273 degrees to it. Fig.5-25 (a) shows the daily temperature ($^{\circ}C$) based on RCP 8.5 and the range of sampling for each temperature.

Step 2. The 100 sets of temperature dependent parameters for each day are given by randomly selected daily temperature. Fig.5-25 (b) shows the 100 realizations of infectious human (I_h) in accordance with the 100 parameter samples.

Step 3. The Partial Rank Correlation Coefficients (PRCCs) measure monotonic relationship. The PRCCs as a function of time are computed for R_s in Fig.5-26. The monotone relationship is positive (negative) as PRCC closes to 1 (-1).

Fig.5-26 shows the significant parameters over the time interval. The change of daily PRCC values is relatively large since the dynamics of R_s over time have the fluctuations due to the daily temperature data. We focus on the PRCC on time interval rather than the daily PRCC values. For example, transmissible rates (β_{hv}, β_{vh}) are strongly positive parameters on R_s over the entire time interval. Meanwhile, mortality rate (μ_v) is strongly negative between day 180 and day 240 when the number of infectious human rapidly increases. Moreover, the values of PRCC are significantly changed, especially for ω in the time interval with the dramatic rise of the number of infectious human. Fig.5-27 investigate the relationship between parameters on R_s at specific time point. We clearly observe that the transmissible rates are strongly influential parameters and mortality rate is negative parameter on R_s at day 180.

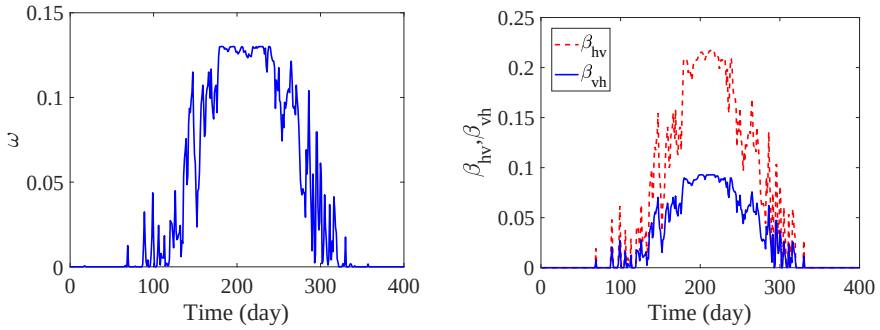

(a) Pre-adult maturation rate (ω) (b) Transmissible rate (β_{hv}, β_{hv})

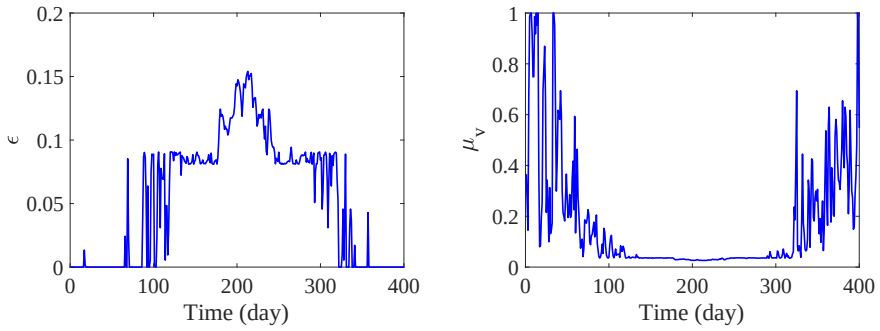

(c) Virus incubation rate (ε) (d) Mortality rate (μ_v)

Figure 5-23: Daily temperature dependent parameters are displayed over the time based on RCP 8.5 scenario starting on Jan. 1, 2017.

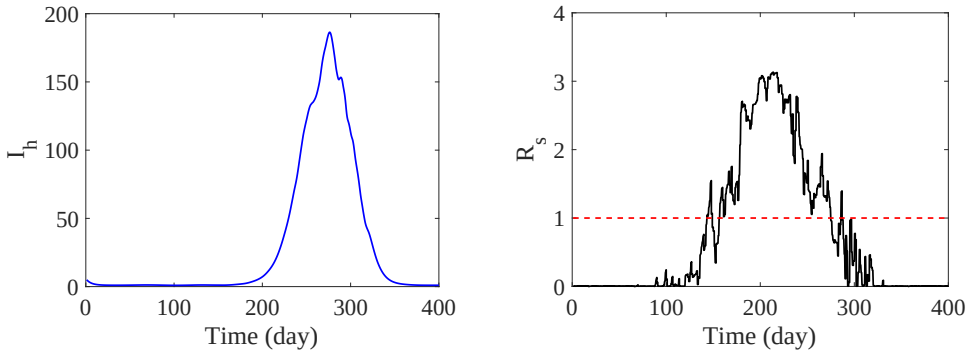

(a) Infectious human (I_h) (b) Seasonal reproduction number (R_s)

Figure 5-24: Infectious human (I_h) and the seasonal reproduction number for primary infection model are displayed. (b) red dashed line refers to $R_s = 1$.

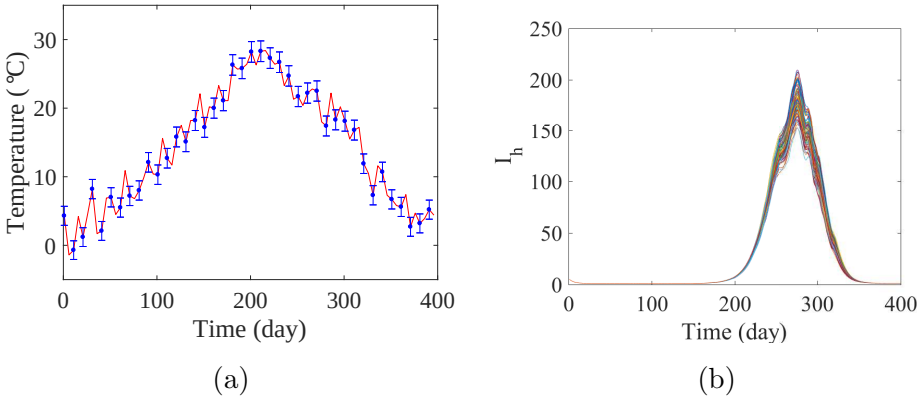

Figure 5-25: Random sampling: (a) daily temperature based on RCP 8.5 (red solid) and the range of sampling for each temperature (blue line). (b) dynamics of infectious human under the 100 sets of temperature dependent parameters given by randomly selected temperature.

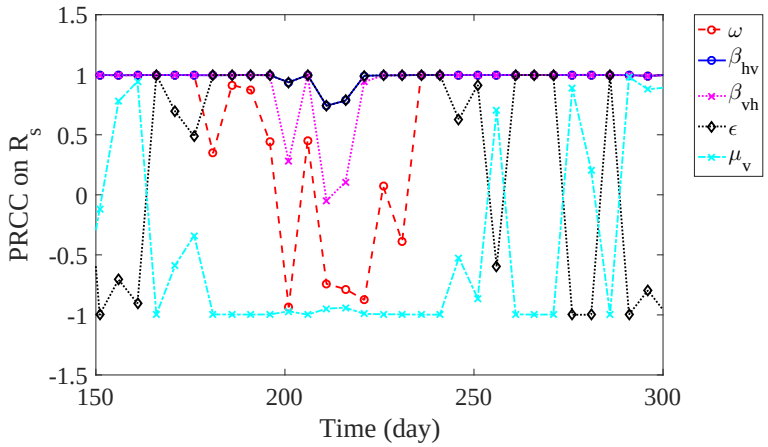

Figure 5-26: Partial Rank Correlation Coefficients on R_s over time.

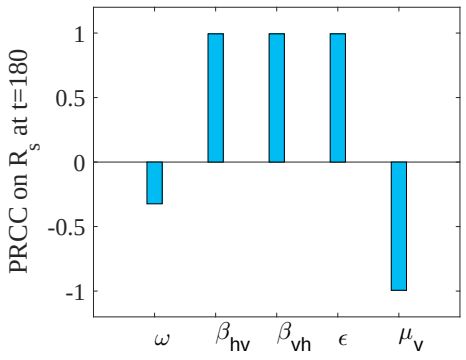

Figure 5-27: Partial Rank Correlation Coefficients on R_s at specific time, day 180.

6

Conclusion and Further Study

6.1 Mathematical modeling in South Korea

In chapter 4, we investigate how H1N1 influenza progresses and how the control measures influence on the outcome of an epidemic. The control measures consist of non-pharmaceutical isolation, antiviral treatment, and vaccination in terms of pharmaceutical interventions. We consider the spread of H1N1 influenza which prevailed for a year in Korea in 2009 and suggest the model to describe it with control measures.

The purpose in this chapter 4 is to construct an influenza transmission model regarding the control strategies. We focus on the impact of control interventions on the spread of H1N1 influenza. By applying the intervention strategies, the time-evolution dynamics for deterministic and stochastic models are compared. Moreover, we investigate the effect of control scenarios for vaccination and antiviral treatment on the dispersion of influenza for the stochastic model. Our model is based on the SLIAR with treatment model introduced in [42]. There are three modifications as follows:

(1) To focus on the dynamics of short-time scale, the relapses from treatment compartments – I_T and A_T – to disease compartments – I and A – do not occur.

(2) Compared to I_T and A_T, latent class receives treatment infrequently, so we set the rate (ϕ_L) equal to 0 for transitions from L to L_T.

(3) Our record shows that this vaccination was available six months after the first case was detected in Korea in 2009. We consider this event and add this vaccination factor during the epidemic.

The countermeasure is applied to the control parameters of the model. The epidemic duration is divided into four different periods according to different counter measure goals implemented by the Korean government from 2009 to 2010: day $0 \sim 79$ (period P_1), day $80 \sim 110$ (P_2), day $111 \sim 176$ (P_3), and day $177 \sim 400$ (P_4).

The conclusion is as follows. First, the earlier vaccination reduces the peak size of the number of infectives and the delays the time for the dynamics to reach the peak. If the vaccination policy is advanced by 10 days, the peak size of infectives is reduced by 31.2% compared to the actual peak size of infectives at time when the first vaccination was available in Korea.

Second, if the amount of antiviral treatment is increased beyond the baseline spent for each period, the peak size of the infectives decreases but is not effective at delaying the time to reach the peak. If one increases the amount of antiviral treatment by 50% in period P_3, where the number of infectives rapidly increases, the peak size is reduced by 8.2%. Therefore, we observe that the early vaccination is more effective in reducing the peak size and delaying the time to reach the peak than increasing the amount of antiviral treatment.

In chapter 5, we investigate the impact of the climate change and international travels on dengue transmission dynamics. We construct the dengue transmission model based on the climate change to estimate the epidemic outcomes in Jeju Island, Korea. The primary infection model has already been presented in [27], containing the SEI mosquito population and SIR human population with the temperature-dependent entomological parameters. One observes that temperature indirectly affects mosquito populations. Based on this model, we propose a modified primary infection model by adding the E compartment in consideration of the latent period for human infections. Moreover, the secondary infection model with two strains is formulated by extending the modified primary infection model in order to explore the severe outbreaks of DHF and DSS. In consideration of the winter-season in Korea, the temperature dependent functions are extend to a wide temperature range. Since the indigenous dengue cases have not been reported yet and all dengue cases of travelers returning from the endemic areas have been identified, the risk of dengue outbreaks may increase due to the increase of international travels. So, in the model, we incorporate the inflow rate of imported dengue cases by international travelers as a factor. To verify the validity of the parameters in the model, we compare the dengue incidence data in Taiwan with numerical simulation results without imported dengue cases. We carry out numerical simulations to estimate the dengue prevalence in Jeju Island in terms of seasonal patterns and the annual peak size. First, the time evolution dynamics of the deterministic model are shown by the daily temperature data based on RCP 4.5 and RCP 8.5 scenarios during the first 50 years in 2017. The results show the re-emerging of dengue fever with the periodic patterns. Second, the effect of the inflow rate of imported dengue cases by international travel is investigated. If the inflow rate of imported dengue cases is decreased due to the control interventions, the peak size of the number of infectives for both deterministic and stochastic models decreases. However, the discrepancy between two models becomes relatively larger due to the decrease of the imported cases.

6.2 Applications of stochastic computational method

Although deterministic model is a direct approach to estimating time evolution of dynamics, stochastic model is essential when randomness or uncertainty is crucial in the system. Furthermore, if there are only a few infected people in the large population system, the change in individuals due to a reaction is considered as a discrete integer. In that case, stochastic model can accurately describe the infection process involving the stochastic properties such as intrinsic fluctuation.

In chapter 3, we explain the difficulty of solving the stochastic system analytically. For simple stochastic enzyme-substrate reaction model, we derive the explicit representation of the solution. By expressing them in block matrix form, we can reduce the computational intensity, while maintaining efficiency and accuracy. Thus, this method gives us the motivation to use it as a computational method for complex stochastic system near necessity.

Generally, epidemic model includes a non-linear or high dimensional term. In that case, it may be impractical to find the stochastic governing equation. We apply the computational method such as stochastic simulation algorithm (SSA) and moment closure method (MCM) into the epidemic models. In section 2.2, we compare the time evolution of susceptible and infectious individuals for stochastic SEIR model by using SSA and MCM. Both solutions for mean and standard deviation between SSA and MCM are compared and accurately matched. In chapter 5, we compare the time evolution of mean and standard deviation for infectious human and mosquitoes considering climate changes and inflow rate induced by international travels. As a result, MCM can accurately capture the stochastic solutions. In the aspect of the computational efficacy, MCM is much faster than SSA for simulating sufficiently large number of realizations.

We adopt MCM instead of SSA to solve the stochastic epidemic models by applying various scenarios for large population in chapter 4 and chapter 5. In chapter 4, we explore the difference between deterministic and stochastic model for a few different number of initial infectives such as $10, 50$, and 250. If there is a small number of initial infectives, for example 10, then there is significant discrepancy between the two solutions, which can be observed by the exceeding of the confidence interval of the stochastic solution. However, the discrepancy becomes smaller as the number of initial infectives becomes larger. Here, we conclude that the solution of stochastic model converges to the solution of the deterministic model. Mcquarrie [92] illustrates that as the number of reactants increases, the coefficient of variation (CV) decreases, meaning that the relative fluctuations is reduced, where CV=standard deviation/mean measures the fluctuation relative to the mean.

In chapter 5, we compare the time-evolution of the dengue outbreaks of the ODEs with the stochastic solutions. When a small number of infectives is presented in the system, the dynamical behavior of two models has a considerable discrepancy at the peak. However, if a

sufficiently large number of infectives is initiated in the system, the discrepancy between the two solutions becomes smaller. Thus, when one simulates the stochastic system for various parameter sets and deals with the stochastic system which has a high dimensional system or large population size, MCM is efficient and useful since the method can give the stochastic properties such as mean, variance, and the higher order moments.

6.3 Further remarks

In chapter 3, we express the exact solution for the stochastic enzyme-substrate model by using the block matrix form of the Markov chain generator. Acedo [93] presented the exact solution analytically for the deterministic SIRS model. Yamand [94] found the exact solution of the stochastic SI model only for when the initial conditions were given with different control interventions of vaccination, isolation, and treatment. Hence, if we develop our method to find the stochastic solution analytically, not in terms of the block structures, we can find the analytic solution for stochastic SIR model and the stochastic SEIR model with general initial conditions which has not been presented yet.

In chapter 4, we only focus on the time-evolution dynamics of infectious individuals. The control measures of using antiviral treatment and vaccination are compared in terms of time to peak, peak size, and final attack ratio. Optimal control theory described in [95, 96] has been used in vector host models [97, 98]. The optimal control efforts are carried out to prevent the spread of disease. Since the average information for control policies in four different periods (P_1–P_4) is available, the control parameters are represented as a constant step function. So if we employ the optimal control methods for continuous control parameter, we can suggest the most effective control strategy.

In chapter 5, the dengue transmission model for primary infection and secondary infection is developed. It takes into account the climate change and inflow rate of imported dengue cases by international travel in the model. We investigate the impact of the two factors on dengue transmission dynamics in Jeju Island, Korea. Entomological parameters were expressed as polynomial functions of temperature. However, it is insufficient to clarify the dynamics of dengue outbreaks only by the effect of temperature, so we will consider the other meteorological factors such as relative humidity and rainfall. Moreover, due to the seasonal variation, the extinction of the mosquitoes in the winter and recurrent dengue outbreaks are observed. In [99], a stochastic two-dimensional model was developed to describe the recurrence and extinction patterns measles outbreaks and identify the factors related to the extinction of a disease. For further studies, we will find the probability distribution of extinction and derive the thresholds which determines the extinction of the epidemics.

MCM gives the moment equations without the Monte-Carlo simulation; however, it is difficult to find the probability distribution from the MCM. There are approximation methods

that allow us to compute the realizations of the state vector much faster than the SSA. For example, tau leaping method is an approximation for the SSA [17]. This method counts the number of reactions that occur in a small time interval with almost no change in the propensity, where the number of reactions is considered as a simple Poisson process. In addition, stochastic differential equations (SDE) is differential equations involving stochastic process [16]. If the reactions occur many times in a small time interval, Poisson random numbers approximate to normal random numbers, so one can derive the SDE from tau leaping. For future studies, we will apply stochastic computational method such as tau-leaping or SDE into the model and compute the probability distribution numerically to investigate the effect of the climate change and international travels on the periodic pattern of dengue outbreaks.

Appendices

Appendix A

Moment Equations for SLIAR with Treatment Model

For the moments $\mu_i = E[x_i]$ and $\sigma_{i,j} = E[(x_i - \mu_i)(x_j - \mu_j)]$, we have

$$
\begin{aligned}
\frac{d\mu_1}{dt} &= -c_{21}\mu_1 - c_1\sigma_{1,5} - c_2\sigma_{1,6} - c_3\sigma_{1,7} - c_4\sigma_{1,8} - c_1\mu_1\mu_5 - c_2\mu_1\mu_6 \\
&\quad -c_3\mu_1\mu_7 - c_4\mu_1\mu_8 \\
\frac{d\mu_2}{dt} &= c_{21}\mu_1 - c_5\sigma_{2,5} - c_6\sigma_{2,6} - c_7\sigma_{2,7} - c_8\sigma_{2,8} - c_5\mu_2\mu_5 - c_6\mu_2\mu_6 \\
&\quad -c_7\mu_2\mu_7 - c_8\mu_2\mu_8 \\
\frac{d\mu_3}{dt} &= c_1\sigma_{1,5} + c_2\sigma_{1,6} + c_3\sigma_{1,7} + c_4\sigma_{1,8} - c_{10}\mu_3 - c_9\mu_3 + c_1\mu_1\mu_5 + c_2\mu_1\mu_6 \\
&\quad +c_3\mu_1\mu_7 + c_4\mu_1\mu_8 \\
\frac{d\mu_4}{dt} &= c_5\sigma_{2,5} + c_6\sigma_{2,6} + c_7\sigma_{2,7} + c_8\sigma_{2,8} - c_{11}\mu_4 - c_{12}\mu_4 + c_5\mu_2\mu_5 + c_6\mu_2\mu_6 \\
&\quad +c_7\mu_2\mu_7 + c_8\mu_2\mu_8 \\
\frac{d\mu_5}{dt} &= c_9\mu_3 - c_{13}\mu_5 - c_{14}\mu_5 - c_{15}\mu_5 \\
\frac{d\mu_6}{dt} &= c_{11}\mu_4 + c_{13}\mu_5 - c_{16}\mu_6 - c_{17}\mu_6 \\
\frac{d\mu_7}{dt} &= c_{10}\mu_3 - c_{18}\mu_7 - c_{19}\mu_7, \quad \frac{d\mu_8}{dt} = c_{12}\mu_4 + c_{18}\mu_7 - c_{20}\mu_8 \\
\frac{d\mu_9}{dt} &= c_{14}\mu_5 + c_{16}\mu_6 + c_{19}\mu_7 + c_{20}\mu_8, \quad \frac{d\mu_{10}}{dt} = c_{15}\mu_5 + c_{17}\mu_6 \\
\frac{d\sigma_{1,1}}{dt} &= c_{21}\mu_1 + c_1\sigma_{1,5} - 2c_1\mu_1\sigma_{1,5} + c_2\sigma_{1,6} - 2c_2\mu_1\sigma_{1,6} + c_3\sigma_{1,7} - 2c_3\mu_1\sigma_{1,7} \\
&\quad +c_4\sigma_{1,8} - 2c_4\mu_1\sigma_{1,8} + c_1\mu_1\mu_5 - 2c_{21}\sigma_{1,1} - 2c_1\mu_5\sigma_{1,1} + c_2\mu_1\mu_6 \\
&\quad -2c_2\sigma_{1,1}\mu_6 + c_3\mu_1\mu_7 - 2c_3\sigma_{1,1}\mu_7 + c_4\mu_1\mu_8 - 2c_4\sigma_{1,1}\mu_8 \\
\frac{d\sigma_{2,2}}{dt} &= c_{21}\mu_1 + 2c_{21}\sigma_{1,2} + c_5\sigma_{2,5} - 2c_5\mu_2\sigma_{2,5} + c_6\sigma_{2,6} - 2c_6\mu_2\sigma_{2,6} + c_7\sigma_{2,7} \\
&\quad -2c_7\mu_2\sigma_{2,7} + c_8\sigma_{2,8} - 2c_8\mu_2\sigma_{2,8} + c_5\mu_2\mu_5 - 2c_5\mu_5\sigma_{2,2} + c_6\mu_2\mu_6 \\
&\quad -2c_6\sigma_{2,2}\mu_6 + c_7\mu_2\mu_7 - 2c_7\sigma_{2,2}\mu_7 + c_8\mu_2\mu_8 - 2c_8\sigma_{2,2}\mu_8
\end{aligned}
$$

$$
\begin{aligned}
\frac{d\sigma_{3,3}}{dt} &= c_1\sigma_{1,5} + c_2\sigma_{1,6} + c_3\sigma_{1,7} + c_4\sigma_{1,8} + 2c_1\mu_1\sigma_{3,5} + c_{10}\mu_3 + c_9\mu_3 \\
&\quad +2c_2\mu_1\sigma_{3,6} + 2c_3\mu_1\sigma_{3,7} + 2c_4\mu_1\sigma_{3,8} + c_1\mu_1\mu_5 + 2c_1\sigma_{1,3}\mu_5 \\
&\quad -2c_{10}\sigma_{3,3} - 2c_9\sigma_{3,3} + c_2\mu_1\mu_6 + 2c_2\sigma_{1,3}\mu_6 + c_3\mu_1\mu_7 \\
&\quad +2c_3\sigma_{1,3}\mu_7 + c_4\mu_1\mu_8 + 2c_4\sigma_{1,3}\mu_8 \\
\frac{d\sigma_{4,4}}{dt} &= c_5\sigma_{2,5} + c_6\sigma_{2,6} + c_7\sigma_{2,7} + c_8\sigma_{2,8} + 2c_5\mu_2\sigma_{4,5} + 2c_6\mu_2\sigma_{4,6} \\
&\quad +2c_7\mu_2\sigma_{4,7} + 2c_8\mu_2\sigma_{4,8} + c_{11}\mu_4 + c_{12}\mu_4 + c_5\mu_2\mu_5 + 2c_5\sigma_{2,4}\mu_5 \\
&\quad -2c_{11}\sigma_{4,4} - 2c_{12}\sigma_{4,4} + c_6\mu_2\mu_6 + 2c_6\sigma_{2,4}\mu_6 + c_7\mu_2\mu_7 + 2c_7\sigma_{2,4}\mu_7 \\
&\quad +c_8\mu_2\mu_8 + 2c_8\sigma_{2,4}\mu_8 \\
\frac{d\sigma_{5,5}}{dt} &= 2c_9\sigma_{3,5} + c_9\mu_3 + c_{13}\mu_5 + c_{14}\mu_5 + c_{15}\mu_5 - 2c_{13}\sigma_{5,5} - 2c_{14}\sigma_{5,5} \\
&\quad -2c_{15}\sigma_{5,5} \\
\frac{d\sigma_{6,6}}{dt} &= 2c_{11}\sigma_{4,6} + c_{11}\mu_4 + 2c_{13}\sigma_{5,6} + c_{13}\mu_5 + c_{16}\mu_6 + c_{17}\mu_6 - 2c_{16}\sigma_{6,6} \\
&\quad -2c_{17}\sigma_{6,6} \\
\frac{d\sigma_{7,7}}{dt} &= c_{10}\mu_3 + 2c_{10}\sigma_{3,7} - 2c_{18}\sigma_{7,7} - 2c_{19}\sigma_{7,7} + c_{18}\mu_7 + c_{19}\mu_7 \\
\frac{d\sigma_{8,8}}{dt} &= 2c_{12}\sigma_{4,8} + c_{12}\mu_4 + 2c_{18}\sigma_{7,8} - 2c_{20}\sigma_{8,8} + c_{18}\mu_7 + c_{20}\mu_8 \\
\frac{d\sigma_{9,9}}{dt} &= 2c_{14}\sigma_{5,9} + 2c_{16}\sigma_{6,9} + c_{14}\mu_5 + 2c_{19}\sigma_{7,9} + 2c_{20}\sigma_{8,9} + c_{16}\mu_6 \\
&\quad +c_{19}\mu_7 + c_{20}\mu_8 \\
\frac{d\sigma_{10,10}}{dt} &= 2c_{15}\sigma_{5,10} + 2c_{17}\sigma_{6,10} + c_{15}\mu_5 + c_{17}\mu_6 \\
\frac{d\sigma_{1,2}}{dt} &= -c_{21}\mu_1 - c_{21}\sigma_{1,2} - c_5\sigma_{1,5}\mu_2 - c_6\sigma_{1,6}\mu_2 - c_7\sigma_{1,7}\mu_2 - c_8\sigma_{1,8}\mu_2 \\
&\quad -c_1\mu_1\sigma_{2,5} - c_2\mu_1\sigma_{2,6} - c_3\mu_1\sigma_{2,7} - c_4\mu_1\sigma_{2,8} - c_1\sigma_{1,2}\mu_5 - c_5\sigma_{1,2}\mu_5 \\
&\quad +c_{21}\sigma_{1,1} - c_2\sigma_{1,2}\mu_6 - c_6\sigma_{1,2}\mu_6 - c_3\sigma_{1,2}\mu_7 - c_7\sigma_{1,2}\mu_7 - c_4\sigma_{1,2}\mu_8 \\
&\quad -c_8\sigma_{1,2}\mu_8 \\
\frac{d\sigma_{1,3}}{dt} &= -c_{10}\sigma_{1,3} - c_{21}\sigma_{1,3} - c_9\sigma_{1,3} - c_1\sigma_{1,5} + c_1\mu_1\sigma_{1,5} - c_2\sigma_{1,6} + c_2\mu_1\sigma_{1,6} \\
&\quad -c_3\sigma_{1,7} + c_3\mu_1\sigma_{1,7} - c_4\sigma_{1,8} + c_4\mu_1\sigma_{1,8} - c_1\mu_1\sigma_{3,5} - c_2\mu_1\sigma_{3,6} \\
&\quad -c_3\mu_1\sigma_{3,7} - c_4\mu_1\sigma_{3,8} - c_1\mu_1\mu_5 - c_1\sigma_{1,3}\mu_5 + c_1\mu_5\sigma_{1,1} - c_2\mu_1\mu_6 \\
&\quad -c_2\sigma_{1,3}\mu_6 + c_2\sigma_{1,1}\mu_6 - c_3\mu_1\mu_7 - c_3\sigma_{1,3}\mu_7 + c_3\sigma_{1,1}\mu_7 - c_4\mu_1\mu_8 \\
&\quad -c_4\sigma_{1,3}\mu_8 + c_4\sigma_{1,1}\mu_8 \\
\frac{d\sigma_{1,4}}{dt} &= -c_{11}\sigma_{1,4} - c_{12}\sigma_{1,4} - c_{21}\sigma_{1,4} + c_5\sigma_{1,5}\mu_2 + c_6\sigma_{1,6}\mu_2 + c_7\sigma_{1,7}\mu_2 \\
&\quad +c_8\sigma_{1,8}\mu_2 - c_1\mu_1\sigma_{4,5} - c_2\mu_1\sigma_{4,6} - c_3\mu_1\sigma_{4,7} - c_4\mu_1\sigma_{4,8} + c_5\sigma_{1,2}\mu_5 \\
&\quad -c_1\sigma_{1,4}\mu_5 + c_6\sigma_{1,2}\mu_6 - c_2\sigma_{1,4}\mu_6 + c_7\sigma_{1,2}\mu_7 - c_3\sigma_{1,4}\mu_7 + c_8\sigma_{1,2}\mu_8 \\
&\quad -c_4\sigma_{1,4}\mu_8
\end{aligned}
$$

$$
\begin{aligned}
\frac{d\sigma_{1,5}}{dt} &= c_9\sigma_{1,3} - c_{13}\sigma_{1,5} - c_{14}\sigma_{1,5} - c_{15}\sigma_{1,5} - c_{21}\sigma_{1,5} - c_2\mu_1\sigma_{5,6} - c_3\mu_1\sigma_{5,7} \\
&\quad -c_4\mu_1\sigma_{5,8} - c_1\sigma_{1,5}\mu_5 - c_2\sigma_{1,5}\mu_6 - c_1\mu_1\sigma_{5,5} - c_3\sigma_{1,5}\mu_7 - c_4\sigma_{1,5}\mu_8 \\
\frac{d\sigma_{1,6}}{dt} &= c_{11}\sigma_{1,4} + c_{13}\sigma_{1,5} - c_{16}\sigma_{1,6} - c_{17}\sigma_{1,6} - c_{21}\sigma_{1,6} - c_1\mu_1\sigma_{5,6} - c_3\mu_1\sigma_{6,7} \\
&\quad -c_4\mu_1\sigma_{6,8} - c_1\sigma_{1,6}\mu_5 - c_2\sigma_{1,6}\mu_6 - c_2\mu_1\sigma_{6,6} - c_3\sigma_{1,6}\mu_7 - c_4\sigma_{1,6}\mu_8 \\
\frac{d\sigma_{1,7}}{dt} &= c_{10}\sigma_{1,3} - c_{18}\sigma_{1,7} - c_{19}\sigma_{1,7} - c_{21}\sigma_{1,7} - c_1\mu_1\sigma_{5,7} - c_2\mu_1\sigma_{6,7} - c_1\sigma_{1,7}\mu_5 \\
&\quad -c_4\mu_1\sigma_{7,8} - c_2\sigma_{1,7}\mu_6 - c_3\mu_1\sigma_{7,7} - c_3\sigma_{1,7}\mu_7 - c_4\sigma_{1,7}\mu_8 \\
\frac{d\sigma_{1,8}}{dt} &= c_{12}\sigma_{1,4} + c_{18}\sigma_{1,7} - c_{20}\sigma_{1,8} - c_{21}\sigma_{1,8} - c_1\mu_1\sigma_{5,8} - c_2\mu_1\sigma_{6,8} - c_1\sigma_{1,8}\mu_5 \\
&\quad -c_3\mu_1\sigma_{7,8} - c_2\sigma_{1,8}\mu_6 - c_4\mu_1\sigma_{8,8} - c_3\sigma_{1,8}\mu_7 - c_4\sigma_{1,8}\mu_8 \\
\frac{d\sigma_{1,9}}{dt} &= c_{14}\sigma_{1,5} + c_{16}\sigma_{1,6} + c_{19}\sigma_{1,7} + c_{20}\sigma_{1,8} - c_{21}\sigma_{1,9} - c_1\mu_1\sigma_{5,9} - c_2\mu_1\sigma_{6,9} \\
&\quad -c_1\sigma_{1,9}\mu_5 - c_3\mu_1\sigma_{7,9} - c_4\mu_1\sigma_{8,9} - c_2\sigma_{1,9}\mu_6 - c_3\sigma_{1,9}\mu_7 - c_4\sigma_{1,9}\mu_8 \\
\frac{d\sigma_{1,10}}{dt} &= c_{15}\sigma_{1,5} + c_{17}\sigma_{1,6} - c_{21}\sigma_{1,10} - c_1\mu_1\sigma_{5,10} - c_2\mu_1\sigma_{6,10} - c_1\sigma_{1,10}\mu_5 \\
&\quad -c_3\mu_1\sigma_{7,10} - c_4\mu_1\sigma_{8,10} - c_2\sigma_{1,10}\mu_6 - c_3\sigma_{1,10}\mu_7 - c_4\sigma_{1,10}\mu_8 \\
\frac{d\sigma_{2,3}}{dt} &= c_{21}\sigma_{1,3} - c_{10}\sigma_{2,3} - c_9\sigma_{2,3} + c_1\mu_1\sigma_{2,5} + c_2\mu_1\sigma_{2,6} + c_3\mu_1\sigma_{2,7} + c_4\mu_1\sigma_{2,8} \\
&\quad -c_5\mu_2\sigma_{3,5} - c_6\mu_2\sigma_{3,6} - c_7\mu_2\sigma_{3,7} - c_8\mu_2\sigma_{3,8} + c_1\sigma_{1,2}\mu_5 - c_5\sigma_{2,3}\mu_5 \\
&\quad +c_2\sigma_{1,2}\mu_6 - c_6\sigma_{2,3}\mu_6 + c_3\sigma_{1,2}\mu_7 - c_7\sigma_{2,3}\mu_7 + c_4\sigma_{1,2}\mu_8 - c_8\sigma_{2,3}\mu_8 \\
\frac{d\sigma_{2,4}}{dt} &= c_{21}\sigma_{1,4} - c_{11}\sigma_{2,4} - c_{12}\sigma_{2,4} - c_5\sigma_{2,5} + c_5\mu_2\sigma_{2,5} - c_6\sigma_{2,6} + c_6\mu_2\sigma_{2,6} \\
&\quad -c_7\sigma_{2,7} + c_7\mu_2\sigma_{2,7} - c_8\sigma_{2,8} + c_8\mu_2\sigma_{2,8} - c_5\mu_2\sigma_{4,5} - c_6\mu_2\sigma_{4,6} \\
&\quad -c_7\mu_2\sigma_{4,7} - c_8\mu_2\sigma_{4,8} - c_5\mu_2\mu_5 - c_5\sigma_{2,4}\mu_5 + c_5\mu_5\sigma_{2,2} - c_6\mu_2\mu_6 \\
&\quad -c_6\sigma_{2,4}\mu_6 + c_6\sigma_{2,2}\mu_6 - c_7\mu_2\mu_7 - c_7\sigma_{2,4}\mu_7 + c_7\sigma_{2,2}\mu_7 - c_8\mu_2\mu_8 \\
&\quad -c_8\sigma_{2,4}\mu_8 + c_8\sigma_{2,2}\mu_8 \\
\frac{d\sigma_{2,5}}{dt} &= c_{21}\sigma_{1,5} + c_9\sigma_{2,3} - c_{13}\sigma_{2,5} - c_{14}\sigma_{2,5} - c_{15}\sigma_{2,5} - c_6\mu_2\sigma_{5,6} - c_7\mu_2\sigma_{5,7} \\
&\quad -c_8\mu_2\sigma_{5,8} - c_5\sigma_{2,5}\mu_5 - c_6\sigma_{2,5}\mu_6 - c_5\mu_2\sigma_{5,5} - c_7\sigma_{2,5}\mu_7 - c_8\sigma_{2,5}\mu_8 \\
\frac{d\sigma_{2,6}}{dt} &= c_{21}\sigma_{1,6} + c_{11}\sigma_{2,4} + c_{13}\sigma_{2,5} - c_{16}\sigma_{2,6} - c_{17}\sigma_{2,6} - c_5\mu_2\sigma_{5,6} - c_7\mu_2\sigma_{6,7} \\
&\quad -c_8\mu_2\sigma_{6,8} - c_5\sigma_{2,6}\mu_5 - c_6\sigma_{2,6}\mu_6 - c_6\mu_2\sigma_{6,6} - c_7\sigma_{2,6}\mu_7 - c_8\sigma_{2,6}\mu_8 \\
\frac{d\sigma_{2,7}}{dt} &= c_{21}\sigma_{1,7} + c_{10}\sigma_{2,3} - c_{18}\sigma_{2,7} - c_{19}\sigma_{2,7} - c_5\mu_2\sigma_{5,7} - c_6\mu_2\sigma_{6,7} - c_5\sigma_{2,7}\mu_5 \\
&\quad -c_8\mu_2\sigma_{7,8} - c_6\sigma_{2,7}\mu_6 - c_7\mu_2\sigma_{7,7} - c_7\sigma_{2,7}\mu_7 - c_8\sigma_{2,7}\mu_8 \\
\frac{d\sigma_{2,8}}{dt} &= c_{21}\sigma_{1,8} + c_{12}\sigma_{2,4} + c_{18}\sigma_{2,7} - c_{20}\sigma_{2,8} - c_5\mu_2\sigma_{5,8} - c_6\mu_2\sigma_{6,8} - c_5\sigma_{2,8}\mu_5 \\
&\quad -c_7\mu_2\sigma_{7,8} - c_6\sigma_{2,8}\mu_6 - c_8\mu_2\sigma_{8,8} - c_7\sigma_{2,8}\mu_7 - c_8\sigma_{2,8}\mu_8 \\
\frac{d\sigma_{2,9}}{dt} &= c_{21}\sigma_{1,9} + c_{14}\sigma_{2,5} + c_{16}\sigma_{2,6} + c_{19}\sigma_{2,7} + c_{20}\sigma_{2,8} - c_5\mu_2\sigma_{5,9} - c_6\mu_2\sigma_{6,9} \\
&\quad -c_5\sigma_{2,9}\mu_5 - c_7\mu_2\sigma_{7,9} - c_8\mu_2\sigma_{8,9} - c_6\sigma_{2,9}\mu_6 - c_7\sigma_{2,9}\mu_7 - c_8\sigma_{2,9}\mu_8
\end{aligned}
$$

$$
\begin{aligned}
\frac{d\sigma_{2,10}}{dt} &= c_{21}\sigma_{1,10} + c_{15}\sigma_{2,5} + c_{17}\sigma_{2,6} - c_5\mu_2\sigma_{5,10} - c_6\mu_2\sigma_{6,10} - c_5\sigma_{2,10}\mu_5 \\
&\quad -c_7\mu_2\sigma_{7,10} - c_8\mu_2\sigma_{8,10} - c_6\sigma_{2,10}\mu_6 - c_7\sigma_{2,10}\mu_7 - c_8\sigma_{2,10}\mu_8 \\
\frac{d\sigma_{3,4}}{dt} &= -c_{10}\sigma_{3,4} - c_{11}\sigma_{3,4} - c_{12}\sigma_{3,4} - c_9\sigma_{3,4} + c_5\mu_2\sigma_{3,5} + c_6\mu_2\sigma_{3,6} + c_7\mu_2\sigma_{3,7} \\
&\quad +c_8\mu_2\sigma_{3,8} + c_1\mu_1\sigma_{4,5} + c_2\mu_1\sigma_{4,6} + c_3\mu_1\sigma_{4,7} + c_4\mu_1\sigma_{4,8} + c_1\sigma_{1,4}\mu_5 \\
&\quad +c_5\sigma_{2,3}\mu_5 + c_2\sigma_{1,4}\mu_6 + c_6\sigma_{2,3}\mu_6 + c_3\sigma_{1,4}\mu_7 + c_7\sigma_{2,3}\mu_7 \\
&\quad +c_4\sigma_{1,4}\mu_8 + c_8\sigma_{2,3}\mu_8 \\
\frac{d\sigma_{3,5}}{dt} &= -c_{10}\sigma_{3,5} - c_{13}\sigma_{3,5} - c_{14}\sigma_{3,5} - c_{15}\sigma_{3,5} - c_9\sigma_{3,5} - c_9\mu_3 + c_2\mu_1\sigma_{5,6} \\
&\quad +c_3\mu_1\sigma_{5,7} + c_4\mu_1\sigma_{5,8} + c_1\sigma_{1,5}\mu_5 + c_9\sigma_{3,3} + c_2\sigma_{1,5}\mu_6 + c_1\mu_1\sigma_{5,5} \\
&\quad +c_3\sigma_{1,5}\mu_7 + c_4\sigma_{1,5}\mu_8 \\
\frac{d\sigma_{3,6}}{dt} &= c_{11}\sigma_{3,4} + c_{13}\sigma_{3,5} - c_{10}\sigma_{3,6} - c_{16}\sigma_{3,6} - c_{17}\sigma_{3,6} - c_9\sigma_{3,6} + c_1\mu_1\sigma_{5,6} \\
&\quad +c_3\mu_1\sigma_{6,7} + c_4\mu_1\sigma_{6,8} + c_1\sigma_{1,6}\mu_5 + c_2\sigma_{1,6}\mu_6 + c_2\mu_1\sigma_{6,6} + c_3\sigma_{1,6}\mu_7 \\
&\quad +c_4\sigma_{1,6}\mu_8 \\
\frac{d\sigma_{3,7}}{dt} &= -c_{10}\mu_3 - c_{10}\sigma_{3,7} - c_{18}\sigma_{3,7} - c_{19}\sigma_{3,7} - c_9\sigma_{3,7} + c_1\mu_1\sigma_{5,7} + c_2\mu_1\sigma_{6,7} \\
&\quad +c_1\sigma_{1,7}\mu_5 + c_4\mu_1\sigma_{7,8} + c_{10}\sigma_{3,3} + c_2\sigma_{1,7}\mu_6 + c_3\mu_1\sigma_{7,7} + c_3\sigma_{1,7}\mu_7 \\
&\quad +c_4\sigma_{1,7}\mu_8 \\
\frac{d\sigma_{3,8}}{dt} &= c_{12}\sigma_{3,4} + c_{18}\sigma_{3,7} - c_{10}\sigma_{3,8} - c_{20}\sigma_{3,8} - c_9\sigma_{3,8} + c_1\mu_1\sigma_{5,8} + c_2\mu_1\sigma_{6,8} \\
&\quad +c_1\sigma_{1,8}\mu_5 + c_3\mu_1\sigma_{7,8} + c_2\sigma_{1,8}\mu_6 + c_4\mu_1\sigma_{8,8} + c_3\sigma_{1,8}\mu_7 + c_4\sigma_{1,8}\mu_8 \\
\frac{d\sigma_{3,9}}{dt} &= c_{14}\sigma_{3,5} + c_{16}\sigma_{3,6} + c_{19}\sigma_{3,7} + c_{20}\sigma_{3,8} - c_{10}\sigma_{3,9} - c_9\sigma_{3,9} + c_1\mu_1\sigma_{5,9} \\
&\quad +c_2\mu_1\sigma_{6,9} + c_1\sigma_{1,9}\mu_5 + c_3\mu_1\sigma_{7,9} + c_4\mu_1\sigma_{8,9} + c_2\sigma_{1,9}\mu_6 + c_3\sigma_{1,9}\mu_7 \\
&\quad +c_4\sigma_{1,9}\mu_8 \\
\frac{d\sigma_{3,10}}{dt} &= c_{15}\sigma_{3,5} + c_{17}\sigma_{3,6} - c_{10}\sigma_{3,10} - c_9\sigma_{3,10} + c_1\mu_1\sigma_{5,10} + c_2\mu_1\sigma_{6,10} \\
&\quad +c_1\sigma_{1,10}\mu_5 + c_3\mu_1\sigma_{7,10} + c_4\mu_1\sigma_{8,10} + c_2\sigma_{1,10}\mu_6 \\
&\quad +c_3\sigma_{1,10}\mu_7 + c_4\sigma_{1,10}\mu_8 \\
\frac{d\sigma_{4,5}}{dt} &= c_9\sigma_{3,4} - c_{11}\sigma_{4,5} - c_{12}\sigma_{4,5} - c_{13}\sigma_{4,5} - c_{14}\sigma_{4,5} - c_{15}\sigma_{4,5} + c_6\mu_2\sigma_{5,6} \\
&\quad +c_7\mu_2\sigma_{5,7} + c_8\mu_2\sigma_{5,8} + c_5\sigma_{2,5}\mu_5 + c_6\sigma_{2,5}\mu_6 + c_5\mu_2\sigma_{5,5} \\
&\quad +c_7\sigma_{2,5}\mu_7 + c_8\sigma_{2,5}\mu_8 \\
\frac{d\sigma_{4,6}}{dt} &= c_{13}\sigma_{4,5} - c_{11}\sigma_{4,6} - c_{12}\sigma_{4,6} - c_{16}\sigma_{4,6} - c_{17}\sigma_{4,6} - c_{11}\mu_4 + c_5\mu_2\sigma_{5,6} \\
&\quad +c_7\mu_2\sigma_{6,7} + c_8\mu_2\sigma_{6,8} + c_5\sigma_{2,6}\mu_5 + c_{11}\sigma_{4,4} + c_6\sigma_{2,6}\mu_6 + c_6\mu_2\sigma_{6,6} \\
&\quad +c_7\sigma_{2,6}\mu_7 + c_8\sigma_{2,6}\mu_8 \\
\frac{d\sigma_{4,7}}{dt} &= c_{10}\sigma_{3,4} - c_{11}\sigma_{4,7} - c_{12}\sigma_{4,7} - c_{18}\sigma_{4,7} - c_{19}\sigma_{4,7} + c_5\mu_2\sigma_{5,7} + c_6\mu_2\sigma_{6,7} \\
&\quad +c_5\sigma_{2,7}\mu_5 + c_8\mu_2\sigma_{7,8} + c_6\sigma_{2,7}\mu_6 + c_7\mu_2\sigma_{7,7} + c_7\sigma_{2,7}\mu_7 + c_8\sigma_{2,7}\mu_8
\end{aligned}
$$

$$
\begin{aligned}
\frac{d\sigma_{4,8}}{dt} &= c_{18}\sigma_{4,7} - c_{11}\sigma_{4,8} - c_{12}\sigma_{4,8} - c_{20}\sigma_{4,8} - c_{12}\mu_4 + c_5\mu_2\sigma_{5,8} + c_6\mu_2\sigma_{6,8} \\
&\quad + c_5\sigma_{2,8}\mu_5 + c_7\mu_2\sigma_{7,8} + c_{12}\sigma_{4,4} + c_6\sigma_{2,8}\mu_6 + c_8\mu_2\sigma_{8,8} \\
&\quad + c_7\sigma_{2,8}\mu_7 + c_8\sigma_{2,8}\mu_8 \\
\frac{d\sigma_{4,9}}{dt} &= c_{14}\sigma_{4,5} + c_{16}\sigma_{4,6} + c_{19}\sigma_{4,7} + c_{20}\sigma_{4,8} - c_{11}\sigma_{4,9} - c_{12}\sigma_{4,9} + c_5\mu_2\sigma_{5,9} \\
&\quad + c_6\mu_2\sigma_{6,9} + c_5\sigma_{2,9}\mu_5 + c_7\mu_2\sigma_{7,9} + c_8\mu_2\sigma_{8,9} + c_6\sigma_{2,9}\mu_6 + c_7\sigma_{2,9}\mu_7 \\
&\quad + c_8\sigma_{2,9}\mu_8 \\
\frac{d\sigma_{4,10}}{dt} &= c_{15}\sigma_{4,5} + c_{17}\sigma_{4,6} - c_{11}\sigma_{4,10} - c_{12}\sigma_{4,10} + c_5\mu_2\sigma_{5,10} + c_6\mu_2\sigma_{6,10} \\
&\quad + c_5\sigma_{2,10}\mu_5 + c_7\mu_2\sigma_{7,10} + c_8\mu_2\sigma_{8,10} + c_6\sigma_{2,10}\mu_6 \\
&\quad + c_7\sigma_{2,10}\mu_7 + c_8\sigma_{2,10}\mu_8 \\
\frac{d\sigma_{5,6}}{dt} &= c_9\sigma_{3,6} + c_{11}\sigma_{4,5} - c_{13}\sigma_{5,6} - c_{14}\sigma_{5,6} - c_{15}\sigma_{5,6} - c_{16}\sigma_{5,6} - c_{17}\sigma_{5,6} \\
&\quad - c_{13}\mu_5 + c_{13}\sigma_{5,5} \\
\frac{d\sigma_{5,7}}{dt} &= c_{10}\sigma_{3,5} + c_9\sigma_{3,7} - c_{13}\sigma_{5,7} - c_{14}\sigma_{5,7} - c_{15}\sigma_{5,7} - c_{18}\sigma_{5,7} - c_{19}\sigma_{5,7} \\
\frac{d\sigma_{5,8}}{dt} &= c_9\sigma_{3,8} + c_{12}\sigma_{4,5} + c_{18}\sigma_{5,7} - c_{13}\sigma_{5,8} - c_{14}\sigma_{5,8} - c_{15}\sigma_{5,8} - c_{20}\sigma_{5,8} \\
\frac{d\sigma_{5,9}}{dt} &= c_9\sigma_{3,9} + c_{16}\sigma_{5,6} + c_{19}\sigma_{5,7} + c_{20}\sigma_{5,8} - c_{13}\sigma_{5,9} - c_{14}\sigma_{5,9} - c_{15}\sigma_{5,9} \\
&\quad - c_{14}\mu_5 + c_{14}\sigma_{5,5} \\
\frac{d\sigma_{5,10}}{dt} &= c_9\sigma_{3,10} + c_{17}\sigma_{5,6} - c_{13}\sigma_{5,10} - c_{14}\sigma_{5,10} - c_{15}\sigma_{5,10} - c_{15}\mu_5 + c_{15}\sigma_{5,5} \\
\frac{d\sigma_{6,7}}{dt} &= c_{10}\sigma_{3,6} + c_{11}\sigma_{4,7} + c_{13}\sigma_{5,7} - c_{16}\sigma_{6,7} - c_{17}\sigma_{6,7} - c_{18}\sigma_{6,7} - c_{19}\sigma_{6,7} \\
\frac{d\sigma_{6,8}}{dt} &= c_{12}\sigma_{4,6} + c_{11}\sigma_{4,8} + c_{13}\sigma_{5,8} + c_{18}\sigma_{6,7} - c_{16}\sigma_{6,8} - c_{17}\sigma_{6,8} - c_{20}\sigma_{6,8} \\
\frac{d\sigma_{6,9}}{dt} &= c_{11}\sigma_{4,9} + c_{14}\sigma_{5,6} + c_{13}\sigma_{5,9} + c_{19}\sigma_{6,7} + c_{20}\sigma_{6,8} - c_{16}\sigma_{6,9} - c_{17}\sigma_{6,9} \\
&\quad - c_{16}\mu_6 + c_{16}\sigma_{6,6} \\
\frac{d\sigma_{6,10}}{dt} &= c_{11}\sigma_{4,10} + c_{15}\sigma_{5,6} + c_{13}\sigma_{5,10} - c_{16}\sigma_{6,10} - c_{17}\sigma_{6,10} - c_{17}\mu_6 + c_{17}\sigma_{6,6} \\
\frac{d\sigma_{7,8}}{dt} &= c_{10}\sigma_{3,8} + c_{12}\sigma_{4,7} - c_{18}\sigma_{7,8} - c_{19}\sigma_{7,8} - c_{20}\sigma_{7,8} + c_{18}\sigma_{7,7} - c_{18}\mu_7 \\
\frac{d\sigma_{7,9}}{dt} &= c_{10}\sigma_{3,9} + c_{14}\sigma_{5,7} + c_{16}\sigma_{6,7} + c_{20}\sigma_{7,8} - c_{18}\sigma_{7,9} - c_{19}\sigma_{7,9} + c_{19}\sigma_{7,7} \\
&\quad - c_{19}\mu_7 \\
\frac{d\sigma_{7,10}}{dt} &= c_{10}\sigma_{3,10} + c_{15}\sigma_{5,7} + c_{17}\sigma_{6,7} - c_{18}\sigma_{7,10} - c_{19}\sigma_{7,10} \\
\frac{d\sigma_{8,9}}{dt} &= c_{12}\sigma_{4,9} + c_{14}\sigma_{5,8} + c_{16}\sigma_{6,8} + c_{19}\sigma_{7,8} + c_{18}\sigma_{7,9} - c_{20}\sigma_{8,9} + c_{20}\sigma_{8,8} \\
&\quad - c_{20}\mu_8 \\
\frac{d\sigma_{8,10}}{dt} &= c_{12}\sigma_{4,10} + c_{15}\sigma_{5,8} + c_{17}\sigma_{6,8} + c_{18}\sigma_{7,10} - c_{20}\sigma_{8,10} \\
\frac{d\sigma_{9,10}}{dt} &= c_{15}\sigma_{5,9} + c_{14}\sigma_{5,10} + c_{17}\sigma_{6,9} + c_{16}\sigma_{6,10} + c_{19}\sigma_{7,10} + c_{20}\sigma_{8,10}
\end{aligned}
$$

Appendix B

Moment Equation for the Primary Infection Model for Dengue Fever

For the moments $\mu_i = E[x_i]$ and $\sigma_{i,j} = E[(x_i - \mu_i)(x_j - \mu_j)]$, for simplify,
$\mu_M := \sum_{i=3}^{5} \mu_i$ and $\mu_H := \sum_{i=6}^{9} \mu_i$ we have

$$
\begin{aligned}
\frac{d\mu_1}{dt} &= -\mu_1 c_2 + c_1(1 + (\sigma_{3,5}(\mu_3 + \mu_4 - \mu_5)c_{11})/\mu_M^3 - (2\sigma_{3,4}\mu_5 c_{11})/\mu_M^3 \\
&- (2\sigma_{4,5}\mu_5 c_{11})/\mu_M^3 - (\sigma_{3,3}\mu_5 c_{11})/\mu_M^3 - (\sigma_{4,4}\mu_5 c_{11})/\mu_M^3 \\
&+ (\sigma_{4,5}c_{11})/\mu_M^2 - (\mu_5 c_{11})/\mu_M - (\mu_5\sigma_{5,5}c_{11})/\mu_M^3 + (\sigma_{5,5}c_{11})/\mu_M^2) \\
\frac{d\mu_2}{dt} &= -\mu_2 c_2 + (2\sigma_{3,4}\mu_5 c_1 c_{11})/\mu_M^3 + (2\sigma_{3,5}\mu_5 c_1 c_{11})/\mu_M^3 + (2\sigma_{4,5}\mu_5 c_1 c_{11})/\mu_M^3 \\
&+ (\sigma_{3,3}\mu_5 c_1 c_{11})/\mu_M^3 + (\sigma_{4,4}\mu_5 c_1 c_{11})/\mu_M^3 - (\sigma_{3,5}c_1 c_{11})/\mu_M^2 \\
&+ (\mu_5 c_1 c_{11})/\mu_M + (\mu_5\sigma_{5,5}c_1 c_{11})/\mu_M^3 - (\sigma_{5,5}c_1 c_{11})/\mu_M^2 - (\sigma_{4,5}c_1 c_{11})/\mu_M^2 \\
\frac{d\mu_3}{dt} &= \mu_1 c_2 + (\sigma_{3,6}\mu_8 c_3)/\mu_H^2 + (\sigma_{3,7}\mu_8 c_3)/\mu_H^2 + (\sigma_{3,8}\mu_8 c_3)/\mu_H^2 + (\sigma_{3,9}\mu_8 c_3)/\mu_H^2 \\
&- (\sigma_{3,8}c_3)/\mu_H + \mu_3(-((2\sigma_{6,7}\mu_8 c_3)/\mu_H^3) - (2\sigma_{6,8}\mu_8 c_3)/\mu_H^3 - (2\sigma_{6,9}\mu_8 c_3)/\mu_H^3 \\
&- (2\sigma_{7,8}\mu_8 c_3)/\mu_H^3 - (2\sigma_{7,9}\mu_8 c_3)/\mu_H^3 - (2\sigma_{8,9}\mu_8 c_3)/\mu_H^3 - (\sigma_{6,6}\mu_8 c_3)/\mu_H^3 \\
&- (\sigma_{7,7}\mu_8 c_3)/\mu_H^3 - (\sigma_{8,8}\mu_8 c_3)/\mu_H^3 - (\sigma_{9,9}\mu_8 c_3)/\mu_H^3 + (\sigma_{6,8}c_3)/\mu_H^2 \\
&+ (\sigma_{7,8}c_3)/\mu_H^2 + (\sigma_{8,9}c_3)/\mu_H^2 + (\sigma_{8,8}c_3)/\mu_H^2 - (\mu_8 c_3)/\mu_H - c_6) \\
\frac{d\mu_4}{dt} &= -(\sigma_{3,6}\mu_8 c_3)/\mu_H^2 - (\sigma_{3,7}\mu_8 c_3)/\mu_H^2 - (\sigma_{3,8}\mu_8 c_3)/\mu_H^2 - (\sigma_{3,9}\mu_8 c_3)/\mu_H^2 \\
&+ (\sigma_{3,8}c_3)/\mu_H + (\mu_3(-\sigma_{8,9}\mu_6 - \sigma_{8,8}\mu_6 - \sigma_{8,9}\mu_7 - \sigma_{8,8}\mu_7 + 2\sigma_{6,7}\mu_8 \\
&+ 2\sigma_{6,9}\mu_8 + 2\sigma_{7,9}\mu_8 + \sigma_{8,9}\mu_8 + \sigma_{6,6}\mu_8 + \sigma_{7,7}\mu_8 + \sigma_{9,9}\mu_8 + \mu_6^2\mu_8 \\
&+ 2\mu_6\mu_7\mu_8 + \mu_7^2\mu_8 + 2\mu_6\mu_8^2 + 2\mu_7\mu_8^2 + \mu_8^3 + \sigma_{6,8}(-\mu_6 - \mu_7 + \mu_8 - \mu_9) \\
&+ 2\mu_6\mu_8\mu_9 + \sigma_{7,8}(-\mu_6 - \mu_7 + \mu_8 - \mu_9) - \sigma_{8,9}\mu_9 - \sigma_{8,8}\mu_9 + 2\mu_7\mu_8\mu_9 \\
&+ 2\mu_8^2\mu_9 + \mu_8\mu_9^2)c_3)/\mu_H^3 - \mu_4 c_5 - \mu_4 c_6
\end{aligned}
$$

$$
\begin{aligned}
\frac{d\mu_5}{dt} &= +\mu_2 c_2 + \mu_4 c_5 - \mu_5 c_6 \\
\frac{d\mu_6}{dt} &= -(\mu_5\mu_6 c_4)/\mu_H + ((-\sigma_{6,9}\mu_5\mu_6 - 2\sigma_{7,8}\mu_5\mu_6 - 2\sigma_{7,9}\mu_5\mu_6 - 2\sigma_{8,9}\mu_5\mu_6 \\
&- \mu_5\sigma_{7,7}\mu_6 - \mu_5\sigma_{8,8}\mu_6 - \mu_5\sigma_{9,9}\mu_6 + \sigma_{5,7}\mu_6^2 + \sigma_{5,8}\mu_6^2 + \sigma_{5,9}\mu_6^2 \\
&+ \mu_5\sigma_{6,6}\mu_7 - \sigma_{5,6}\mu_6\mu_7 + \sigma_{5,7}\mu_6\mu_7 + \sigma_{5,8}\mu_6\mu_7 + \sigma_{5,9}\mu_6\mu_7 - \sigma_{5,6}\mu_7^2 \\
&+ \mu_5\sigma_{6,6}\mu_8 - \sigma_{5,6}\mu_6\mu_8 + \sigma_{5,7}\mu_6\mu_8 + \sigma_{5,8}\mu_6\mu_8 + \sigma_{5,9}\mu_6\mu_8 - 2\sigma_{5,6}\mu_7\mu_8 \\
&- \sigma_{5,6}\mu_8^2 + \sigma_{6,9}\mu_5\mu_9 + \mu_5\sigma_{6,6}\mu_9 - \sigma_{5,6}\mu_6\mu_9 + \sigma_{5,7}\mu_6\mu_9 + \sigma_{5,8}\mu_6\mu_9 \\
&- 2\sigma_{5,6}\mu_7\mu_9 - 2\sigma_{5,6}\mu_8\mu_9 - \sigma_{5,6}\mu_9^2 + \sigma_{6,7}\mu_5(-\mu_6 + \mu_7 + \mu_8 + \mu_9) \\
&+ \sigma_{6,8}\mu_5(-\mu_6 + \mu_7 + \mu_8 + \mu_9))c_4)/\mu_H^3 - \mu_6 c_7 + \mu_H c_9 - \mu_6 c_{10} \\
&+ \sigma_{6,9}\mu_5\mu_7 + \sigma_{6,9}\mu_5\mu_8 + \sigma_{5,9}\mu_6\mu_9 \\
\frac{d\mu_7}{dt} &= +(2\sigma_{6,9}\mu_5\mu_6 c_4)/\mu_H^3 + (2\sigma_{7,8}\mu_5\mu_6 c_4)/\mu_H^3 + (2\sigma_{7,9}\mu_5\mu_6 c_4)/\mu_H^3 \\
&+ (2\sigma_{8,9}\mu_5\mu_6 c_4)/\mu_H^3 + (\mu_5\sigma_{6,6}\mu_6 c_4)/\mu_H^3 + (\mu_5\sigma_{7,7}\mu_6 c_4)/\mu_H^3 \\
&+ (\mu_5\sigma_{9,9}\mu_6 c_4)/\mu_H^3 + (\sigma_{6,7}\mu_5(\mu_6 - \mu_7 - \mu_8 - \mu_9)c_4)/\mu_H^3 - \mu_7 c_{12} \\
&+ (\sigma_{6,8}\mu_5(\mu_6 - \mu_7 - \mu_8 - \mu_9)c_4)/\mu_H^3 - (\sigma_{6,9}\mu_5 c_4)/\mu_H^2 - (\mu_5\sigma_{6,6}c_4)/\mu_H^2 \\
&- (\sigma_{5,6}\mu_6 c_4)/\mu_H^2 - (\sigma_{5,7}\mu_6 c_4)/\mu_H^2 - (\sigma_{5,8}\mu_6 c_4)/\mu_H^2 - (\sigma_{5,9}\mu_6 c_4)/\mu_H^2 \\
&+ (\sigma_{5,6}c_4)/\mu_H + (\mu_5\mu_6 c_4)/\mu_H + \mu_6 c_7 - \mu_7 c_{10} + (\mu_5\sigma_{8,8}\mu_6 c_4)/\mu_H^3 \\
\frac{d\mu_8}{dt} &= -\mu_8(c_8 + c_{10}) + \mu_7 c_{12} \\
\frac{d\mu_9}{dt} &= +\mu_8 c_8 - \mu_9 c_{10} \\
\frac{d\sigma_{1,1}}{dt} &= +\mu_1 c_2 - 2\sigma_{1,1}c_2 + c_1(1 + (\sigma_{3,5}(\mu_3 + \mu_4 - \mu_5)c_{11})/\mu_M^3 \\
&- (2\sigma_{4,5}\mu_5 c_{11})/\mu_M^3 - (\sigma_{3,3}\mu_5 c_{11})/\mu_M^3 - (\sigma_{4,4}\mu_5 c_{11})/\mu_M^3 \\
&+ (2\sigma_{1,3}\mu_5 c_{11})/\mu_M^2 + (2\sigma_{1,4}\mu_5 c_{11})/\mu_M^2 + (2\sigma_{1,5}\mu_5 c_{11})/\mu_M^2 \\
&- (\mu_5 c_{11})/\mu_M - (\mu_5\sigma_{5,5}c_{11})/\mu_M^3 + (\sigma_{5,5}c_{11})/\mu_M^2) \\
&- (2\sigma_{3,4}\mu_5 c_{11})/\mu_M^3 - (2\sigma_{1,5}c_{11})/\mu_M + (\sigma_{4,5}c_{11})/\mu_M^2 \\
\frac{d\sigma_{2,2}}{dt} &= +\mu_2 c_2 - 2\sigma_{2,2}c_2 + (2\sigma_{3,4}\mu_5 c_1 c_{11})/\mu_M^3 + (2\sigma_{3,5}\mu_5 c_1 c_{11})/\mu_M^3 \\
&+ (2\sigma_{4,5}\mu_5 c_1 c_{11})/\mu_M^3 - (\sigma_{3,5}c_1 c_{11})/\mu_M^2 + (\sigma_{3,3}\mu_5 c_1 c_{11})/\mu_M^3 \\
&- (\sigma_{4,5}c_1 c_{11})/\mu_M^2 - (2\sigma_{2,3}\mu_5 c_1 c_{11})/\mu_M^2 - (2\sigma_{2,4}\mu_5 c_1 c_{11})/\mu_M^2 \\
&- (2\sigma_{2,5}\mu_5 c_1 c_{11})/\mu_M^2 + (2\sigma_{2,5}c_1 c_{11})/\mu_M + (\mu_5 c_1 c_{11})/\mu_M \\
&+ (\sigma_{4,4}\mu_5 c_1 c_{11})/\mu_M^3 + (\mu_5\sigma_{5,5}c_1 c_{11})/\mu_M^3 - (\sigma_{5,5}c_1 c_{11})/\mu_M^2
\end{aligned}
$$

$$
\begin{aligned}
\frac{d\sigma_{3,3}}{dt} &= +\mu_1 c_2 + 2\sigma_{1,3}c_2 + (2\mu_3\sigma_{6,7}\mu_8 c_3)/\mu_H^3 + (2\mu_3\sigma_{6,8}\mu_8 c_3)/\mu_H^3 \\
&+ (2\mu_3\sigma_{7,8}\mu_8 c_3)/\mu_H^3 + (2\mu_3\sigma_{7,9}\mu_8 c_3)/\mu_H^3 + (2\mu_3\sigma_{8,9}\mu_8 c_3)/\mu_H^3 \\
&+ (\mu_3\sigma_{7,7}\mu_8 c_3)/\mu_H^3 + (\mu_3\sigma_{8,8}\mu_8 c_3)/\mu_H^3 + (\mu_3\sigma_{9,9}\mu_8 c_3)/\mu_H^3 \\
&- (\mu_3\sigma_{7,8}c_3)/\mu_H^2 - (\mu_3\sigma_{8,9}c_3)/\mu_H^2 - (\mu_3\sigma_{8,8}c_3)/\mu_H^2 - (\sigma_{3,6}\mu_8 c_3)/\mu_H^2 \\
&- (\sigma_{3,7}\mu_8 c_3)/\mu_H^2 - (\sigma_{3,8}\mu_8 c_3)/\mu_H^2 + (2\sigma_{3,6}\mu_3\mu_8 c_3)/\mu_H^2 + (2\sigma_{3,7}\mu_3\mu_8 c_3)/\mu_H^2 \\
&+ (2\sigma_{3,8}\mu_3\mu_8 c_3)/\mu_H^2 - (\sigma_{3,9}\mu_8 c_3)/\mu_H^2 + (2\mu_3\sigma_{3,9}\mu_8 c_3)/\mu_H^2 + (\sigma_{3,8}c_3)/\mu_H \\
&- (2\sigma_{3,8}\mu_3 c_3)/\mu_H + (\mu_3\mu_8 c_3)/\mu_H - (2\sigma_{3,3}\mu_8 c_3)/\mu_H + \mu_3 c_6 - 2\sigma_{3,3}c_6 \\
&+ (2\mu_3\sigma_{6,9}\mu_8 c_3)/\mu_H^3 + (\mu_3\sigma_{6,6}\mu_8 c_3)/\mu_H^3 - (\mu_3\sigma_{6,8}c_3)/\mu_H^2 \\
\frac{d\sigma_{4,4}}{dt} &= -(\sigma_{3,6}\mu_8 c_3)/\mu_H^2 - (\sigma_{3,7}\mu_8 c_3)/\mu_H^2 - (\sigma_{3,8}\mu_8 c_3)/\mu_H^2 - (\sigma_{3,9}\mu_8 c_3)/\mu_H^2 \\
&+ (\sigma_{3,8}c_3)/\mu_H + +(2\sigma_{3,4}\mu_8 c_3)/\mu_H + (\mu_3(2\sigma_{6,7}\mu_8 + 2\sigma_{6,8}\mu_8 + 2\sigma_{6,9}\mu_8 \\
&+ 2\sigma_{7,8}\mu_8 + 2\sigma_{7,9}\mu_8 + 2\sigma_{8,9}\mu_8 + \sigma_{6,6}\mu_8 + \sigma_{7,7}\mu_8 + \sigma_{8,8}\mu_8 + \sigma_{9,9}\mu_8 - \sigma_{6,8}\mu_H \\
&- \sigma_{7,8}\mu_H - \sigma_{8,9}\mu_H - \sigma_{8,8}\mu_H - 2\sigma_{4,6}\mu_8\mu_H - 2\sigma_{4,7}\mu_8\mu_H - 2\sigma_{4,8}\mu_8\mu_H \\
&- 2\sigma_{4,9}\mu_8\mu_H + \sigma_{4,8}\mu_H^2 + \mu_8\mu_H^2)c_3)/\mu_H^3 + \mu_4 c_5 - 2\sigma_{4,4}c_5 + \mu_4 c_6 - 2\sigma_{4,4}c_6 \\
\frac{d\sigma_{5,5}}{dt} &= \mu_2 c_2 + 2\sigma_{2,5}c_2 + 2\sigma_{4,5}c_5 + \mu_4 c_5 + \mu_5 c_6 - 2\sigma_{5,5}c_6 \\
\frac{d\sigma_{6,6}}{dt} &= (2\sigma_{6,7}\mu_5\mu_6 c_4)/\mu_H^2 + (2\sigma_{6,8}\mu_5\mu_6 c_4)/\mu_H^2 + (2\sigma_{6,9}\mu_5\mu_6 c_4)/\mu_H^2 \\
&- (2\mu_5\sigma_{6,6}(\mu_7 + \mu_8 + \mu_9)c_4)/\mu_H^2 - (2\sigma_{5,6}\mu_6 c_4)/\mu_H + (\mu_5\mu_6 c_4)/\mu_H \\
&+ ((\sigma_{6,9}\mu_5\mu_6 + 2\sigma_{7,8}\mu_5\mu_6 + 2\sigma_{7,9}\mu_5\mu_6 + 2\sigma_{8,9}\mu_5\mu_6 + \mu_5\sigma_{7,7}\mu_6 + \mu_5\sigma_{8,8}\mu_6 \\
&+ \mu_5\sigma_{9,9}\mu_6 - \sigma_{5,7}\mu_6^2 - \sigma_{5,8}\mu_6^2 - \sigma_{5,9}\mu_6^2 - \sigma_{6,9}\mu_5\mu_7 - \mu_5\sigma_{6,6}\mu_7 + \sigma_{5,6}\mu_6\mu_7 \\
&- \sigma_{5,7}\mu_6\mu_7 - \sigma_{5,8}\mu_6\mu_7 - \sigma_{5,9}\mu_6\mu_7 + \sigma_{5,6}\mu_7^2 - \sigma_{6,9}\mu_5\mu_8 - \mu_5\sigma_{6,6}\mu_8 \\
&- \sigma_{5,7}\mu_6\mu_8 - \sigma_{5,8}\mu_6\mu_8 - \sigma_{5,9}\mu_6\mu_8 + 2\sigma_{5,6}\mu_7\mu_8 + \sigma_{5,6}\mu_8^2 + \sigma_{5,6}\mu_6\mu_8 \\
&+ \sigma_{6,7}\mu_5(\mu_6 - \mu_7 - \mu_8 - \mu_9) + \sigma_{6,8}\mu_5(\mu_6 - \mu_7 - \mu_8 - \mu_9) - \sigma_{6,9}\mu_5\mu_9 \\
&- \mu_5\sigma_{6,6}\mu_9 + \sigma_{5,6}\mu_6\mu_9 - \sigma_{5,7}\mu_6\mu_9 - \sigma_{5,8}\mu_6\mu_9 - \sigma_{5,9}\mu_6\mu_9 + 2\sigma_{5,6}\mu_7\mu_9 \\
&+ 2\sigma_{5,6}\mu_8\mu_9 + \sigma_{5,6}\mu_9^2)c_4)/\mu_H^3 - 2\sigma_{6,6}c_7 + \mu_6 c_7 + 2\sigma_{6,7}c_9 \\
&+ 2\sigma_{6,8}c_9 + 2\sigma_{6,9}c_9 + 2\sigma_{6,6}c_9 + \mu_H c_9 - 2\sigma_{6,6}c_{10} + \mu_6 c_{10} \\
\frac{d\sigma_{7,7}}{dt} &= +(2\sigma_{6,9}\mu_5\mu_6 c_4)/\mu_H^3 + (2\sigma_{7,8}\mu_5\mu_6 c_4)/\mu_H^3 + (2\sigma_{7,9}\mu_5\mu_6 c_4)/\mu_H^3 \\
&+ (2\sigma_{8,9}\mu_5\mu_6 c_4)/\mu_H^3 + (\mu_5\sigma_{6,6}\mu_6 c_4)/\mu_H^3 + (\mu_5\sigma_{7,7}\mu_6 c_4)/\mu_H^3 \\
&+ (\mu_5\sigma_{8,8}\mu_6 c_4)/\mu_H^3 + (\mu_5\sigma_{9,9}\mu_6 c_4)/\mu_H^3 - (\sigma_{6,9}\mu_5 c_4)/\mu_H^2 \\
&+ (\sigma_{6,8}\mu_5(\mu_6 - \mu_7 - \mu_8 - \mu_9)c_4)/\mu_H^3 - (\mu_5\sigma_{6,6}c_4)/\mu_H^2 - (\sigma_{5,6}\mu_6 c_4)/\mu_H^2 \\
&- (\sigma_{5,7}\mu_6 c_4)/\mu_H^2 - (\sigma_{5,8}\mu_6 c_4)/\mu_H^2 - (\sigma_{5,9}\mu_6 c_4)/\mu_H^2 - (2\sigma_{7,8}\mu_5\mu_6 c_4)/\mu_H^2
\end{aligned}
$$

$$
\begin{aligned}
& - (2\sigma_{7,9}\mu_5\mu_6 c_4)/\mu_H^2 - (2\mu_5\sigma_{7,7}\mu_6 c_4)/\mu_H^2 + (\sigma_{5,6}c_4)/\mu_H - 2\sigma_{7,7}c_{10} \\
& + (\mu_5\mu_6 c_4)/\mu_H + \sigma_{6,7}((\mu_5(2\mu_6 - \mu_H - 2\mu_6\mu_H + 2\mu_H^2)c_4)/\mu_H^3 + 2c_7) \\
& + \mu_6 c_7 + \mu_7 c_{10} - 2\sigma_{7,7}c_{12} + \mu_7 c_{12} + (2\sigma_{5,7}\mu_6 c_4)/\mu_H \\
\frac{d\sigma_{8,8}}{dt} &= -2\sigma_{8,8}(c_8 + c_{10}) + \mu_8(c_8 + c_{10}) + 2\sigma_{7,8}c_{12} + \mu_7 c_{12} \\
\frac{d\sigma_{9,9}}{dt} &= +2\sigma_{8,9}c_8 + \mu_8 c_8 - 2\sigma_{9,9}c_{10} + \mu_9 c_{10} \\
\frac{d\sigma_{1,2}}{dt} &= (1/\mu_M^2)(-2\sigma_{1,2}\mu_M^2 c_2 + (\sigma_{1,5}(\mu_3 + \mu_4) - \sigma_{2,5}(\mu_3 + \mu_4) \\
& + (-\sigma_{1,3} - \sigma_{1,4} + \sigma_{2,3} + \sigma_{2,4})\mu_5)c_1 c_{11}) \\
\frac{d\sigma_{1,3}}{dt} &= -\mu_1 c_2 + \sigma_{1,1}c_2 + (\sigma_{1,6}\mu_3\mu_8 c_3)/\mu_H^2 + (\sigma_{1,7}\mu_3\mu_8 c_3)/\mu_H^2 \\
& + (\sigma_{1,8}\mu_3\mu_8 c_3)/\mu_H^2 + (\sigma_{1,9}\mu_3\mu_8 c_3)/\mu_H^2 - (\sigma_{1,8}\mu_3 c_3)/\mu_H \\
& + \sigma_{1,3}(-c_2 - (\mu_8 c_3)/\mu_H - c_6) + (\sigma_{3,4}\mu_5 c_1 c_{11})/\mu_M^2 \\
& + (\sigma_{3,5}\mu_5 c_1 c_{11})/\mu_M^2 + (\sigma_{3,3}\mu_5 c_1 c_{11})/\mu_M^2 - (\sigma_{3,5}c_1 c_{11})/\mu_M \\
\frac{d\sigma_{1,4}}{dt} &= (-\sigma_{1,4})c_2 - (\sigma_{1,6}\mu_3\mu_8 c_3)/\mu_H^2 - (\sigma_{1,7}\mu_3\mu_8 c_3)/\mu_H^2 \\
& - (\sigma_{1,9}\mu_3\mu_8 c_3)/\mu_H^2 + (\sigma_{1,8}\mu_3(\mu_6 + \mu_7 + \mu_9)c_3)/\mu_H^2 \\
& - \sigma_{1,4}c_6 - (\sigma_{4,5}(\mu_3 + \mu_4)c_1 c_{11})/\mu_M^2 + (\sigma_{3,4}\mu_5 c_1 c_{11})/\mu_M^2 \\
& - \sigma_{1,4}c_5 + (\sigma_{1,3}\mu_8 c_3)/\mu_H + (\sigma_{4,4}\mu_5 c_1 c_{11})/\mu_M^2 \\
\frac{d\sigma_{1,5}}{dt} &= \sigma_{1,2}c_2 - \sigma_{1,5}c_2 + \sigma_{1,4}c_5 - \sigma_{1,5}c_6 + (\sigma_{3,5}\mu_5 c_1 c_{11})/\mu_M^2 \\
& - ((\mu_3 + \mu_4)\sigma_{5,5}c_1 c_{11})/\mu_M^2 + (\sigma_{4,5}\mu_5 c_1 c_{11})/\mu_M^2 \\
\frac{d\sigma_{1,6}}{dt} &= (\sigma_{1,8}\mu_5\mu_6 c_4)/\mu_H^2 + (\sigma_{1,9}\mu_5\mu_6 c_4)/\mu_H^2 - (\sigma_{1,5}\mu_6 c_4)/\mu_H \\
& + \sigma_{1,7}((\mu_5\mu_6 c_4)/\mu_H^2 + c_9) + \sigma_{1,6}(-c_2 - (\mu_5(\mu_7 + \mu_8 + \mu_9)c_4)/\mu_H^2 \\
& - c_7 + c_9 - c_{10}) + (\sigma_{3,6}\mu_5 c_1 c_{11})/\mu_M^2 + (\sigma_{4,6}\mu_5 c_1 c_{11})/\mu_M^2 \\
& + (\sigma_{5,6}\mu_5 c_1 c_{11})/\mu_M^2 - (\sigma_{5,6}c_1 c_{11})/\mu_M + \sigma_{1,8}c_9 + \sigma_{1,9}c_9 \\
\frac{d\sigma_{1,7}}{dt} &= (-\sigma_{1,7})c_2 - (\sigma_{1,7}\mu_5\mu_6 c_4)/\mu_H^2 - (\sigma_{1,8}\mu_5\mu_6 c_4)/\mu_H^2 \\
& + (\sigma_{1,6}\mu_5(\mu_7 + \mu_8 + \mu_9)c_4)/\mu_H^2 + (\sigma_{1,5}\mu_6 c_4)/\mu_H + \sigma_{1,6}c_7 - \sigma_{1,7}c_{10} \\
& - (\sigma_{5,7}(\mu_3 + \mu_4)c_1 c_{11})/\mu_M^2 + (\sigma_{3,7}\mu_5 c_1 c_{11})/\mu_M^2 + (\sigma_{4,7}\mu_5 c_1 c_{11})/\mu_M^2 \\
& - (\sigma_{1,9}\mu_5\mu_6 c_4)/\mu_H^2 - \sigma_{1,7}c_{12} \\
\frac{d\sigma_{1,8}}{dt} &= (-\sigma_{1,8})c_2 - \sigma_{1,8}c_8 - \sigma_{1,8}c_{10} - (\sigma_{5,8}(\mu_3 + \mu_4)c_1 c_{11})/\mu_M^2 \\
& + (\sigma_{4,8}\mu_5 c_1 c_{11})/\mu_M^2 + \sigma_{1,7}c_{12} + (\sigma_{3,8}\mu_5 c_1 c_{11})/\mu_M^2 \\
\frac{d\sigma_{1,9}}{dt} &= (-\sigma_{1,9})(c_2 + c_{10}) + (1/\mu_M^2)(\sigma_{1,8}\mu_M^2 c_8 + ((-\mu_3)\sigma_{5,9} - \sigma_{5,9}\mu_4 \\
& + (\sigma_{3,9} + \sigma_{4,9})\mu_5)c_1 c_{11})
\end{aligned}
$$

$$
\begin{aligned}
\frac{d\sigma_{2,3}}{dt} &= \sigma_{1,2}c_2 + (\sigma_{2,6}\mu_3\mu_8c_3)/\mu_H^2 + (\sigma_{2,7}\mu_3\mu_8c_3)/\mu_H^2 + (\sigma_{2,8}\mu_3\mu_8c_3)/\mu_H^2 \\
&+ (\sigma_{2,9}\mu_3\mu_8c_3)/\mu_H^2 - (\sigma_{2,8}\mu_3c_3)/\mu_H + \sigma_{2,3}(-c_2 - (\mu_8c_3)/\mu_H - c_6) \\
&- (\sigma_{3,4}\mu_5c_1c_{11})/\mu_M^2 - (\sigma_{3,5}\mu_5c_1c_{11})/\mu_M^2 - (\sigma_{3,3}\mu_5c_1c_{11})/\mu_M^2 + (\sigma_{3,5}c_1c_{11})/\mu_M \\
\frac{d\sigma_{2,4}}{dt} &= -((\sigma_{2,6}\mu_3\mu_8c_3)/\mu_H^2) - (\sigma_{2,7}\mu_3\mu_8c_3)/\mu_H^2 - (\sigma_{2,8}\mu_3\mu_8c_3)/\mu_H^2 \\
&- (\sigma_{2,9}\mu_3\mu_8c_3)/\mu_H^2 + (\sigma_{2,8}\mu_3c_3)/\mu_H + (\sigma_{2,3}\mu_8c_3)/\mu_H - \sigma_{2,4}(c_2 + c_5 + c_6) \\
&- (\sigma_{3,4}\mu_5c_1c_{11})/\mu_M^2 - (\sigma_{4,5}\mu_5c_1c_{11})/\mu_M^2 - (\sigma_{4,4}\mu_5c_1c_{11})/\mu_M^2 + (\sigma_{4,5}c_1c_{11})/\mu_M \\
\frac{d\sigma_{2,5}}{dt} &= -\mu_2c_2 + \sigma_{2,2}c_2 + \sigma_{2,4}c_5 - \sigma_{2,5}(c_2 + c_6) - (\sigma_{3,5}\mu_5c_1c_{11})/\mu_M^2 \\
&- (\sigma_{4,5}\mu_5c_1c_{11})/\mu_M^2 - (\mu_5\sigma_{5,5}c_1c_{11})/\mu_M^2 + (\sigma_{5,5}c_1c_{11})/\mu_M \\
\frac{d\sigma_{2,6}}{dt} &= (\sigma_{2,8}\mu_5\mu_6c_4)/\mu_H^2 + (\sigma_{2,9}\mu_5\mu_6c_4)/\mu_H^2 - (\sigma_{2,5}\mu_6c_4)/\mu_H + \sigma_{2,8}c_9 + \sigma_{2,9}c_9 \\
&+ \sigma_{2,7}((\mu_5\mu_6c_4)/\mu_H^2 + c_9) - (\sigma_{3,6}\mu_5c_1c_{11})/\mu_M^2 - (\sigma_{4,6}\mu_5c_1c_{11})/\mu_M^2 \\
&+ \sigma_{2,6}(-c_2 - (\mu_5(\mu_7 + \mu_8 + \mu_9)c_4)/\mu_H^2 - c_7 + c_9 - c_{10}) + (\sigma_{5,6}c_1c_{11})/\mu_M \\
&- (\sigma_{5,6}\mu_5c_1c_{11})/\mu_M^2 \\
\frac{d\sigma_{2,7}}{dt} &= -((\sigma_{2,8}\mu_5\mu_6c_4)/\mu_H^2) - (\sigma_{2,9}\mu_5\mu_6c_4)/\mu_H^2 + (\sigma_{2,5}\mu_6c_4)/\mu_H \\
&+ \sigma_{2,6}((\mu_5(\mu_7 + \mu_8 + \mu_9)c_4)/\mu_H^2 + c_7) - (\sigma_{3,7}\mu_5c_1c_{11})/\mu_M^2 \\
&- (\sigma_{5,7}\mu_5c_1c_{11})/\mu_M^2 + (\sigma_{5,7}c_1c_{11})/\mu_M - (\sigma_{4,7}\mu_5c_1c_{11})/\mu_M^2 \\
&+ \sigma_{2,7}(-c_2 - (\mu_5\mu_6c_4)/\mu_H^2 - c_{10} - c_{12}) \\
\frac{d\sigma_{2,8}}{dt} &= (-\sigma_{2,8})(c_2 + c_8 + c_{10}) - (\sigma_{3,8}\mu_5c_1c_{11})/\mu_M^2 - (\sigma_{4,8}\mu_5c_1c_{11})/\mu_M^2 \\
&- (\sigma_{5,8}\mu_5c_1c_{11})/\mu_M^2 + (\sigma_{5,8}c_1c_{11})/\mu_M + \sigma_{2,7}c_{12} \\
\frac{d\sigma_{2,9}}{dt} &= (-\sigma_{2,9})(c_2 + c_{10}) + (1/\mu_M^2)(\sigma_{2,8}\mu_M^2c_8 + (\mu_3\sigma_{5,9} + \sigma_{5,9}\mu_4 \\
&- (\sigma_{3,9} + \sigma_{4,9})\mu_5)c_1c_{11}) \\
\frac{d\sigma_{3,4}}{dt} &= \sigma_{1,4}c_2 + (\sigma_{3,6}\mu_8c_3)/\mu_H^2 + (\sigma_{3,7}\mu_8c_3)/\mu_H^2 + (\sigma_{3,8}\mu_8c_3)/\mu_H^2 \\
&- (\sigma_{3,8}c_3)/\mu_H - (\sigma_{3,4}\mu_8c_3)/\mu_H + (\sigma_{3,3}\mu_8c_3)/\mu_H + (\sigma_{3,9}\mu_8c_3)/\mu_H^2 \\
&+ (\mu_3(-2\sigma_{6,7}\mu_8 - 2\sigma_{6,8}\mu_8 - 2\sigma_{6,9}\mu_8 - 2\sigma_{7,8}\mu_8 - 2\sigma_{7,9}\mu_8 - 2\sigma_{8,9}\mu_8 \\
&- \sigma_{6,6}\mu_8 - \sigma_{7,7}\mu_8 - \sigma_{8,8}\mu_8 - \sigma_{9,9}\mu_8 + \sigma_{6,8}\mu_H + \sigma_{7,8}\mu_H + \sigma_{8,9}\mu_H \\
&+ \sigma_{8,8}\mu_H - \sigma_{3,6}\mu_8\mu_H - \sigma_{3,7}\mu_8\mu_H - \sigma_{3,8}\mu_8\mu_H - \sigma_{3,9}\mu_8\mu_H + \sigma_{4,6}\mu_8\mu_H \\
&+ \sigma_{4,7}\mu_8\mu_H + \sigma_{4,8}\mu_8\mu_H + \sigma_{4,9}\mu_8\mu_H + \sigma_{3,8}\mu_H^2 - \mu_8\mu_H^2)c_3)/\mu_H^3 \\
&- \sigma_{3,4}c_5 - 2\sigma_{3,4}c_6 - \sigma_{4,8}\mu_H^2 \\
\frac{d\sigma_{3,5}}{dt} &= \sigma_{1,5}c_2 + \sigma_{2,3}c_2 + (\mu_3\sigma_{5,6}\mu_8c_3)/\mu_H^2 + (\mu_3\sigma_{5,7}\mu_8c_3)/\mu_H^2 + (\mu_3\sigma_{5,8}\mu_8c_3)/\mu_H^2 \\
&+ (\mu_3\sigma_{5,9}\mu_8c_3)/\mu_H^2 - (\mu_3\sigma_{5,8}c_3)/\mu_H - (\sigma_{3,5}\mu_8c_3)/\mu_H + \sigma_{3,4}c_5 - 2\sigma_{3,5}c_6 \\
\frac{d\sigma_{3,6}}{dt} &= \sigma_{1,6}c_2 - (\sigma_{3,6}\mu_8c_3)/\mu_H - (\mu_3((-(\sigma_{6,7} + \sigma_{6,9} + \sigma_{6,6}))\mu_8 \\
&+ \sigma_{6,8}(\mu_6 + \mu_7 + \mu_9))c_3)/\mu_H^2 + (\sigma_{3,6}\mu_5\mu_6c_4)/\mu_H^2 + (\sigma_{3,7}\mu_5\mu_6c_4)/\mu_H^2 \\
&+ (\sigma_{3,8}\mu_5\mu_6c_4)/\mu_H^2 + (\sigma_{3,9}\mu_5\mu_6c_4)/\mu_H^2 - (\sigma_{3,6}\mu_5c_4)/\mu_H - (\sigma_{3,5}\mu_6c_4)/\mu_H \\
&- \sigma_{3,6}c_6 - \sigma_{3,6}c_7 + \sigma_{3,6}c_9 + \sigma_{3,7}c_9 + \sigma_{3,8}c_9 + \sigma_{3,9}c_9 - \sigma_{3,6}c_{10}
\end{aligned}
$$

$$
\begin{aligned}
\frac{d\sigma_{3,7}}{dt} &= \sigma_{1,7}c_2 - (\sigma_{3,7}\mu_8 c_3)/\mu_H - (\mu_3((-(\sigma_{6,7}+\sigma_{7,9}+\sigma_{7,7}))\mu_8 \\
&+ \sigma_{7,8}(\mu_6+\mu_7+\mu_9))c_3)/\mu_H^2 - (\sigma_{3,6}\mu_5\mu_6 c_4)/\mu_H^2 - (\sigma_{3,7}\mu_5\mu_6 c_4)/\mu_H^2 \\
&- (\sigma_{3,8}\mu_5\mu_6 c_4)/\mu_H^2 - (\sigma_{3,9}\mu_5\mu_6 c_4)/\mu_H^2 + (\sigma_{3,6}\mu_5 c_4)/\mu_H \\
&+ (\sigma_{3,5}\mu_6 c_4)/\mu_H - \sigma_{3,7}c_6 + \sigma_{3,6}c_7 - \sigma_{3,7}c_{10} - \sigma_{3,7}c_{12} \\
\frac{d\sigma_{3,8}}{dt} &= \sigma_{1,8}c_2 - (\sigma_{3,8}\mu_8 c_3)/\mu_H - (\mu_3((-(\sigma_{6,8}+\sigma_{7,8}+\sigma_{8,9}))\mu_8 - \sigma_{3,8}c_8 \\
&+ \sigma_{8,8}(\mu_6+\mu_7+\mu_9))c_3)/\mu_H^2 - \sigma_{3,8}c_6 - \sigma_{3,8}c_{10} + \sigma_{3,7}c_{12} \\
\frac{d\sigma_{3,9}}{dt} &= \sigma_{1,9}c_2 - (\sigma_{3,9}\mu_8 c_3)/\mu_H - (\mu_3((-(\sigma_{6,9}+\sigma_{7,9}+\sigma_{9,9}))\mu_8 \\
&+ \sigma_{8,9}(\mu_6+\mu_7+\mu_9))c_3)/\mu_H^2 - \sigma_{3,9}c_6 + \sigma_{3,8}c_8 - \sigma_{3,9}c_{10} \\
\frac{d\sigma_{4,5}}{dt} &= +\sigma_{2,4}c_2 + (\sigma_{3,5}\mu_8 c_3)/\mu_H + (\mu_3((-(\sigma_{5,6}+\sigma_{5,7}+\sigma_{5,9}))\mu_8 \\
&+ \sigma_{5,8}(\mu_6+\mu_7+\mu_9))c_3)/\mu_H^2 - \sigma_{4,5}c_5 - \mu_4 c_5 + \sigma_{4,4}c_5 - 2\sigma_{4,5}c_6 \\
\frac{d\sigma_{4,6}}{dt} &= (\sigma_{3,6}\mu_8 c_3)/\mu_H + (\mu_3((-(\sigma_{6,7}+\sigma_{6,9}+\sigma_{6,6}))\mu_8 \\
&+ \sigma_{6,8}(\mu_6+\mu_7+\mu_9))c_3)/\mu_H^2 + (\sigma_{4,6}\mu_5\mu_6 c_4)/\mu_H^2 - \sigma_{4,6}c_{10} \\
&+ (\sigma_{4,7}\mu_5\mu_6 c_4)/\mu_H^2 + (\sigma_{4,8}\mu_5\mu_6 c_4)/\mu_H^2 + (\sigma_{4,9}\mu_5\mu_6 c_4)/\mu_H^2 \\
&- (\sigma_{4,5}\mu_6 c_4)/\mu_H - \sigma_{4,6}c_5 - \sigma_{4,6}c_6 - \sigma_{4,6}c_7 + \sigma_{4,6}c_9 + \sigma_{4,7}c_9 \\
&- (\sigma_{4,6}\mu_5 c_4)/\mu_H + \sigma_{4,8}c_9 + \sigma_{4,9}c_9 \\
\frac{d\sigma_{4,7}}{dt} &= (\sigma_{3,7}\mu_8 c_3)/\mu_H + (\mu_3((-(\sigma_{6,7}+\sigma_{7,9}+\sigma_{7,7}))\mu_8 \\
&- (\sigma_{4,6}\mu_5\mu_6 c_4)/\mu_H^2 - (\sigma_{4,7}\mu_5\mu_6 c_4)/\mu_H^2 - (\sigma_{4,8}\mu_5\mu_6 c_4)/\mu_H^2 \\
&+ (\sigma_{4,6}\mu_5 c_4)/\mu_H + (\sigma_{4,5}\mu_6 c_4)/\mu_H - \sigma_{4,7}c_5 - \sigma_{4,7}c_6 - (\sigma_{4,9}\mu_5\mu_6 c_4)/\mu_H^2 \\
&+ \sigma_{4,6}c_7 - \sigma_{4,7}c_{10} - \sigma_{4,7}c_{12} + \sigma_{7,8}(\mu_6+\mu_7+\mu_9))c_3)/\mu_H^2 \\
\frac{d\sigma_{4,8}}{dt} &= (\sigma_{3,8}\mu_8 c_3)/\mu_H + (\mu_3((-(\sigma_{6,8}+\sigma_{7,8}+\sigma_{8,9}))\mu_8 \\
&- \sigma_{4,8}c_5 - \sigma_{4,8}c_6 - \sigma_{4,8}c_8 - \sigma_{4,8}c_{10} + \sigma_{4,7}c_{12} + \sigma_{8,8}(\mu_6+\mu_7+\mu_9))c_3)/\mu_H^2 \\
\frac{d\sigma_{4,9}}{dt} &= (\sigma_{3,9}\mu_8 c_3)/\mu_H + (\mu_3((-(\sigma_{6,9}+\sigma_{7,9}+\sigma_{9,9}))\mu_8 \\
&- \sigma_{4,9}c_5 - \sigma_{4,9}c_6 + \sigma_{4,8}c_8 - \sigma_{4,9}c_{10} + \sigma_{8,9}(\mu_6+\mu_7+\mu_9))c_3)/\mu_H^2 \\
\frac{d\sigma_{5,6}}{dt} &= \sigma_{2,6}c_2 + (\sigma_{5,7}\mu_5\mu_6 c_4)/\mu_H^2 + (\sigma_{5,8}\mu_5\mu_6 c_4)/\mu_H^2 + (\sigma_{5,9}\mu_5\mu_6 c_4)/\mu_H^2 \\
&- (\sigma_{5,5}\mu_6 c_4)/\mu_H + \sigma_{4,6}c_5 + \sigma_{5,7}c_9 + \sigma_{5,8}c_9 + \sigma_{5,9}c_9 \\
&+ \sigma_{5,6}(-((\mu_5(\mu_7+\mu_8+\mu_9)c_4)/\mu_H^2) - c_6 - c_7 + c_9 - c_{10}) \\
\frac{d\sigma_{5,7}}{dt} &= \sigma_{2,7}c_2 - (\sigma_{5,7}\mu_5\mu_6 c_4)/\mu_H^2 + \sigma_{4,7}c_5 - \sigma_{5,7}c_6 \\
&+ (\sigma_{5,5}\mu_6 c_4)/\mu_H - (\sigma_{5,9}\mu_5\mu_6 c_4)/\mu_H^2 - (\sigma_{5,8}\mu_5\mu_6 c_4)/\mu_H^2 \\
&- \sigma_{5,7}c_{10} - \sigma_{5,7}c_{12} + \sigma_{5,6}((\mu_5(\mu_7+\mu_8+\mu_9)c_4)/\mu_H^2 + c_7) \\
\frac{d\sigma_{5,8}}{dt} &= \sigma_{2,8}c_2 + \sigma_{4,8}c_5 - \sigma_{5,8}c_6 - \sigma_{5,8}c_8 - \sigma_{5,8}c_{10} + \sigma_{5,7}c_{12} \\
\frac{d\sigma_{5,9}}{dt} &= \sigma_{2,9}c_2 + \sigma_{4,9}c_5 - \sigma_{5,9}c_6 + \sigma_{5,8}c_8 - \sigma_{5,9}c_{10}
\end{aligned}
$$

$$
\begin{aligned}
\frac{d\sigma_{6,7}}{dt} &= -(2\sigma_{6,9}\mu_5\mu_6c_4)/\mu_H^3 - (2\sigma_{7,8}\mu_5\mu_6c_4)/\mu_H^3 - (2\sigma_{7,9}\mu_5\mu_6c_4)/\mu_H^3 \\
&- (2\sigma_{8,9}\mu_5\mu_6c_4)/\mu_H^3 - (\mu_5\sigma_{6,6}\mu_6c_4)/\mu_H^3 - (\mu_5\sigma_{7,7}\mu_6c_4)/\mu_H^3 \\
&- (\mu_5\sigma_{9,9}\mu_6c_4)/\mu_H^3 + (\sigma_{6,9}\mu_5c_4)/\mu_H^2 + (\mu_5\sigma_{6,6}c_4)/\mu_H^2 + (\sigma_{5,6}\mu_6c_4)/\mu_H^2 \\
&+ (\sigma_{5,7}\mu_6c_4)/\mu_H^2 + (\sigma_{5,8}\mu_6c_4)/\mu_H^2 + (\sigma_{5,9}\mu_6c_4)/\mu_H^2 - (\sigma_{6,9}\mu_5\mu_6c_4)/\mu_H^2 \\
&+ (\sigma_{7,8}\mu_5\mu_6c_4)/\mu_H^2 + (\sigma_{7,9}\mu_5\mu_6c_4)/\mu_H^2 - (\mu_5\sigma_{6,6}\mu_6c_4)/\mu_H^2 \\
&- (\sigma_{5,6}c_4)/\mu_H + (\mu_5\sigma_{6,6}c_4)/\mu_H + (\sigma_{5,6}\mu_6c_4)/\mu_H - (\sigma_{5,7}\mu_6c_4)/\mu_H \\
&+ (\sigma_{6,8}\mu_5(-2\mu_6 + \mu_H - \mu_6\mu_H)c_4)/\mu_H^3 + \sigma_{6,6}c_7 - \mu_6c_7 + \sigma_{7,8}c_9 \\
&+ \sigma_{6,7}((\mu_5(-2\mu_6 + \mu_H - \mu_H^2)c_4)/\mu_H^3 - c_7 + c_9 - 2c_{10} - c_{12}) + \sigma_{7,9}c_9 \\
&- (\mu_5\sigma_{8,8}\mu_6c_4)/\mu_H^3 + (\mu_5\sigma_{7,7}\mu_6c_4)/\mu_H^2 - (\mu_5\mu_6c_4)/\mu_H + \sigma_{7,7}c_9 \\
\frac{d\sigma_{6,8}}{dt} &= (\sigma_{8,9}\mu_5\mu_6c_4)/\mu_H^2 + (\mu_5\sigma_{8,8}\mu_6c_4)/\mu_H^2 - (\sigma_{5,8}\mu_6c_4)/\mu_H + \sigma_{8,9}c_9 \\
&+ \sigma_{8,8}c_9 + \sigma_{7,8}((\mu_5\mu_6c_4)/\mu_H^2 + c_9) + \sigma_{6,7}c_{12} \\
&+ \sigma_{6,8}(-((\mu_5(\mu_7 + \mu_8 + \mu_9)c_4)/\mu_H^2) - c_7 - c_8 + c_9 - 2c_{10}) \\
\frac{d\sigma_{6,9}}{dt} &= (\sigma_{8,9}\mu_5\mu_6c_4)/\mu_H^2 + (\mu_5\sigma_{9,9}\mu_6c_4)/\mu_H^2 - (\sigma_{5,9}\mu_6c_4)/\mu_H \\
&+ \sigma_{6,8}c_8 + \sigma_{8,9}c_9 + \sigma_{9,9}c_9 + \sigma_{7,9}((\mu_5\mu_6c_4)/\mu_H^2 + c_9) \\
&+ \sigma_{6,9}(-((\mu_5(\mu_7 + \mu_8 + \mu_9)c_4)/\mu_H^2) - c_7 + c_9 - 2c_{10}) \\
\frac{d\sigma_{7,8}}{dt} &= -(\sigma_{8,9}\mu_5\mu_6c_4)/\mu_H^2 - (\mu_5\sigma_{8,8}\mu_6c_4)/\mu_H^2 + (\sigma_{5,8}\mu_6c_4)/\mu_H \\
&+ \sigma_{6,8}((\mu_5(\mu_7 + \mu_8 + \mu_9)c_4)/\mu_H^2 + c_7) + \sigma_{7,8}(-((\mu_5\mu_6c_4)/\mu_H^2) \\
&- c_8 - 2c_{10} - c_{12}) + \sigma_{7,7}c_{12} - \mu_7c_{12} \\
\frac{d\sigma_{7,9}}{dt} &= -((\sigma_{8,9}\mu_5\mu_6c_4)/\mu_H^2) - (\mu_5\sigma_{9,9}\mu_6c_4)/\mu_H^2 + (\sigma_{5,9}\mu_6c_4)/\mu_H \\
&+ \sigma_{6,9}((\mu_5(\mu_7 + \mu_8 + \mu_9)c_4)/\mu_H^2 + c_7) \\
&+ \sigma_{7,8}c_8 + \sigma_{7,9}(-((\mu_5\mu_6c_4)/\mu_H^2) - 2c_{10} - c_{12}) \\
\frac{d\sigma_{8,9}}{dt} &= +\sigma_{8,8}c_8 - \mu_8c_8 - \sigma_{8,9}(c_8 + 2c_{10}) + \sigma_{7,9}c_{12}
\end{aligned}
$$

References

[1] H. Lee, S. Lee, and C. H. Lee, "Stochastic methods for epidemic models: An application to the 2009 h1n1 influenza outbreak in korea," *Applied Mathematics and Computation*, vol. 286, pp. 232–249, 2016. ix, 11, 16, 20

[2] A. G. McKendrick, "Applications of mathematics to medical problems," *Proceedings of the Edinburgh Mathematical Society*, vol. 44, pp. 98–130, 1925. 1

[3] W. O. Kermack and A. G. McKendrick, "A contribution to the mathematical theory of epidemics," in *Proceedings of the Royal Society of London A: mathematical, physical and engineering sciences*, vol. 115, pp. 700–721, The Royal Society, 1927. 1

[4] A. Alexanderian, M. K. Gobbert, K. R. Fister, H. Gaff, S. Lenhart, and E. Schaefer, "An age-structured model for the spread of epidemic cholera: analysis and simulation," *Nonlinear Analysis: Real World Applications*, vol. 12, no. 6, pp. 3483–3498, 2011. 1

[5] E. M. Lotfi, M. Maziane, K. Hattaf, and N. Yousfi, "Partial differential equations of an epidemic model with spatial diffusion," *International Journal of Partial Differential Equations*, vol. 2014, 2014. 1

[6] L. J. Allen and G. E. Lahodny Jr, "Extinction thresholds in deterministic and stochastic epidemic models," *Journal of biological dynamics*, vol. 6, no. 2, pp. 590–611, 2012. 1

[7] J. A. Jacquez and P. O'Neill, "Reproduction numbers and thresholds in stochastic epidemic models i. homogeneous populations," *Mathematical Biosciences*, vol. 107, no. 2, pp. 161–186, 1991. 1

[8] T. Britton, "Stochastic epidemic models: a survey," *Mathematical biosciences*, vol. 225, no. 1, pp. 24–35, 2010. 2

[9] D. G. Kendall, "Deterministic and stochastic epidemics in closed populations," in *Proc. 3rd Berkeley Symp. Math. Statist. Prob*, vol. 4, pp. 149–165, 1956. 2

[10] M. Bartlett, "Some evolutionary stochastic processes," *Journal of the Royal Statistical Society. Series B (Methodological)*, vol. 11, no. 2, pp. 211–229, 1949. 2

[11] L. J. Allen and A. M. Burgin, "Comparison of deterministic and stochastic SIS and SIR models in discrete time," *Mathematical biosciences*, vol. 163, no. 1, pp. 1–33, 2000. 2

[12] N. Samat and D. Percy, "Vector-borne infectious disease mapping with stochastic difference equations: an analysis of dengue disease in malaysia," *Journal of Applied Statistics*, vol. 39, no. 9, pp. 2029–2046, 2012. 2

[13] Y. Cao and D. Denu, "Analysis of stochastic vector-host epidemic model with direct transmission.," *Discrete & Continuous Dynamical Systems-Series B*, vol. 21, no. 7, 2016. 2

[14] M. Otero and H. Solari, "Stochastic eco-epidemiological model of dengue disease transmission by aedes aegypti mosquito," *Mathematical biosciences*, vol. 223, no. 1, pp. 32–46, 2010. 2

[15] D. T. Gillespie, "A general method for numerically simulating the stochastic time evolution of coupled chemical reactions," *Journal of computational physics*, vol. 22, no. 4, pp. 403–434, 1976. 2

[16] D. T. Gillespie, "The chemical langevin equation," *The Journal of Chemical Physics*, vol. 113, no. 1, pp. 297–306, 2000. 2, 80

[17] D. T. Gillespie, "Approximate accelerated stochastic simulation of chemically reacting systems," *The Journal of Chemical Physics*, vol. 115, no. 4, pp. 1716–1733, 2001. 2, 80

[18] A. L. Lloyd, "Estimating variability in models for recurrent epidemics: assessing the use of moment closure techniques," *Theoretical population biology*, vol. 65, no. 1, pp. 49–65, 2004. 2

[19] I. Krishnarajah, A. Cook, G. Marion, and G. Gibson, "Novel moment closure approximations in stochastic epidemics," *Bulletin of mathematical biology*, vol. 67, no. 4, pp. 855–873, 2005. 2

[20] C. H. Lee, K.-H. Kim, and P. Kim, "A moment closure method for stochastic reaction networks," *The Journal of chemical physics*, vol. 130, no. 13, p. 134107, 2009. 2, 18, 19

[21] National Center for Emerging and Zoonotic Infectious Disease, Centers for Disease Control and Prevention(CDC), "Mosquito life cycle." 4

[22] S.-C. Chen, C.-M. Liao, C.-P. Chio, H.-H. Chou, S.-H. You, and Y.-H. Cheng, "Lagged temperature effect with mosquito transmission potential explains dengue variability in southern taiwan: insights from a statistical analysis," *Science of the total environment*, vol. 408, no. 19, pp. 4069–4075, 2010. 4

[23] S. Janreung and W. Chinviriyasit, "Dengue fever with two strains in thailand," *International Journal of Applied Physics and Mathematics*, vol. 4, no. 1, p. 55, 2014. 4, 57

[24] B. W. Kooi, M. Aguiar, and N. Stollenwerk, "Analysis of an asymmetric two-strain dengue model," *Mathematical biosciences*, vol. 248, pp. 128–139, 2014. 4

[25] K. Hu, C. Thoens, S. Bianco, S. Edlund, M. Davis, J. Douglas, and J. Kaufman, "Modeling the dynamics of dengue fever," in *Social Computing, Behavioral-Cultural Modeling and Prediction*, pp. 486–494, Springer, 2013. 4, 53, 57, 62

[26] E. Chikaki and H. Ishikawa, "A dengue transmission model in thailand considering sequential infections with all four serotypes," *The Journal of Infection in Developing Countries*, vol. 3, no. 09, pp. 711–722, 2009. 4

[27] S.-C. Chen and M.-H. Hsieh, "Modeling the transmission dynamics of dengue fever: implications of temperature effects," *Science of the Total Environment*, vol. 431, pp. 385–391, 2012. 4, 42, 57, 77

[28] M. Andraud, N. Hens, and P. Beutels, "A simple periodic-forced model for dengue fitted to incidence data in singapore," *Mathematical biosciences*, vol. 244, no. 1, pp. 22–28, 2013. 4

[29] M. G. Teixeira, J. B. Siqueira Jr, G. L. Ferreira, L. Bricks, and G. Joint, "Epidemiological trends of dengue disease in brazil (2000–2010): a systematic literature search and analysis," *PLoS Negl Trop Dis*, vol. 7, no. 12, p. e2520, 2013. 4

[30] S. Naish, P. Dale, J. S. Mackenzie, J. McBride, K. Mengersen, and S. Tong, "Climate change and dengue: a critical and systematic review of quantitative modelling approaches," *BMC infectious diseases*, vol. 14, no. 1, p. 1, 2014. 4

[31] S. Polwiang, "The seasonal reproduction number of dengue fever: impacts of climate on transmission," *PeerJ*, vol. 3, p. e1069, 2015. 4, 41, 46, 52, 53, 57

[32] H. Yang, M. Macoris, K. Galvani, M. Andrighetti, and D. Wanderley, "Assessing the effects of temperature on the population of aedes aegypti, the vector of dengue," *Epidemiology and infection*, vol. 137, no. 08, pp. 1188–1202, 2009. 4, 52, 53

[33] H. M. Yang, M. d. L. da Graca Macoris, K. C. Galvani, and M. T. M. Andrighetti, "Follow up estimation of aedes aegypti entomological parameters and mathematical modellings," *Biosystems*, vol. 103, no. 3, pp. 360–371, 2011. 4

[34] S. Berger *et al.*, *Infectious Diseases of South Korea*. GIDEON Informatics Inc, 2015. 4

[35] Y. E. Jeong, W.-C. Lee, J. E. Cho, M.-G. Han, and W.-J. Lee, "Comparison of the epidemiological aspects of imported dengue cases between korea and japan, 2006–2010," *Osong public health and research perspectives*, vol. 7, no. 1, pp. 71–74, 2016. 4

[36] S. H. Choi, Y. J. Kim, J. H. Shin, K. H. Yoo, K. W. Sung, and H. H. Koo, "International travel of korean children and dengue fever: A single institutional analysis," *Korean journal of pediatrics*, vol. 53, no. 6, pp. 701–704, 2010. 4, 54

[37] H. Guo and M. Y. Li, "Impacts of migration and immigration on disease transmission dynamics in heterogeneous populations," *Discrete Contin. Dyn. Syst. Ser. B*, vol. 17, no. 7, pp. 2413–2430, 2012. 4

[38] M. Y. Li and L. Wang, "Global stability in some seir epidemic models," in *Mathematical approaches for emerging and reemerging infectious diseases: models, methods, and theory*, pp. 295–311, Springer, 2002. 4

[39] F. Brauer, C. Castillo-Chavez, and C. Castillo-Chavez, *Mathematical models in population biology and epidemiology*, vol. 40. Springer, 2001. 6, 46

[40] L. J. Allen, F. Brauer, P. Van den Driessche, and J. Wu, *Mathematical epidemiology*. Springer, 2008. 7, 10

[41] J. Arino, F. Brauer, P. van den Driessche, and J. Watmough, "Simple models for containment of a pandemic," *Journal of the Royal Society Interface*, vol. 3, no. 8, pp. 453–457, 2006. 7

[42] J. Arino, F. Brauer, P. Van Den Driessche, and J. Watmough, "A model for influenza with vaccination and antiviral treatment," *Journal of theoretical biology*, vol. 253, no. 1, pp. 118–130, 2008. 7, 8, 13, 32, 34, 76

[43] J. Heffernan, R. Smith, and L. Wahl, "Perspectives on the basic reproductive ratio," *Journal of the Royal Society Interface*, vol. 2, no. 4, pp. 281–293, 2005. 10

[44] P. Van den Driessche and J. Watmough, "Reproduction numbers and sub-threshold endemic equilibria for compartmental models of disease transmission," *Mathematical biosciences*, vol. 180, no. 1, pp. 29–48, 2002. 10, 14

[45] J. Arino, F. Brauer, P. Van Den Driessche, and J. Watmough, "A final size relation for epidemic models," *Mathematical Biosciences and Engineering*, vol. 4, no. 2, pp. 159 – 175, 2007. 11, 13

[46] D. J. Higham, "Modeling and simulating chemical reactions," *SIAM review*, vol. 50, no. 2, pp. 347–368, 2008. 15

[47] C. H. Lee and R. Lui, "A reduction method for multiple time scale stochastic reaction networks," *Journal of mathematical chemistry*, vol. 46, no. 4, pp. 1292–1321, 2009. 15, 22

[48] D. T. Gillespie, "Exact stochastic simulation of coupled chemical reactions," *The journal of physical chemistry*, vol. 81, no. 25, pp. 2340–2361, 1977. 17

[49] D. Blount, "Fourier analysis applied to spdes," *Stochastic processes and their applications*, vol. 62, no. 2, pp. 223–242, 1996. 19

[50] M. Lipsitch, S. Riley, S. Cauchemez, and A. C. Ghani, "Managing and reducing uncertainty in an emerging influenza pandemic," *New England Journal of Medicine*, vol. 361, no. 2, pp. 112–115, 2009. 19

[51] S. S. Kim, S. W. Lee, and B. Y. Choi, "A review of mathematical models and strategies for pandemic influenza control," *Korean Journal of Epidemiology*, vol. 30, no. 2, pp. 156–167, 2008. 19, 34, 36

[52] B. Munsky and M. Khammash, "The finite state projection algorithm for the solution of the chemical master equation," *The Journal of chemical physics*, vol. 124, no. 4, p. 044104, 2006. 22

[53] L. Michaelis and M. L. Menten, "Die kinetik der invertinwirkung," *Biochem. z*, vol. 49, no. 333-369, p. 352, 1913. 22

[54] M. B. Elowitz, A. J. Levine, E. D. Siggia, and P. S. Swain, "Stochastic gene expression in a single cell," *Science*, vol. 297, no. 5584, pp. 1183–1186, 2002. 22

[55] M. Thattai and A. Van Oudenaarden, "Intrinsic noise in gene regulatory networks," *Proceedings of the National Academy of Sciences*, vol. 98, no. 15, pp. 8614–8619, 2001. 22

[56] A. Kumar and K. Josić, "Reduced models of networks of coupled enzymatic reactions," *Journal of theoretical biology*, vol. 278, no. 1, pp. 87–106, 2011. 22

[57] P. Staff, "A stochastic development of the reversible michaelis-menten mechanism," *Journal of theoretical biology*, vol. 27, no. 2, pp. 221–232, 1970. 22

[58] H. Qian and E. L. Elson, "Single-molecule enzymology: stochastic michaelis–menten kinetics," *Biophysical chemistry*, vol. 101, pp. 565–576, 2002. 22

[59] É. Dóka and G. Lente, "Stochastic mapping of the michaelis-menten mechanism," *The Journal of chemical physics*, vol. 136, no. 5, p. 054111, 2012. 22

[60] P. Arányi and J. Tóth, "A full stochastic description of the michaelis-menten reaction for small systems.," *Acta biochimica et biophysica; Academiae Scientiarum Hungaricae*, vol. 12, no. 4, pp. 375–388, 1976. 22

[61] C. H. Lee and P. Kim, "An analytical approach to solutions of master equations for stochastic nonlinear reactions," *Journal of Mathematical Chemistry*, vol. 50, no. 6, pp. 1550–1569, 2012. 25

[62] J. Wilkinson, "Calculation of the eigenvectors of a symmetric tridiagonal matrix by inverse iteration," *Numerische Mathematik*, vol. 4, no. 1, pp. 368–376, 1962. 25

[63] L. Elsner, A. Fasse, and E. Langmann, "A divide-and-conquer method for the tridiagonal generalized eigenvalue problem," *Journal of computational and applied mathematics*, vol. 86, no. 1, pp. 141–148, 1997. 25

[64] I. S. Dhillon and B. N. Parlett, "Multiple representations to compute orthogonal eigenvectors of symmetric tridiagonal matrices," *Linear Algebra and its Applications*, vol. 387, pp. 1–28, 2004. 25

[65] H. Lee and C. H. Lee, "An analytic approach to a stochastic enzyme kinetic model," *MATCH-Communications in Mathematical and in Computer Chemistry*, vol. 73, no. 3, pp. 691–704, 2015. 27

[66] M. Suh, J. Lee, H. J. Chi, and Y. K. Kim, "Mathematical modeling of the novel influenza a (h1n1) virus and evaluation of the epidemic response strategies in the republic of korea," *Journal of preventive medicine and public health= Yebang Uihakhoe chi*, vol. 43, no. 2, pp. 109–116, 2010. 34, 36

[67] M.-J. Zhang, X. Zhang, and T. H. Scheike, "Modeling cumulative incidence function for competing risks data," *Expert review of clinical pharmacology*, vol. 1, no. 3, pp. 391–400, 2008. 36

[68] KOrean Statistical Information Service(KOSIS), "Population census," 2005, 2010. 36

[69] W. S. Choi, W. J. Kim, and H. J. Cheong, "The evaluation of policies on 2009 influenza pandemic in korea," *Journal of preventive medicine and public health= Yebang Uihakhoe chi*, vol. 43, no. 2, pp. 105–108, 2010. 36

[70] The immunization control team, Korea Centers for Disease Control and Prevention(KCDC), "2009-2010 Influenza A (H1N1) vaccination program in Korea, Public Health Weekly Report, 22 (3)," 2010. 36

[71] T. G. Kurtz, "Solutions of ordinary differential equations as limits of pure jump markov processes," *Journal of applied Probability*, vol. 7, no. 1, pp. 49–58, 1970. 37

[72] T. G. Kurtz, "Limit theorems for sequences of jump markov processes approximating ordinary differential processes," *Journal of Applied Probability*, vol. 8, no. 2, pp. 344–356, 1971. 37

[73] S. N. Ethier and T. G. Kurtz, *Markov processes: characterization and convergence*, vol. 282. John Wiley & Sons, 2009. 37

[74] P. L. Simon and I. Z. Kiss, "From exact stochastic to mean-field ode models: a new approach to prove convergence results," *IMA Journal of Applied Mathematics*, vol. 78, no. 5, pp. 945–964, 2013. 38

[75] R. Graham, M. Juffrie, R. Tan, C. Hayes, I. Laksono, C. Ma'Roef, K. Porter, S. Halstead, *et al.*, "A prospective seroepidemiologic study on dengue in children four to nine years of age in yogyakarta, indonesia i. studies in 1995-1996.," *The American Journal of Tropical Medicine and Hygiene*, vol. 61, no. 3, pp. 412–419, 1999. 41

[76] M. Derouich, A. Boutayeb, and E. Twizell, "A model of dengue fever," *BioMedical Engineering OnLine*, vol. 2, no. 1, p. 1, 2003. 42, 57

[77] N. Ferguson, R. Anderson, and S. Gupta, "The effect of antibody-dependent enhancement on the transmission dynamics and persistence of multiple-strain pathogens," *Proceedings of the National Academy of Sciences*, vol. 96, no. 2, pp. 790–794, 1999. 43

[78] J. Liu-Helmersson, H. Stenlund, A. Wilder-Smith, and J. Rocklöv, "Vectorial capacity of aedes aegypti: effects of temperature and implications for global dengue epidemic potential," *PloS one*, vol. 9, no. 3, p. e89783, 2014. 52, 53

[79] B. W. Alto and D. Bettinardi, "Temperature and dengue virus infection in mosquitoes: independent effects on the immature and adult stages," *The American journal of tropical medicine and hygiene*, vol. 88, no. 3, pp. 497–505, 2013. 52

[80] N. B. Tjaden, S. M. Thomas, D. Fischer, and C. Beierkuhnlein, "Extrinsic incubation period of dengue: knowledge, backlog, and applications of temperature dependence," *PLoS Negl Trop Dis*, vol. 7, no. 6, p. e2207, 2013. 53

[81] B. Adams and M. Boots, "How important is vertical transmission in mosquitoes for the persistence of dengue? insights from a mathematical model," *Epidemics*, vol. 2, no. 1, pp. 1–10, 2010. 53, 57, 58

[82] M. Q. Benedict, R. S. Levine, W. A. Hawley, and L. P. Lounibos, "Spread of the tiger: global risk of invasion by the mosquito aedes albopictus," *Vector-borne and zoonotic diseases*, vol. 7, no. 1, pp. 76–85, 2007. 54

[83] S. H. Lee, K. W. Nam, J. Y. Jeong, S. J. Yoo, Y.-S. Koh, S. Lee, S. T. Heo, S.-Y. Seong, and K. H. Lee, "The effects of climate change and globalization on mosquito vectors: evidence from jeju island, south korea on the potential for asian tiger mosquito (aedes albopictus) influxes and survival from vietnam rather than japan," *PloS one*, vol. 8, no. 7, p. e68512, 2013. 54

[84] Korea Centers for Disease Control and Prevention(KCDC), *Infectious Diseases Surveillance Yearbook 2015*. KCDC, 2016. 55, 57

[85] KOrean Statistical Information Service(KOSIS), "Population census," 2010. 56, 57, 62

[86] H. J. Wearing and P. Rohani, "Ecological and immunological determinants of dengue epidemics," *Proceedings of the National Academy of Sciences*, vol. 103, no. 31, pp. 11802–11807, 2006. 57

[87] L. K. Gallos and N. H. Fefferman, "The effect of disease-induced mortality on structural network properties," *PloS one*, vol. 10, no. 8, p. e0136704, 2015. 57

[88] S.-F. Wang, K. Chang, R.-W. Lu, W.-H. Wang, Y.-H. Chen, M. Chen, D.-C. Wu, and Y.-M. A. Chen, "Large dengue virus type 1 outbreak in taiwan," *Emerging microbes & infections*, vol. 4, no. 8, p. e46, 2015. 57

[89] S.-F. Wang, K. Chang, E.-W. Loh, W.-H. Wang, S.-P. Tseng, P.-L. Lu, Y.-H. Chen, and Y.-M. A. Chen, "Consecutive large dengue outbreaks in taiwan in 2014–2015," *Emerging Microbes & Infections*, vol. 5, no. 12, p. e123, 2016. 57

[90] Jeju special self-governing province, "Population statistics based on resident registration," 2014. 62

[91] H. S. Rodrigues, M. T. T. Monteiro, and D. F. Torres, "Sensitivity analysis in a dengue epidemiological model," in *Conference Papers in Science*, vol. 2013, Hindawi Publishing Corporation, 2013. 71

[92] D. A. McQuarrie, "Stochastic approach to chemical kinetics," *Journal of applied probability*, vol. 4, no. 3, pp. 413–478, 1967. 78

[93] L. Acedo, G. González-Parra, and A. J. Arenas, "An exact global solution for the classical sirs epidemic model," *Nonlinear Analysis: Real World Applications*, vol. 11, no. 3, pp. 1819–1825, 2010. 79

[94] H. Yarmand and J. S. Ivy, "Analytic solution of the susceptible-infective epidemic model with state-dependent contact rates and different intervention policies," *Simulation*, p. 0037549713479052, 2013. 79

[95] S. Lenhart and J. T. Workman, *Optimal control applied to biological models*. CRC Press, 2007. 79

[96] A. W. Wymore, *A mathematical theory of systems engineering: the elements*. Wiley, 1967. 79

[97] D. Aldila, T. Götz, and E. Soewono, "An optimal control problem arising from a dengue disease transmission model," *Mathematical biosciences*, vol. 242, no. 1, pp. 9–16, 2013. 79

[98] F. B. Agusto, N. Marcus, and K. O. Okosun, "Application of optimal control to the epidemiology of malaria," *Electronic Journal of Differential Equations*, vol. 2012, no. 81, pp. 1–22, 2012. 79

[99] B. F. Finkenstädt, O. N. Bjørnstad, and B. T. Grenfell, "A stochastic model for extinction and recurrence of epidemics: estimation and inference for measles outbreaks," *Biostatistics*, vol. 3, no. 4, pp. 493–510, 2002. 79

ACKNOWLEDGEMENTS

I would like to thank all the people who contributed in this dissertation, which would never have been possible without their support. Frist and foremost, I would like to express my gratitude to advisor Chang Hyeong Lee, who has continuously supported me by not only introducing me to the interesting topic on mathematical modeling and stochastic simulation but also giving me so many wonderful opportunities. He has encouraged me academically and emotionally to complete my PhD thesis be an independent researcher. He has always answered my questions through the insightful discussion despite his busy schedules. I was impressed he said to me something like "First, sincerity is important, but it is also important for me to do better." It has encouraged me to study more deeply and keep my focus and motivation. I think I was lucky because I had a great mentor. It has been an honor to be his first Ph.D. student. I appreciate all his contributions of time, his constant guidance, suggestions, and endless encouragement, and full support during last six years of my graduate studies.

I would like to thank my reading committee members: Pilwon Kim, Chang Yeol Jung, Jin Hyuk Choi, for investing time and their encouragement. I feel proud and honoured that they accepted to be on my committee. I am also deeply grateful to Prof. Pilwon Kim for providing his warm encouragement, thoughtful guidance, and critical comments on various research projects. I am very grateful that he has been actively interested in my work and gave me scientific advice all the time. I would like to express my thanks to Jin Hyuk Choi for providing interesting and valuable comments on exact probability solution with block structures of stochastic system. I also would like to thank Chang Yeol Jung for providing helpful comments and insightful questions on stochastic computational methods and teaching me about numerical methods.

I would like to express my thanks to Prof. Sunmi Lee for providing me valuable comments and my next step of on-going project. I also would like to offer my sincere thanks to her for wonderful collaboration on the H1N1 influenza transmission model with control measures as well as the dengue transmission modeling with seasonality. I am very grateful for her patience, motivation, enthusiasm, and immense knowledge in mathematical modeling for infectious disease.

I would like to express my sincere appreciation to the faculties of Mathematical Sciences for helping me at various phases of my research and providing academic support. All of professors have played an important role in my journey to be a researcher. I will forever be grateful to Prof. Bongsuk Kwon for providing advice many times and valuable guides during my graduate school. I realized the attitude of a good researcher from his enthusiasm and confidence for research. I am greatly indebted to Prof. Bongsoo Jang for helping me having a confidence by developing my computational skills for his lectures about dynamical system and numerical methods. I would like to express my deep thanks to Dr. Jung Eun Kim for the insightful discussion, valuable advice, and friendly assistance on deterministic and stochastic approaches of epidemic model all the time. I feel that it was a great pleasure working with her and I very much appreciate her enthusiasm, patience. I also express my gratitude to her for caring and concern about this dissertation. I express my gratitude to Dr. Sunghwan Moon for his skill in spreading happiness and friendly assistance all the time. I am grateful for encouraging me to focus on my research and overcome both personal or academic difficulties.

I want to thank great labmates of Stochastic Simulation and Analysis, Yongin Choi and James Seulgi Kim for the stimulating discussions and the sleepless nights we were working together, and all the fun we have had in the last two years. They gave me strength to overcome my difficulties. I will not forget their consideration and friendship as well as their support I felt in every conferences and summer programs we took participated in together. I especially thank James for helping me with detail review of proofreading my thesis. I am very grateful to Kyunghoon Kim for providing critical advice as well as endless encouragement. We had been supporting each other to realize our dreams of being a great researcher together since we started the graduate program at the same time. I will also not forget his help and He will still be there as a supportive friend. I am grateful for time spent with many colleagues at UNIST that became an unforgettable part of my life. I would like to thank to all my friends, Junho, Junsik, Wanyong, Hyunki, Minho, Jongha, Jongo, Soyoung for all their supports the and sharing wonderful and enjoyable time at UNIST. I also would like to thank to Eunji, Hoyeon, Seyeon, Keon ho for the joyful activities and friendship and all the nice conversations during tea and lunch time. I am very grateful to celebrate my birthday without forgetting each year and I will never forget it as wonderful memories.

I want to express my gratitude to Prof. Eunok Jung (Konkuk Univ.), Prof. Yongkuk Kim (Kyungpook National Univ.) for contributing to a rewarding graduate school experience by supporting my attendance at various research activities and being interested in my research and providing critical comments. I am very grateful to

Prof. Jae Kyoung Kim (KAIST) for giving me good advice of importance of the active and challenging spirit for new research topic when I consider postdoc positions.

Specially, I would like to express my deep gratitude to Giphil Cho and Kwang Su Kim at Pusan National University for giving me positive comments and continuously encouraging me. We have often met mostly in the conferences, discussed interesting research and provided valuable advice. I hope that there will be the opportunity to work together to be an excellent researcher in the future.

I would like to express my sincere thanks to Kwang Mo Hwang, who was a math teacher encouraging me and providing advice whenever I was discouraged. It was a very valuable opportunity that I realized the pleasure of mathematics and statistics through his lectures.

Lastly, I warmly appreciate my parents Taeman Lee and Hyeyoung Lee and my brother Hyungduk for all their unconditional love and encouragement in all aspects of my life. They have given me the more strength and enthusiasm that make me overcome any problems I encounter. Thank you for always being there for me.